Structure and hydrodesulfurization activity of carbon-supported catalysts

STRUCTURE AND HYDRODESULFURIZATION ACTIVITY OF CARBON-SUPPORTED SULFIDE CATALYSTS

Proefschrift

ter verkrijging van de graad van doctor in de technische wetenschappen aan de Technische Hogeschool Eindhoven, op gezag van de rector magnificus, prof. dr. S.T.M. Ackermans, voor een commissie aangewezen door het college van dekanen in het openbaar te verdedigen op dinsdag 26 maart 1985 te 16.00 uur

door

Jan Paul Rene Vissers

geboren te Merksem

Dit proefschrift is goedgekeurd door de promotoren

Prof. dr. R. Prins
Prof. dr. J.C. Duchet

en door de copromotor

Dr. ir. V.H.J. de Beer

Dit proefschrift is tot stand gekomen mede dankzij de steun van NORIT N.V., Amersfoort.

CONTENTS

CHAPTER 1

INTRODUCTION

CATALYTIC PROCESSES.

Catalytic processes are of tremendous importance in the modern industrialized society. Altogether, they account for as much as 90% of the chemical manufacturing processes in use throughout the world. The role of the catalyst in these processes consists in increasing the rate as well as controlling the selectivity of the chemical reactions involved. Many process improvements result from the discovery of better chemical routes, usually based on new catalysts.

Heterogeneous catalysis is widely applied in the petroleum industry covering reactions such as cracking, catalytic reforming and catalytic hydrotreating. The catalysts applied for these reactions are zeolites or silica-aluminas, alumina-supported metal catalysts and alumina-supported metal sulfide catalysts respectively.

The fastest growing group of catalysts (predicted rate about 13% per year) is that of the hydrotreating catalysts (1). The increased need for a more efficient utilization of the various fossil fuel feedstocks, requiring more severe processing of still heavier feedstocks, made that sulfide catalysts are or will become within a few years, the most important of all catalyst systems with close to 1/4 of the total world catalyst market (2).

HYDROTREATING.

In the petroleum refining industry, catalytic hydrogen treating can be defined as the contacting of petroleum feedstocks with hydrogen in the presence of suitable catalyst and under suitable operating conditions to effect conversion to low molecular weight hydrocarbons, to prepare the feedstocks for further conversion downstream, and to improve the quality of the finished products (3,4). In Fig. 1 the location of hydrotreatment units in relationship to other major refinery process operations is depicted.

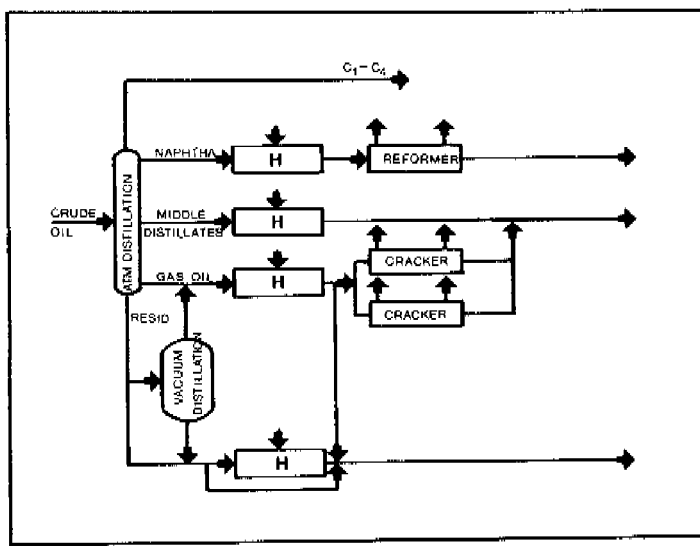

Fig. 1 Location of hydrotreating (H) units in refinery flow scheme (4).

Quite a number of reactions occur during the process which in principle can be subdivided into two classes, hydrogenation and hydrogenolysis reactions. These are in turn subdivided into the following reactions :

a. hydrocracking or C-C bond cleavage
b. olefin and aromatic saturation
c. hydrodesulfurization or C-S bond cleavage (HDS)
d. hydrodenitrogenation or C-N bond cleavage (HDN)
e. hydrodeoxygenation or C-O bond cleavage (HDO)
f. hydrodemetallation or C-Me bond cleavage (HDMe)

The relative shortage of crude oil, the increased processing of coal and tar sand-derived liquids (high in S, N and metal content), and the definite trend towards complete elimination of the residual oil fractions caused by the declining market for heavy fuel oils, give a strong incentive to the research and the development of the hydrotreatment catalysts and the process technology involved.

The study described in this dissertation, is focussed on the hydrodesulfurization reaction which frequently is the most important objective of hydrotreatment. Hydrodesulfurization involves the removal of sulfur from S-containing molecules present in the feedstock, the reaction being schematically as :

$$R - SH + H_2 \longrightarrow RH + H_2S$$

The following classes of sulfur containing compounds, listed in order of decreasing reactivity in hydrodesulfurization rate, are present in petroleum feedstocks : thiols, disulfides, sulfides, thiophenes, benzothiophenes, dibenzothiophenes, benzonaphtothiophenes etc. Hydrodesulfurization is applied to naphtha to prevent poisoning of platinum metal-containing catalysts in the reforming process with sulfur and, in the treatment of gasoline to obtain sweetened and stabilized products. Nowadays, one of its most important objectives is the removal of sulfur from fuels to prevent the pollution of the

atmosphere with SO_2 (acid rain).

SULFIDE CATALYSTS.

The catalysts applied in hydrodesulfurization processes must be highly resistant to poisoning and operate efficiently under severe reaction conditions, requirements which are only fulfilled by transition metal sulfides. Historically, sulfide catalysts have evolved from those developed in prewar Germany for the hydrogenation of coal and coal-derived liquids. After a systematic study it was found that metal sulfides, especially molybdenum and tungsten sulfide were the active catalysts (5,6). Since that time, HDS catalysts have evoluted to the nowadays industrially applied catalytic ensembles composed of molybdenum (or tungsten) sulfide promoted with cobalt (or nickel) sulfide supported on a porous alumina carrier. The term promotor being related to the fact that the HDS activity of sulfided alumina-supported molybdenum is largely enhanced by the addition of cobalt sulfide, while sulfided alumina-supported cobalt is considered to be inactive.

Whereas most of the knowledge on sulfide catalysts in the past was based on rather empirical observations and nearly arbitrary assumptions related to the hydrodesulfurization process in practice, considerable fundamental research has accumulated on the structure and properties of sulfide catalysts in comparatively recent time. Among the models proposed to describe the structure of the cobalt molybdenum supported on alumina catalyst, are the monolayer model (3,7,8,9), the intercalation (or decoration model) (10-13), the contact synergy model (14,15) and the Co-Mo-S model (16), each of which describes the promotor effect of cobalt in a different way. For a review on this subject we refer to (3,15,17-19). Considerable work has also been and is done aiming to elucidate the location and operation of the

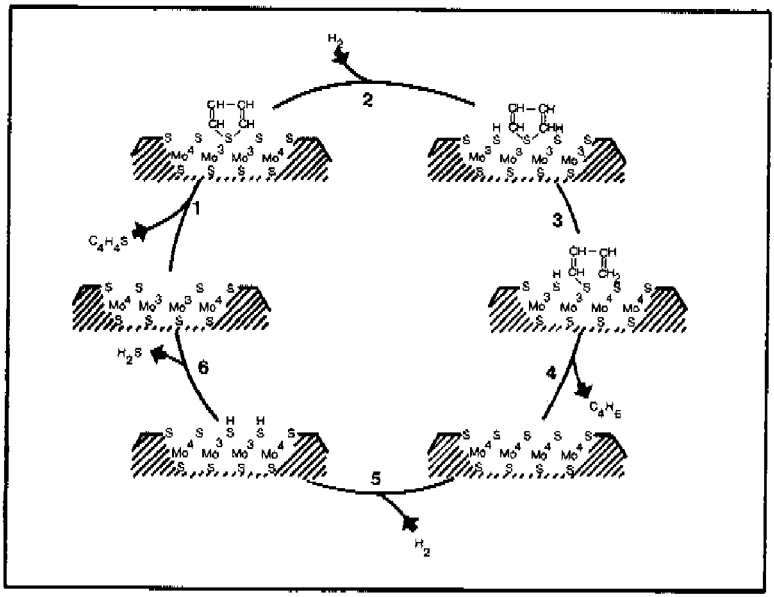

Fig. 2 Schematic thiophene HDS mechanism.

active sites (20-25). Figure 2 depicts a possible schematic thiophene hydrodesulfurization mechanism over a molybdenum sulfide catalyst. In this scheme the electrons are localized which in fact may not be the case. Thiophene adsorbs on a sulfur vacancy which agrees with the common belief that the hydrodesulfurization reaction involves anion vacancies (exposed metal ions). The presence of Mo^{3+} ions has been indicated in ESR studies (26,27). Hydrogen is seen to be provided by SH groups in the reaction process. After desorption of the hydrocarbon, the S vacancy is regenerated to complete the cycle. From the above mechanism it may be

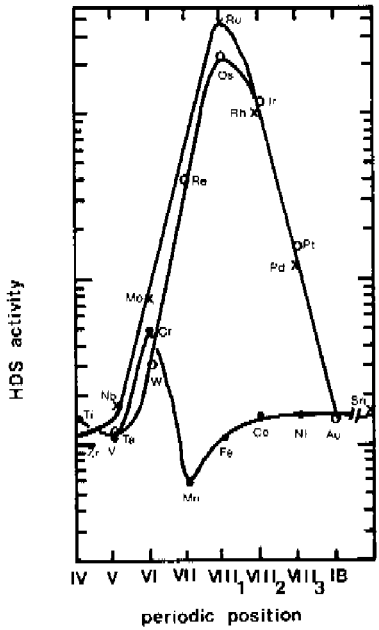

Fig. 3 Periodic HDS activity trends for unsupported metal sulfide catalysts, normalized per gram (27).

argued that there is no need for the exclusive use of molybdenum (or tungsten) sulfide to act as a catalyst. This was indeed shown in a recent study on the hydrodesulfurization activity of unsupported transition metal sulfides (28). As can be seen in Fig. 3 the activity trends for second and third row metal sulfides vary over more than 2 orders of magnitude and display typical volcano type plots with periodic position. Important factors determining the hydrodesulfurization activity seem to be in

this respect the occupation of the highest molecular orbital as well as the metal-sulfur covalent bond strength (29). Despite the numerous research efforts, much detailed fundamental information on the structure and related hydrodesulfurization activity of sulfide catalysts is still lacking.

ROLE AND INFLUENCE OF THE SUPPORT MATERIAL.

Like the majority of the technologically important catalysts, metal sulfides are mostly supported on suitable carriers. The role of the carrier is to maintain the catalytically active phase in a highly dispersed state (high active surface area). In industrial applications, sulfide catalysts are usually exposed to rather extreme conditions, involving high operating temperatures, large catalyst beds necessitating a high mechanical strength of the catalyst, and processing of low-quality materials which contaminate the active surface. To this is added the demand of a long lifetime or, of the possibility of repeated regeneration, so that it is essential for the carriers employed to be of high quality.

Most often employed as support is the gamma-modification of aluminium oxide, prepared such that it has a sufficiently large surface area (150 - 300 m^2/g), a suitable texture and strong mechanical properties. An important property of alumina is its ability to properly disperse large amounts of metal sulfides (up to 20 wt%). Another important type of carrier for sulfide catalysts are the amorphous aluminosilicates (to which sometimes other oxides are added) (6,30). Because of their increased acidity relative to alumina, these materials serve as carriers in hydrotreatment processes where hydrocracking is necessary.

The use of alumina as a carrier material for sulfide catalysts, however, has a considerable drawback, in that the

alumina surface causes unwanted metal-support interactions which lower the hydrodesulfurization activity of the catalyst. In this respect it was observed that small amounts of molybdenum (up to 3 wt% MoO_3) are very strongly adsorbed on the alumina surface such that high sulfiding temperatures are needed to obtain a complete conversion into their active sulfide form (31). Under normal sulfiding conditions this fraction may remain oxidic and as a consequence its activity will be low. Even more pronounced is the interaction with the cobalt and nickel promotor ions. These are known to react with the alumina surface to form $CoAl_2O_4$ ($NiAl_2O_4$) or occupy octahedral or tetrahedral sites inside the alumina latice (3,32), which makes them catalytically inactive. Many studies have been carried out aimed at reducing the active phase-support interaction. Among these studies are those using doped alumina carriers, which allowed some regulation of the active phase-support interaction (33-35).

In their study on the influence of the support, de Beer et al. (36-38) concluded that any support with a high specific surface area (γ- and η -Al_2O_3, SiO_2 or carbon) is acceptable for hydrodesulfurization catalysts, indicating that there is no need for the exclusive use of alumina as a support. They found that substantially more active catalysts could be prepared on the less reactive SiO_2 support material for the cobalt and nickel promotor sulfides, provided that the conventional preparation method was modified somewhat. In this respect it was concluded that even carbon, being an inert support material, should be perfectly suitable as support.

CARBON AS A SUPPORT FOR SULFIDE CATALYSTS.

Amongst the vast number of papers and patents on hydrodesulfurization that have appeared after the second

world war, those dealing with carbon-supported sulfide catalysts are scarce (39-56), despite the fact that the application of carbon carriers was usually reported to lead to interesting results, both from the practical and fundamental point of view.

The advantages that have been claimed for carbon-supported catalysts are :

- Application of a material as inert as carbon results in less complex catalysts, since even after mild sulfidation, all transition metal compounds present in the precursor state will be converted into their sulfide state.
- The inert carbon support material seems very useful in studies on the true catalytic properties of well-dispersed poorly crystallized metal sulfides, unperturbed by strong interactions with the support.
- Carbon-supported sulfide catalysts have high specific hydrodesulfurization activities compared to alumina-supported catalysts, especially at low active phase contents (cf. Fig. 4).
- Due to the fact that carbon has weak adsorption properties for hydrocarbons such as aromatics, the coking propensity on carbon-supported catalysts is considerably lower than on corresponding alumina-supported systems. In this respect, carbon-supported catalysts should be less susceptible to deactivation by coke formation.
- The expensive catalytic metals are readily recoverable from spent catalysts by simply burning off the carbon support.

But in their application as a support for sulfide catalysts, carbon materials do not offer advantages only. The following disadvantages can be discerned , viz. :

- The widely available activated carbons do have a high internal surface but, the major fraction of this area is in narrow mesopores and mostly in micropores. Due to diffusion limitations for reactant and product molecules, the fraction of the catalytically active phase, that is deposited in

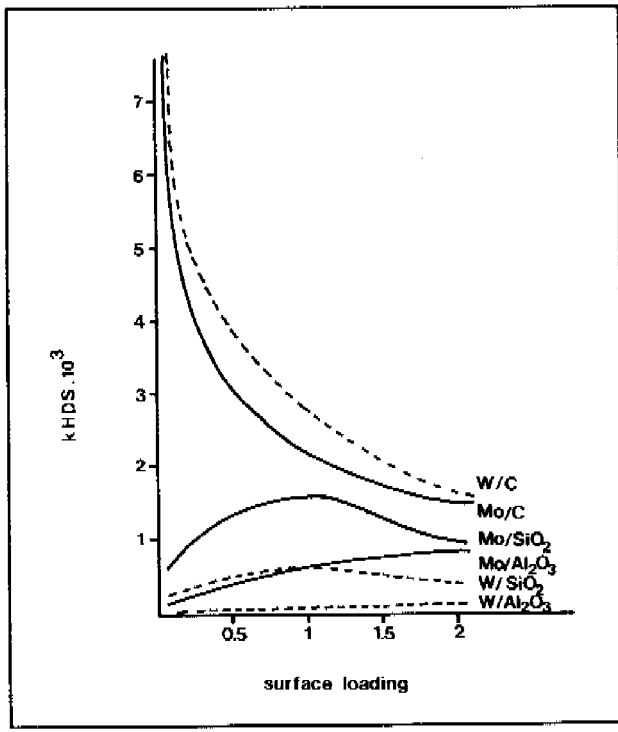

Fig. 4 HDS activity per mol metal of Mo and W-based catalysts on various supports (46).

these pores during catalyst impregnation, will be of little utility in the HDS process and in fact be wasted.

- For most carbon materials enlarging the meso- and macropore structure will be at the expense of their mechanical properties, and will therefore have a poor crushing strength, compared to alumina supports.

- Although on a carbon surface a whole variety of oxygen functional groups is located (cf. Fig. 5), the nature and the concentration of these groups are frequently such that they are insufficient to create and maintain a high active phase dispersion during catalyst preparation and under sulfiding conditions.
- And finally, carbon-supported catalysts cannot be regenerated in the same manner as alumina-supported systems.

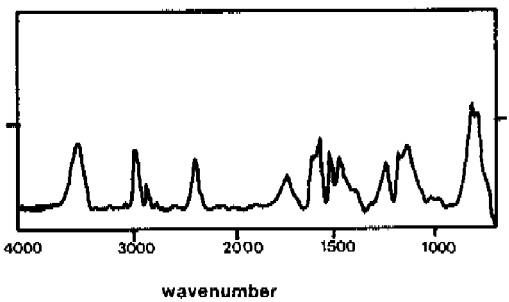

Fig. 5 Fourier transform infrared spectra of a Norit activated carbon sample (57).

cm^{-1}	
3500	OH stretch vibration with weak H-bridge
2966	asymm. and symm. C-H stretch vibration in CH_3 and CH_2 groups
2868	
2347	asymmetric O=C=O stretch vibration of CO_2 adsorbed pores
1735	C=O stretch vibration from CHO, COO-,  or -lactone
1643	methylene vibration
1608	C=O in chinone configuration
1230	C-O stretch vibration (fenol, COO-, epoxide)

SCOPE AND OUTLINE OF THIS INVESTIGATION.

In view of the published advantages of carbon as a support material for sulfide catalysts and considering that they may outweigh the disadvantages, especially when attention is paid to minimize the latter, it was decided to start a systematic study on the relation between the structure and catalytic properties of carbon-supported sulfide catalysts. The present investigation can be subdivided in two parts : one part, which includes chapters 2-5, is devoted to the structure and catalytic activity of various metal sulfides supported on activated carbon ; while the second part, comprising chapters 6-9, is focussed on the influence of textural and surface properties of various carbon supports on the final properties of the catalysts.

In chapters 2 and 3, the results on activated carbon supported molybdenum catalysts are discussed. Dynamic oxygen chemisorption measurements (DOC) were carried out to detect the amount of active surface area, X-ray photoelectron spectroscopy (XPS) was used to measure the dispersion of the catalyst. Temperature programmed sulfidation (TPS), and thiophene hydrodesulfurization (HDS) were measured to study catalyst sulfidation and catalyst activity. A comparison is made with the corresponding alumina-supported catalysts.

Chapter 4 is devoted to the study of activated carbon-supported cobalt catalysts and the role of Co in Co-Mo promoted systems. This includes XPS, TPS and thiophene hydrodesulfurization activity measurements.

A comparative study of the thiophene hydrodesulfurization properties of first, second and third row metal sulfides ranging from group VI to group VIIIc supported on activated carbon is reported in chapter 5. XPS has been used to calculate catalyst dispersion and to identify the sulfide phases present. A comparison is made with unsupported systems, and alumina supported systems.

In chapter 6 the interaction of the oxygen functional groups present at the carbon surface with the impregnated molybdate ions is presented. Fourier transform infrared spectroscopy and XPS are applied for the detection of the different oxygen groups present, while TEM, DOC and XPS are used to study catalyst dispersion.

In chapter 7 the poisoning effect of phosphate (which is frequently present in carbon supports) on the HDS capability of activated carbon supported molybdenum catalysts is discussed.

Chapters 8 and 9 are dedicated to the preparation and evaluation of carbon support materials with optimal textural and mechanical properties. Chapter 8 deals with carbon black composites and chapter 9 with carbon covered alumina.

REFERENCES

1. Bonelle, J.P., Delmon, B., and Derouane, E., in "Surface Properties and Catalysis by Non-metals", (Bonelle, J.P., Delmon, B., and Derouane, E., eds.), p. VII, D. Reidel, Dordrecht (1983).
2. Jacobsen, A.C., in "Surface properties and Catalysis by Non-metals", (Bonelle, J.P., Delmon, B., and Derouane, E., eds.), p. 305, D. Reidel, Dordrecht (1983).
3. Gates, B.C., Katzer, J.R., and Schuit, G.C.A., in "Chemistry of Catalytic Processes", p. 390, Mc-Graw-Hill, New York (1979).
4. Mc Culloch, D.C., in "Applied Industrial Catalysis", (Leach, B.E., Ed.), vol 1, p. 69, Academic press, New York (1983).
5. Kronig, W., in "Die Katalytische Druckhydrierung von Kohlen, Teeren und Mineralolen", Springer - Verlag, Berlin (1950).
6. Weisser, O., and Landa, S., in "Sulphide Catalysts, Their Properties and Applications", Pergamon, New York

(1973).

7. Schuit, G.C.A., and Gates, B.C., AI Ch E.J. 19, 417 (1973).
8. Massoth, F.E., J.Catal. 36, 164 (1975).
9. Massoth, F.E., J.Catal. 47, 316 (1977).
10. Voorhoeve, R.J.H., and Stuiver, J.C.M., J.Catal. 23, 228 (1971).
11. Voorhoeve, R.J.H., and Stuiver, J.C.M., J.Catal. 23, 243 (1971).
12. Voorhoeve, R.J.H., J.Catal. 23, 236 (1971).
13. Farragher, A.L., and Cossee, P., in "Proceedings, 5th International Congress on Catalysis", Palm Beach, 1972 (J.W. Hightower, Ed.), p. 1301, North Holland, Amsterdam (1973).
14. Hagenbach, G., Courty, P., and Delmon, B., J.Catal. 23, 295 (1971).
15. Delmon, B., in "Proceedings of the Climax Third International Conference on the Chemistry and uses of Molybdenum", (W.F. Barry, and P.C.H. Mitchell, Eds.) Climax Molybdenum Company, Ann Arbor, Michigan, p. 73 (1979).
16. Topsøe, H., Clausen, B.S., Candia, R., Wivel, C., and Mørup, S., J.Catal. 68, 433 (1981).
17. Massoth, F.E., Adv. Catal. 27, 265 (1978).
18. Grange, P., Catal. Rev., Sci. Eng. 21 (1), 135 (1980).
19. Topsøe, H., in "Surface Properties and Catalysis by Non-metals", (Bonelle, J.P., Delmon, B., and Derouane, E., Eds.), p. 329, D. Reidel, Dordrecht (1983).
20. Bachelier, J., Duchet, J.C., and Cornet, D., J. Phys. Chem. 84, 1925 (1980).
21. Tauster, S.J., Pecoraro, T.A., and Chianelli, R.R., J. Catal. 63, 515 (1980).
22. Bachelier, J., Tilliette, M.J., Duchet, J.C., and Cornet, D., J. Catal. 76, 300 (1982).
23. Silbernagel, B.G., Pecoraro, T.A., and Chianelli, R.R., J. Catal. 78, 380 (1982).

24. Jung, H.J., Schmitt, J.L., and Ando, H., in "Proceedings of the Climax Fourth Intern. Conf. on Chemistry and Uses of Molybdenum", (H.F. Barry, and P.C.H. Mitchell, Eds.) p. 246, Climax Molybdenum Company, Ann Arbor, Michigan (1982).
25. Candia, R., Clausen, B.S., Bartholdy, J., Topsøe, N.-Y., Lengeler, B., and Topsøe, H., in "Proceedings of the 8th International Congress on Catalysis", Verlag Chemie : Weinheim, Berlin, Vol II, p. 375 (1984).
26. Konings, A.J.A., van Dooren, A.M., Koningsberger, D.C., de Beer, V.H.J., Farragher, A.L., and Schuit, G.C.A., J. Catal. 1, 59 (1978).
27. Konings, A.J.A., Brentjens, W.L.J., Koningsberger, D.C., and de Beer, V.H.J., J. Catal. 67, 145 (1981).
28. Pecoraro, T.A., and Chianelli, R.R., J. Catal. 67, 430 (1981).
29. Harris, S., and Chianelli, R.R., J. Catal. 86, 400 (1984).
30. Muralidhar, G., Massoth, F.E.,and Shabtai, J., J. Catal. 85, 44 (1984).
31. Arnoldy, P., Van den Heijkant, J.A.M., de Bok, G.D., and Moulijn, J.A., J. Catal. accepted for publication.
32. Burggraf, L.W., Leyden, D.E., Chin, R.L., and Hercules, D.M., J. Catal. 78, 360 (1982).
33. Lycourghiotis, A., Vattis, D., and Aroni, P., Z. Phys. Chem. Neue Folge 121, 257 (1980).
34. Lycourghiotis, A., Tsiatsios, A., Katsamos, N.A., Z. Phys. Chem. Neue Folge. 126, 95 (1981).
35. Lo Jacono, M., Schiavello, M., de Beer, V.H.J., and Minelli, J. Phys. Chem. 81, 1583 (1977).
36. de Beer, V.H.J., Van der Aalst, M.J.M., Machiels, C.J., and Schuit, G.C.A., J. Catal. 43, 78 (1976).
37. de Beer, V.H.J., and Schuit, G.C.A., in "Preparation of Catalysts" (B. Delmon, P.A. Jacobs, and G. Poncelet, Eds.), p. 343, Elsevier, Amsterdam (1976).
38. de Beer, V.H.J., van sint Fiet, T.H.M., van der Steen,

G.H.A.M., Zwaga, A.C., and Schuit, G.C.A., J. Catal. 35, 297 (1974).

39. Zdrazil, M., J. Catal. 58, 436 (1979).
40. Kraus, J., and Zdrazil, M., React. Kinet. Catal. Lett. 6, 475 (1977).
41. Yamagata, N., Owada, Y., Okazaki, S., and Tanabe, K., J. Catal. 47, 358 (1977).
42. Topsøe, H., Clausen, B.S., Burriesev, N., Candia, R., and Mørup, S., in "Preparation of Catalysts II" (B. Delmon, P. Grange, P. Jacobs, and G. Poncelet, Eds.) p. 479, Elsevier, Amsterdam (1979).
43. Stevens, G.C., and Edmonds, T., in "Preparation of Catalysts II" (B. Delmon, P. Grange, P. Jacobs, and G. Poncelet, Eds.) p. 507, Elsevier, Amsterdam (1979).
44. de Beer, V.H.J., Duchet, J.C., and Prins, R., J. Catal. 72, 369 (1981).
45. Scaroni, A.W., Ph. D. Thesis, The Pennsylvania State University (1981).
46. Duchet, J.C., van Oers, E.M., de Beer, V.H.J., and Prins, R., J. Catal. 80, 386 (1983).
47. Bridgewater, A.J., Burch, R., and Mitchell, P.C.H., Appl. Catal. 4, 267 (1982).
48. Breysse, M., Bennett, B.A., Chadwick, D., Vrinat, M., Bull. Soc. Chim. Bel. 90, 1271 (1981).
49. Companie Francaise des essences synthetiques, Fr 981468 (1951).
50. Mason, R.B., Springs, D., Hammer, G.P., and Adams, C.E., US Patent 3,367,862 (1968).
51. Urban, P., and Albert, D.J., US Patent 3,725,303 (1973); Ger. Offen. 2,316,029 (1974).
52. Schmitt, J.L., and Castellion, G.A., US Patent 3,997,473 (1976).
53. Schmitt, J.L., and Castellion, G.A., US Patent 4,032,435 (1977).
54. Stevens, G.C., and Tennison, R., British Patent 1,471,588.

55. Voorhies, J.D., US Patent 4,082,652 (1978).

56. Gavin, D.G., and Jones, M.A., UK Patent Application GB 20456478A (1979).

57. "Activated Carbon, a Fascinating Material", published by Norit N.V., Amersfoort (1984).

CHAPTER 2

CHARACTERIZATION OF CARBON AND ALUMINA-SUPPORTED MOLYBDENUM SULFIDE CATALYSTS BY MEANS OF DYNAMIC OXYGEN CHEMISORPTION AND THIOPHENE HYDRODESULFURIZATION ACTIVITY.

ABSTRACT

Dynamic oxygen chemisorption measured in situ at 333 K and thiophene hydrodesulfurization were used to study the quantity and specific activity of catalytic sites present in sulfided Mo/C and Mo/Al_2O_3 catalysts. The molybdenum sulfide phase in the Mo/C catalysts was found to posses a high density of only one type of site with a high turn-over frequency. Comparison of particle size data, obtained from XPS measurements, with oxygen chemisorption measurements indicated that 4/5 or 2/5 (according to the model) of the molybdenum surface atoms in the Mo/C catalysts can be regarded as potential sites. The Al_2O_3-supported molybdenum phase had a lower site density and different types of sites seemed to be present at low and high molybdenum concentration. The decline in activity with run-time of both Mo/C and Mo/Al_2O_3 catalysts was not reproduced by the oxygen chemisorption capacities. Thus initial deactivation cannot be caused by sintering of the active phase or by pore blocking.

INTRODUCTION

Catalysts based on molybdenum sulfide are currently in large-scale use for the removal of sulfur and nitrogen from a variety of petroleum feedstocks. Commercial catalysts

typically contain Al_2O_3 as a carrier material for the active components (1). Recent laboratory-scale studies (2-9) have shown that application of a relatively inert carrier like carbon may result in improved catalysts. Advantages claimed for carbon-supported sulfide catalysts include high activity per Mo atom, especially at low active phase contents. At present it is not clear whether this improved activity is caused by an increase in number of active sites, as a result of a better dispersion or a more favourable morphology of the molybdenum sulfide phase formed on the carbon carrier, or by an enhancement of the activity per site. In the present investigation it was attempted to gain more insight into this matter by means of combined dynamic oxygen chemisorption (DOC) and hydrodesulfurization (HDS) activity measurements, an approach that has been demonstrated to be very useful in similar studies of sulfided Ni/Al_2O_3 catalysts (10,11), unsupported MoS_2 (12), and sulfided Mo/Al_2O_3 catalysts (13,14). X-ray photoelectron spectroscopy was applied to measure the dispersion of the Mo sulfide phase in the Mo/C catalysts. In addition the impact of run time was studied on the chemisorption capacities of both Mo/C and Mo/Al_2O_3 catalysts.

EXPERIMENTAL

Catalyst preparation

An activated carbon (Norit RX3 extra) and an alumina (Rhône-Poulenc) were used as carrier materials. B.E.T. surface area and pore volume were 238 m^2/g, 0.61 ml/g and 1190 m^2/g, 1.0 ml/g for the alumina and carbon support respectively. Series of Mo/C and Mo/Al_2O_3 catalysts (1.3-14.1 wt% Mo) were prepared by pore volume impregnation of the carrier with aqueous solutions of ammonium heptamolybdate (Merck, min 99.9%). All impregnated samples

were dried in air starting at 293 K and slowly increasing up to 383 K where they were kept overnight. Only the Mo/Al_2O_3 samples were subjected to a calcination treatment at 773 K for 2 h. Catalyst compositions were checked by means of atomic absorption spectrometry.

Sulfiding, activity tests and chemisorption measurements

Catalysts sulfiding, thiophene HDS activity test and dynamic oxygen chemisorption measurements were successively carried out, at atmospheric pressure, in one and the same micro flow reactor, without intermission for sample transfer. Two different procedures were applied:

1. Mo/C and Mo/Al_2O_3 samples (0.2 g) were sulfided in a mixture of purified hydrogen and hydrogen sulfide (Matheson, CP grade). The H_2S concentration was 10 mol% and total flow rate 60 ml/min. The following temperature program was used: 10 min at 293 K, linear increase to 673 K in 1 h, and 2 h at 673 K. The freshly sulfided samples were purged in purified He (O_2 concentration << 10^{-3} ppm) for 15 min at 673 K and subsequently cooled to 333 K, within 30 min in a He flow (30 ml/min). Oxygen chemisorption was then measured at 333 K by injecting 2.19 ml pulses of a 5.20 % O_2/He mixture, at 3 min intervals, into the He carrier gas flow. When effluent O_2 peaks had increased to constant size (less than 1% difference between two successive peaks) the total O_2 uptake was calculated.

2. Mo/C and Mo/Al_2O_3 samples (0.2 g) were sulfided according to the method described above. After this sulfiding procedure a mixture of 6.2 mol% thiophene (Merck, min 99%) in purified H_2 was fed to the reactor (flow rate, 50 ml/min) at 673 K. Reaction products were analyzed at 20 min intervals. From the thiophene conversion observed after a 2 h run, the first order HDS rate constant (k_{HDS} at t=2) and the activity per mol Mo (quasi turn-over frequency, QTOF) were calculated. In addition initial activity (k_{HDS}

at t=0) was calculated by extrapolation of the reciprocal conversion curves (straight lines) to zero run time. When activity test was completed the catalyst samples were purged and O_2 chemisorption was measured as described above.

This experimental set-up allowed to determine the oxygen uptake of the freshly sulfided catalysts as well as that of catalysts who had experienced a 2 h run time. In this way the impact of run time on the oxygen chemisorption capacities of the catalysts can be studied.

XPS measurements

Mo/C samples were sulfided, purged and cooled to room temperature (according to the method described under point 1 of the precious section) in a special reactor (15) that allowed transfer of the sample to a dry N_2-flushed glove box attached to the XPS apparatus, without exposure to air. The samples were mounted on the specimen holder by means of double sided adhesive tape. Spectra were recorded on an AEI ES 200 spectrometer at 283 K in steps of 0.1 eV. The C 1s peak was used as internal standard for binding energy calibration. Intensities were calculated from the peak areas after linear background correction. For Mo, the contributions of S 2s and $C_{K\alpha}$ signals were subtracted.

RESULTS

All k_{HDS}, quasi turn-over frequencies (QTOF), DOC, oxygen over molybdenum ratios (O/Mo), and turn-over frequencies (TOF), used throughout this paper have indices t=0, and t=2 indicating the thiophene HDS reaction time in hours, as described in the experimental section for procedure 1 and 2 respectively. All the results are presented in Figs. 1 to 7. However, for the readers convenience the exact experimental data are collected in Table 2, at the end of

the results section.

Carbon-supported catalysts.

Activity and DOC.

The results of the activity measurements are presented in Figs. 1 and 2. Fig. 1 shows that, irrespective of run time, the activity increased with increasing Mo content, and progressively levelled off for higher Mo contents. The activity was found to decline substantially with run time.

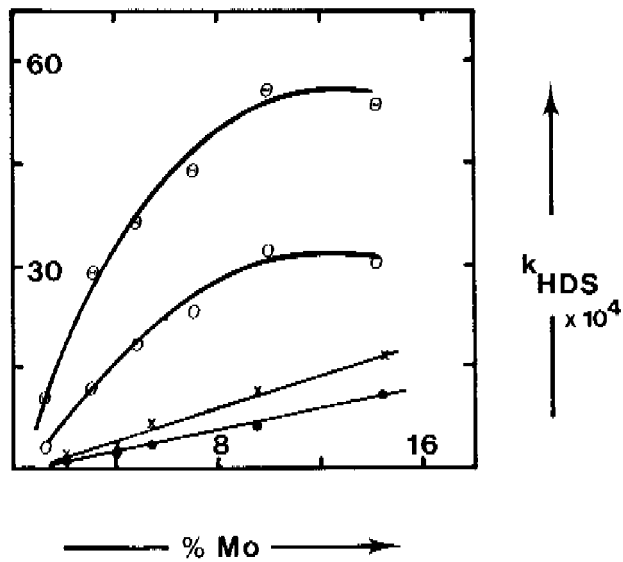

Fig. 1 First order rate constants (k_{HDS}, m^3 total feed per kg catalyst per second) versus wt% Mo for the Mo/C and Mo/Al_2O_3 catalysts.

Θ = values of Mo/C catalysts calculated after presulfidation (t=0, procedure 1)

O = values of Mo/C catalysts calculated after 2 h run time (t=2, procedure 2)

X = values of Mo/Al_2O_3 catalysts calculated after presulfidation (t=0, procedure 1)

● = values of Mo/Al_2O_3 catalysts calculated after 2 h run time (t=2, procedure 2)

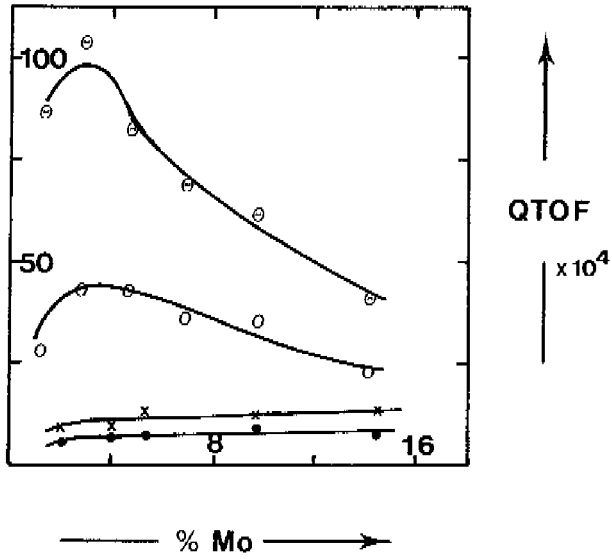

Fig. 2 Quasi Turn-Over Frequency values (QTOF, mol thiophene converted per mol Mo per second) versus wt% Mo for the Mo/C and Mo/Al_2O_3 catalysts. For symbols see Fig. 1.

In Fig. 2 the resulting QTOF values are plotted against Mo content. From this figure it can be seen that QTOF values gradually decrease starting at 4% Mo with increasing Mo content. The relatively low QTOF values at the very low Mo concentration samples may be related to interactions of the Mo phase with surface phosphate impurities present on the carbon surface (16). The results obtained for the DOC

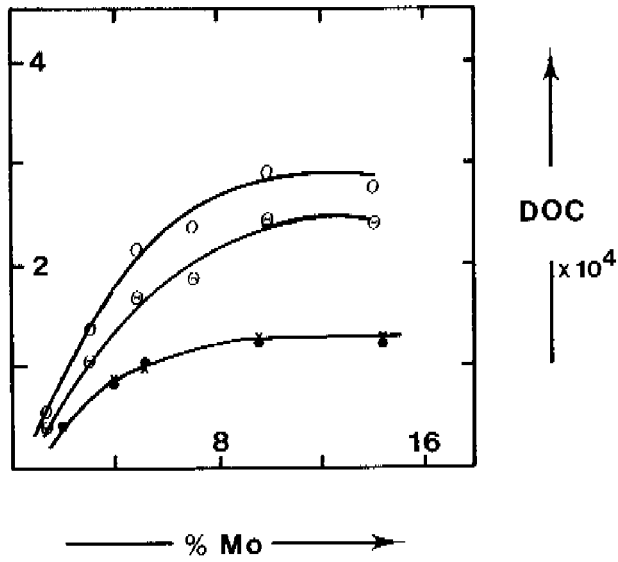

Fig. 3 Dynamic oxygen chemisorption values (DOC, mol O per g catalyst) versus wt% Mo for the Mo/C and Mo/Al_2O_3 catalysts. For symbols see Fig. 1.

measurements are presented in Figs. 3 and 4. The shapes of the curves of oxygen uptake as a function of Mo content (Fig. 3) are similar to the shapes of the activity versus Mo content curves shown in Fig. 1. Surprisingly, however, whereas k_{HDS} decreased with run time, the O_2 uptake did not.

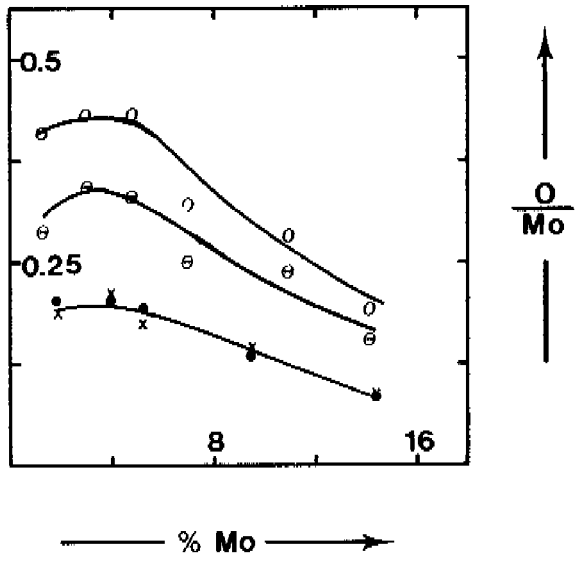

Fig. 4 Oxygen over Molybdenum ratios (O/Mo) versus wt% Mo for the Mo/C and Mo/Al_2O_3 catalysts. For symbols see Fig. 1.

On the contrary, $DOC_{t=0}$ values were even somewhat lower than $DOC_{t=2}$ values. In Fig. 4 O/Mo ratios are plotted versus Mo content. The curves obtained have essentially the same shape as the QTOF curves in Fig. 2 , viz., maximum or plateau around 4% Mo and steady decrease for higher Mo contents.

As shown in Fig. 5 a linear correlation going through the origin was found between DOC and HDS activity for the Mo/C catalysts, provided that the data were taken at the same run time. The slopes decrease with increasing run time as was to be expected from the observation that activity decreased with run time whereas DOC stayed more or less constant. These linear correlations demonstrate that the same kind of active site is present independent of the Mo content. TOF values calculated from the slopes of the curves where : 2.7 x 10^{-2} s^{-1} and 1.1 x 10^{-2} s^{-1} corresponding with the run times t=0 and t=2 respectively.

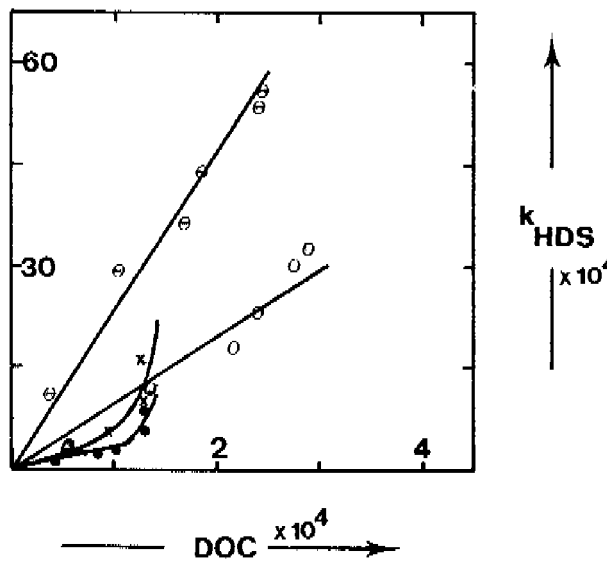

Fig. 5 k_{HDS} values versus DOC values for the Mo/C and Mo/Al_2O_3 catalysts. For symbols see Fig. 1.

XPS measurements.

The XPS results obtained for the Mo/C samples (3.0-14.1% Mo) are presented in Table 1. The Mo $3d_{5/2,3/2}$ photoelectron binding energies (BE) did not change significantly over the Mo concentration range studied and were in good agreement with those measured for the MoS_2 (Shuchardt, min 99%) reference compound. The BE of the S $_{2p3/2,1/2}$ photoelectrons was slightly higher than the one measured for the pure MoS_2. This effect is partly attributable to the presence of sulfur species with BE of 164.0 eV that are deposited on the carbon surface during sulfidation (8). From the Mo/C signal intensity ratios the dispersion of the carbon-supported active phase could be determined. For this purpose the model described by Kerkhof and Moulijn (17) was applied. Deviation of the experimentally determined Mo/C intensity ratio from the intensity ratio predicted under the assumption that the active phase forms a monolayer on the support, indicates the existence of crystallites. The average crystallite size can be calculated using the formula:

$$\frac{[I_{Mo}/I_C]_{exp}}{[I_{Mo}/I_C]_{mono}} = \lambda / c \; [\; 1 - \exp(-c/\lambda)]$$

with c = crystallite size in nm

λ = escape depth (nm) of the Mo electrons through the Mo sulfide phase (1.8nm)

In Fig. 6 are presented $(I_{Mo}/I_C)_e/(I_{Mo}/I_C)_m$ values versus Mo content. They show that, notwithstanding the high surface area of the carbon carrier, the active phase was not present as a monolayer. This implies that Mo sulfide particles were formed in all samples studied. In addition, crystallite size increased with increasing Mo content.

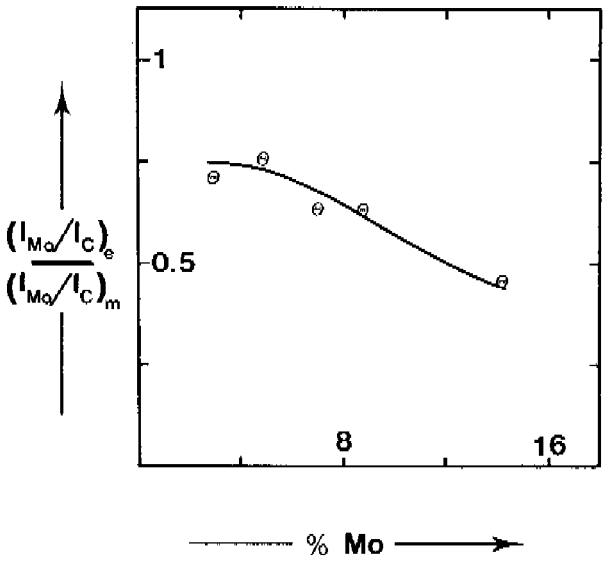

Fig. 6 Mo over C experimental XPS intensity ratio over the calculated ratio for monolayer coverage versus wt% Mo for the Mo/C catalysts after presulfidation (t=0).

TABLE 1. XPS RESULTS

%Mo	Binding energies (ev)			Intensity ratios		Mo sulfide particle size (nm)
	Mo 3d 5/2	Mo 3d 3/2	S 2p	$\frac{I_{Mo}}{I_C}$	$\frac{I_{Mo}}{I_C}$	
-	-	-	164.4	-	-	-
3.0	229.3	232.5	163.0	0.038	0.027	1.2
4.8	229.2	232.5	162.8	0.062	0.047	1.1
7.0	229.3	232.4	162.8	0.098	0.061	1.8
9.9	229.3	232.4	162.8	0.141	0.088	1.8
14.1	229.3	232.5	162.7	0.218	0.099	3.2
MoS_2	229.4	232.5	162.5	-	-	-

It is interesting to compare particle size data with DOC measurements. If DOC is sensitive to surface sites, a linear correlation between $(O/Mo)^{-1}$ values and crystallite size has to be expected. The result shown in Fig. 7 is a linear relation with the following parameters: $(O/Mo)^{-1} = 0.15c + 1.3$ (r=0.997). Moreover extrapolation to 100% dispersion (c=0, all Mo-atoms exposed at the surface) shows that about 4/5 of the Mo surface atoms (assuming that one O atom reacts with one Mo site) were detected by oxygen chemisorption. These results clearly indicate that the DOC technique can indeed be used for the detection of the active Mo sulfide surface area.

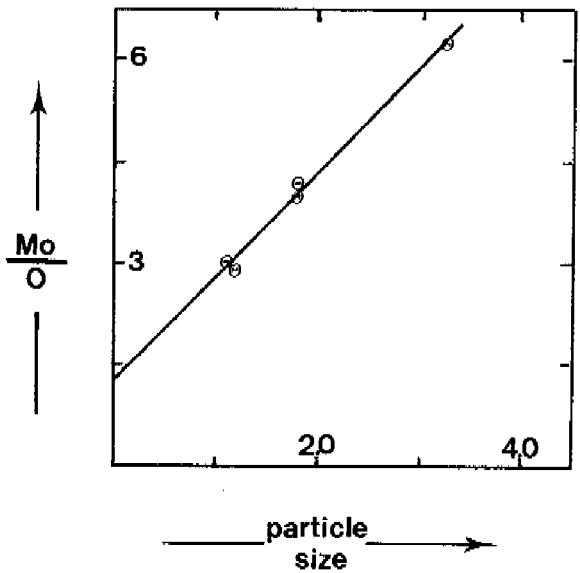

Fig. 7 Molybdenum over oxygen ratios versus calculated XPS particle size (nm) for the Mo/C catalysts after presulfidation.

Alumina-supported catalysts.

The k_{HDS} and QTOF values obtained for the Mo/Al_2O_3 samples are also presented in Figs. 1 and 2. Three major differences between Mo/Al_2O_3 and Mo/C catalysts are observed : (1) HDS activities measured for the Mo/Al_2O_3 catalysts were relatively low ; (2) a small activity threshold was found for the alumina-supported series ; (3) HDS activity of these catalysts increased almost linearly up to the highest Mo loading. It is plausible that these differences must be ascribed to the relatively strong interaction between Al_2O_3 and the active phase (8,18).

Figures 3 and 4 show the oxygen chemisorption results. The $DOC_{t=0}$ and $DOC_{t=2}$ values overlapped almost completely and reached a plateau around 10 wt% Mo. The latter observation was in contrast to the results of the activity measurements where a linear increase up to the highest Mo content was observed. On the other hand the small threshold observed in the k_{HDS} curve was also found in the DOC curves.

The correlation between DOC and activity data is presented in Fig. 5. In contrast to the Mo/C catalysts no linear correlations were found over the entire Mo concentration range studied in the case of the Mo/Al_2O_3 catalysts. Two concentration regions can be distinguished : (1) up to about 6 wt% Mo a linear relation appears to exist ; (2) at higher Mo contents k_{HDS} increased more rapidly than DOC. This clearly illustrates that the nature of the oxygen chemisorption sites present in Mo/Al_2O_3 catalysts depends on the Mo loading. In the low Mo concentration range the calculated TOF values are constant, but a factor of 2-4 lower than the corresponding Mo/C TOF values. At higher Mo contents the TOF values gradually increase until they become comparable with those of the Mo/C samples. This suggests that at very high Mo loadings the active sulfide phases supported on carbon or alumina are essentially the same.

TABLE 2. Activity and DOC results of Mo/C catalysts

%Mo	carrier	$k_{HDS} \times 10^4$ [m^3/kg.s]		QTOF $\times 10^4$ [mol/mol.s]		DOC $\times 10^4$ [molO/g]		O/Mo		TOF $\times 10^4$ [mol/site.s]	
		t=0	t=2	t=0	t=2	t=0	t=2	t=0	t=2	t=0	t=2
0	Al_2O_3	0	0			0	0				
2.07		2.06	1.11	10.7	5.79	0.39	0.42	0.18	0.2	59	30
4.07		3.49	2.22	9.25	5.88	0.91	0.83	0.21	0.2	43	30
5.3		6.28	3.51	12.7	7.10	0.95	1.06	0.17	0.19	74	37
9.6		10.4	6.02	11.7	6.76	1.35	1.31	0.14	0.13	84	52
14.4		16.5	9.31	12.3	6.97	1.26	1.20	0.08	0.08	150	87
0	CARBON	0	0			0	0				
1.3		10.3	3.34	86.8	28.1	0.39	0.55	0.29	0.41	300	70
3.0		28.8	12.0	104	43.4	1.06	1.35	0.34	0.43	300	100
4.8		36.8	18.9	82.8	42.5	1.63	2.14	0.33	0.43	250	100
7.0		44.5	23.8	68.3	36.5	1.83	2.37	0.25	0.32	270	110
9.9		56.2	32.6	61.3	35.6	2.46	2.91	0.24	0.28	260	130
14.1		54.1	30.4	41.3	23.2	2.40	2.76	0.16	0.19	260	120

DISCUSSION

Oxygen chemisorption on Mo sulfide catalysts.

Oxygen chemisorption has been shown to be an appropriate technique for the titration of active sites on sulfides since a proportionality between HDS activity and DOC has been established for sulfided Ni/Al_2O_3 catalysts (11) and for unsupported MoS_2 (12). Extensive results on a large variety of different sulfided systems led, however, to a controversy on the nature of the sites detected by the oxygen chemisorption technique (19-22). The data collected in this paper were an effort to obtain more information on this intriguing problem of detecting active surface sites. In this respect the use of a relatively inert support material such as carbon may enable one to study the surface properties of highly dispersed Mo sulfide unperturbed by interactions with the support.

Most characteristic for the carbon-supported catalyst systems was the existence of different linear correlations between DOC and HDS activity for the entire Mo concentration range studied when samples were compared after presulfidation or 2 h run time. It is obvious that a specific linear correlation exists for every run time. These proportionalities demonstrate that on a Mo sulfide surface the DOC technique indeed measures a parameter directly related to the HDS activity of the catalyst and furthermore that the structure of the active surface of the MoS_2 crystallites remained the same over the entire Mo concentration range and consequently over the entire crystallite range studied. However, the DOC technique proved insensitive to the initial deactivation of the catalyst. This clearly indicates that some other property of the catalyst surface, which does influence the HDS activity, is not measured by the DOC technique. The XPS and DOC data demonstrate that the oxygen uptake was proportional

to the dispersion of the sulfide phase. Moreover, providing that O_2 adsorbs dissociatively on Mo surface atoms it was found that almost all Mo surface atoms (actually about 4/5 of them) are detected by means of DOC. On the other hand, assuming that the O_2 molecule reacts dissociatively on a S vacancy and a neighbouring SH group, as proposed by Bachelier et al. (11), our measurements must be interpreted to indicate that 2/5 of the total Mo surface atoms have sulfur vacancies. But in all this one should of course keep in mind that O_2 chemisorption on sulfides may be corrosive to some extent, like on metal catalysts, and that real TOF values therefore will be somewhat larger than those calculated in the results section. Whatever the exact interaction between the oxygen molecule and the Mo sulfide phase we can conclude on the basis of our combined DOC - HDS activity - XPS measurements that DOC results are proportional to a fraction of the HDS active surface area of the Mo sulfide phase. In this respect our results on the carbon-supported systems confirm the results obtained by Tauster et al. (12) using unsupported MoS_2.

The abrupt changes around 6% Mo in the k_{HDS}-DOC relationship of the Mo/Al_2O_3 catalysts point to different types of Mo sites at low and high concentrations. In the low concentration range a linear proportionality still exists between DOC and k_{HDS}, provided that the catalysts experienced the same run time. The fraction of active surface area is about a factor of 2 lower in the Mo/Al_2O_3 catalysts, as judged from the lower DOC values for the t=0 and t=2 series. At high Mo loadings no proportionallity between DOC and k_{HDS} is found, indicating that the TOF of the sites is changing with Mo content, while the total amount of sites stays constant.

From the above results on the Mo/C and Mo/Al_2O_3 catalysts we conclude that the oxygen chemisorption method is able to determine the fraction of active surface of a Mo sulfide catalyst. However, DOC measures the total active surface

area and differences in TOF of active sites can only be discovered by a combination of DOC and HDS activity measurements. In this respect we can say that the search for a universal chemisorption technique for sulfide catalysts, which measures active sites under all conditions, is still on. Nevertheless the present DOC technique proves to be very useful in comparisons of catalysts.

Structure of the sulfide catalysts.

The results demonstrate that on sulfided Mo/C catalysts MoS_2-like particles are present. A large fraction (4/5 or 2/5 according to the model) of the surface Mo atoms are oxygen detectable sites. It is plausible that a certain morphology of Mo sulfide is favoured on the carbon support explaining this high site density. Assuming that the edge area is the active part of the Mo sulfide surface, we must conclude that small (3 dimensional) particles with the major fraction of the Mo atoms located in the edge planes, are formed. With increasing particle size the amount of surface to bulk Mo atoms decreases (decline in O/Mo ratio and XPS intensity ratio). Nevertheless the surface structure and thus the site density at the surface remains unaffected (linear correlation between Mo/O and particle size). Apparantly the surface structure of the MoS_2 crystallites is not influenced by interactions with the carbon support. The observation that no monolayer type catalysts are formed can also be related to the weak interaction of Mo with the carbon surface.

The results of the Mo/Al_2O_3 catalysts are in perfect agreement with the findings of Bachelier et al. (13) using the same Al_2O_3 support, saying that the surface state of the Mo phase varies according to the Mo content. In the low concentration range a linear proportionality DOC-HDS activity still exists, indicating that one type of Mo sulfide phase with one type of site is formed in this Mo

concentration range. The low site density (O/Mo = 0.2) and moderate TOF (0.6×10^{-2} s^{-1} for freshly sulfided samples) clearly demonstrate that this Mo sulfide phase differs from the small MoS_2 particles observed on the carbon support. It is evident that the strong interaction of the Al_2O_3 surface with the Mo phase plays an important role in this concentration range. Under the sulfidation conditions considered the major part of the Mo oxide monolayer remains intact and is converted to a Mo sulfide monolayer (23). This "single slab" structure in close interaction with the Al_2O_3 support may account for the low site density observed. The moderate TOF of this type of site must also be related to the active phase-support interactions probably leading to a different electronic configuration of the site. Above 6% Mo the proportionality between O_2 uptake and HDS activity is continuously changing with Mo content. This can be explained as follows : At higher Mo contents the Al_2O_3 support is loosing its grip on the Mo sulfide phase. As a result part of the Mo phase becomes relatively free of interactions with the support and formation of a sulfide phase (with sites having a high TOF) comparable with the carbon supported system will occur for this part of the Mo active phase. As we increase the Mo content this fraction increases, leading at the very high Mo concentration to a situation in which the average TOF of the sites tends to that of the Mo/C samples.

In any case we can conclude that in contrast to the Mo/Al_2O_3 catalysts the Mo sulfide phase supported on carbon has only one type of surface structure not influenced by interactions with the carbon support. The high HDS activity of this Mo phase must be attributed partly to a higher fraction of active surface area (site density) and partly to a higher TOF of the type of HDS active site.

Initial deactivation of Mo sulfide catalysts.

This discussion will be limited to the results obtained for the Mo/C catalysts, because in these systems there is no added complication caused by active phase-support interaction, although the same arguments can of course be used for the Mo/Al_2O_3 catalysts. The conditions to be fulfilled by an initial deactivation model, in order to be compatible with our results, are : (1) the number of sites detected by oxygen must essentially remain constant with run time ; (2) a proportionality between DOC and HDS activity must be maintained over the entire Mo concentration range at any given run time.

Various explanations for catalyst deactivation may be suggested : sintering of the active phase, pore blocking by coke formation, poisoning of active sites, coke formation on active sites, etc. Our results definitly rule out the possibilities of sintering and pore blocking, because in these cases the oxygen chemisorption should have been proportional to deactivation. On the other hand deposition of sulfur or coke species in the immediate vicinity of the Mo sites might obstruct access for the thiophene molecule or for spill over hydrogen, but not for the oxygen molecule. For instance in the adsorption mechanism proposed by Kwart et al. (24), the sulfur atom of thiophene is bonded to a S ligand next to the Mo site. Formation of polysulfur species may occur on this S ligand. As a result the neighbouring Mo site becomes catalytically inactive although it remains accessible to the oxygen molecule. A completely different explanation for the observed deactivation could be that after introduction of the feed stream (H_2 + thiophene) the freshly sulfided catalyst slowly reorganises its surface, because there is less H_2S in the gas phase then during sulfidation in H_2 + H_2S. In that respect it is important to note that the flushing procedure of the catalyst samples prior to oxygen chemisorption may alter the surface of the

Mo sulfide to an important extent.

Whatever the explanation of the catalyst deactivation, it is evident that two types of explanations are possible. On one hand deactivation may be due to a decrease in the number of active HDS sites, while oxygen is unable to distinguish between active and poisoned or blocked sites. In that case the TOF of the active site remains constant (e.g. 2.7×10^{-2} s^{-1}) and the apparent decrease of TOF from 2.7×10^{-2} s^{-1} (t=0) to 1.1×10^{-2} s^{-1} (t=2) must be interpreted as a decrease in the number of active sites by 60%. On the other hand the deactivation may be due to some perturbation of the active sites which causes a gradual decrease of their TOF. In that case the total number of active sites remains unaffected. Our present results do not allow us to distinguish between these possibilities, further research has to be performed.

CONCLUSIONS

We conclude that :

- The oxygen chemisorption technique on Mo sulfide catalysts is a surface sensitive technique, which measures a property proportional to the active surface area. However, changes in specific activity which occur with varying Mo content in Mo/Al_2O_3 catalysts or with varying run time, can only be detected by a combination of dynamic oxygen chemisorption and HDS activity.

- The surface structure of carbon-supported Mo sulfide is independent of the dispersion (and thus size) of the Mo sulfide crystallites. Alumina-supported Mo sulfide catalysts have a lower active site density than carbon supported catalysts and different sites are present at low and high Mo concentration.

- Initial deactivation of the Mo sulfide catalysts is not caused by sintering of the active phase or by pore blocking.

- The use of carbon as a support for sulfide catalysts enables one to study the fundamental properties of highly dispersed sulfide particles, unperturbed by interactions with the support.

REFERENCES

1. B.C. Gates, J.R. Katzer, and G.C.A. Schuit, "Chemistry of Catalytic Processes" p. 390, Mc-Graw-Hill, New York, 1979.
2. J.D. Voorhies, US Patent 4.082.652 (1978).
3. G.C. Stevens, and T. Edmonds, in "Preparation of Catalysts II" (B. Delmon, P. Grange, P. Jacobs, and G. Poncelet, Eds.), p. 507, Elsevier, Amsterdam, (1979).
4. D.G. Gavin, and M.A. Jones, U.K. Patent Application GB 20456478A (1979).
   European Patent Application EP 0.024.109 A1 (1980).
5. A.W. Scaroni, Ph.D. Thesis, The Pennsylvania State University (1981).
6. V.H.J. de Beer, J.C. Duchet, and R. Prins, J. Catal. 72 369 (1981).
7. A.J. Bridgewater, R. Burch, and P.C.H. Mitchell, Appl. Catal. 4, 267 (1982).
8. J.C. Duchet, E.M. van Oers, V.H.J. de Beer, and R. Prins, J. Catal. 80, 386 (1983).
9. J.P.R. Vissers, T.J. Lensing, F.P.M. Mercx, V.H.J. de Beer, and R. Prins, in "Hydrogen as an Energy Carrier" (G. Imarisio, and A.S. Strub, Eds.) p. 479, D. Reidel, Dordrecht (1983).
10. J. Bachelier, Ph.D. Thesis, University of Caen (1982).
11. J. Bachelier, J.C. Duchet, and D. Cornet, J. Phys. Chem. 84, 1925 (1980).

12. S.J. Tauster, T.A. Pecoraro, and R.R. Chianelli, J. Catal. 63, 515 (1980).
13. J. Bachelier, M.J. Tilliette, J.C. Duchet, and D. Cornet, J. Catal. 76, 300,(1982).
14. B.G. Silbernagel, T.A. Pecoraro, and R.R. Chianelli, J. Catal. 78, 380 (1982).
15. A.J.A. Konings, A.M. van Doorn, D.C. Koningsberger, V.H.J. de Beer, A.L. Farragher, and G.C.A. Schuit, J. Catal. 54, 1 (1978).
16. J.P.R. Vissers, V.H.J. de Beer, and R. Prins, J. Catal. to be published, chapter 7 of this thesis.
17. F.P.J.M. Kerkhof, and J.A. Moulijn, J. Phys. Chem. 83, 1612 (1979).
18. R. Thomas, E.M. Van Oers, V.H.J. de Beer, J. Medema, and J.A. Moulijn,J. Catal. 76, 241 (1982).
19. K.S. Chung, and F.E. Massoth, J. Catal. 64, 332 (1980).
20. W. Zmierczak, G. Muralidhar, and F.E. Massoth, J. Catal 77, 432 (1982).
21. T.A. Bodrero, C.H. Bartolomew, and K.C. Pratt, J. Catal. 78, 253 (1982).
22. R. Burch, and R. Collins, in "Proceedings of the Climax Fourth International Conference on the Chemistry and Uses of Molybdenum" (H.F. Barry, and P.C.H. Mitchell, Eds.) Climax Molybdenum Company, Ann Arbor, Michigan, p. 397 (1982).
23. J. Grimblot, P. Dufresne, L. Gengembre, and J.P. Bonnelle, Bull. Soc. Chim. Belg. 90, 1261 (1981).
24. H. Kwart, G.C.A. Schuit, and B.C. Gates, J. Catal. 61, 128 (1980).

CHAPTER 3

EFFECT OF THE SUPPORT ON THE STRUCTURE OF Mo-BASED HYDRODESULFURIZATION CATALYSTS : ACTIVATED CARBON VERSUS ALUMINA.

ABSTRACT

The structure of oxidic and sulfided Mo catalysts supported on activated carbon was studied by means of XPS, temperature programmed sulfiding (TPS) and sulfur analysis measurements. In the oxidic state the Mo-phase was highly dispersed as isolated or polymerized monolayer species at Mo loadings below 3 wt% and as very tiny three dimensional particles at higher loadings. Upon sulfiding particle growth took place, although the sulfide particles remained below 3.2 nm even in the sample with the highest Mo loading (14.1 wt%). In the sulfided catalysts only Mo(IV) was detected by XPS, and S/Mo stoichiometries were close to 2 demonstrating that MoS_2 was the major phase present after sulfidation. TPS patterns showed that sulfiding proceeded via a mechanism of O-S substitution reactions and was complete at temperatures below 570 K. The higher catalytic activity for Mo/C compared to Mo/Al_2O_3 is explained by differences in the structure of the sulfide phases present, and in the interaction between these phases and the respective supports.

INTRODUCTION

Previous laboratory studies (1-9) have shown that the application of carbon as a support for sulfide hydrotreating catalysts results in improved catalyst activity compared to the commercial alumina-supported systems. In a recent

publication (4) an attempt was made by means of combined dynamic oxygen chemisorption, X-ray photoelectron spectroscopy and thiophene HDS activity measurements, to explain the observed activity differences between activated carbon-supported (Mo/C) and alumina-supported (Mo/Al_2O_3) Mo catalysts. The salient conclusion was that the observed superior activity of the Mo/C catalysts, especially at low Mo loadings, should be attributed to the presence at the carbon surface of a Mo sulfide phase which has both a higher fraction of catalytically active surface area and a higher HDS activity per active site compared to the Mo sulfide phase present on the Al_2O_3 support surface. This strongly suggests that at low Mo loadings the Mo sulfide phases present on carbon and alumina supports are not identical. Furthermore it was demonstrated that at high Mo loadings the properties of the Mo sulfide phase present on alumina tended towards those of the Mo/C system, emphasizing that at very high Mo loadings the carbon- and alumina-supported sulfide phases are essentially the same.

In the present study it was attempted to gain more insight into this matter by studying the sulfidation process of Mo/C catalysts by means of XPS, temperature programmed sulfidation (TPS) and sulfur analysis and comparing the results with those reported in the literature for Mo/Al_2O_3 catalysts.

EXPERIMENTAL

A Norit activated carbon (RX3-extra; BET surface area 1190 m^2/g, and pore volume 1.0 ml/g) was used as support. Catalysts with Mo loadings ranging from 1.3-14.1 wt% Mo were prepared by pore volume impregnation of the carrier with aqueous solutions of ammonium heptamolybdate (Merck, min 99.9%). All impregnated samples were dried in air starting at 293 K and gradually increasing up to 383 K where they were kept overnight. Catalyst compositions were checked by means

of atomic absorption spectrometry. Catalysts will be denoted as Mo(x)/C or Al_2O_3 with x=wt% Mo.

XPS spectra of the oxidic samples were recorded on a Physical Electronics 550 XPS/AES spectrometer equipped with a magnesium X-ray source (E=1253.6 eV) and a double pass cylindrical mirror analyzer. The powdered samples were pressed on a stainless steel mesh which was mounted on top of the specimen holder. Spectra were recorded in steps of 0.05 eV. The pressure did not exceed 5 x 10^{-8} torr and the temperature was approximately 293 K. Spectra of the sulfided samples were recorded on an AEI ES 200 spectrometer equipped with a dry purified N_2 flushed glove box attached to the XPS introduction chamber. The catalyst samples were sulfided in a H_2S/H_2 flow (10 mol% H_2S, total flow rate 60 ml/min) using the following temperature program : linear increase (6 K/min) from room temperature up to 673 K and holding at this temperature for two additional hours. After sulfidation the catalyst samples were purged with purified He for 15 min at 673 K and subsequently cooled within 30 min to room temperature in flowing He. A special reactor (10) allowed transfer of the sulfided samples to the XPS apparatus, without exposure to air. The samples were mounted on the specimen holder by means of double-sided adhesive tape. Spectra were recorded at 283 K in steps of 0.1 eV. The C 1s peak (284.6 eV) was used as internal standard for binding energy calibration.

Temperature programmed sulfiding of the Mo (9.9)/C catalyst was carried out as described elsewhere (11). A 60 mg catalyst sample was sulfided using a mixture of 3.3% H_2S - 28.1% H_2 - 68.6% Ar at atmospheric pressure (flowrate = 11 x 10^{-6} mol/s). Product analysis during sulfiding was obtained with a mass spectrometer which registered almost continuously the peak intensities of H_2S, H_2O, Ar, CH_4 and CO. The latter ones were recorded to check whether gasification of the carbon carrier would occur. The H_2 concentration was measured using a thermal conductivity detector. The

sulfidation was carried out as follows : the catalyst was subjected to the sulfiding mixture for 0.5 h at room temperature, thereafter, the temperature was increased from room temperature up to 1270 K with a heating rate of 10 K/min, followed by an isothermal stage at 1270 K (30 min).

Total sulfur content of some sulfided catalysts (sulfided and flushed according to the procedure described for the XPS measurements) was determined by combustion of the in situ sulfided catalysts in an O_2 flow (150 ml/min) at temperatures starting from 673 K and rapidly (30 min) increasing up to 1420 K. The emerging SO_2 and SO_3 were trapped in two vessels containing an ice-cooled aqueous solution of H_2O_2 (1%). From the amount of a 0.1 M $Na_2B_4O_7.10H_2O$ solution needed to neutralize the sulfuric acid, the total sulfur content was calculated.

RESULTS

In Table 1 the XPS data are collected for both the oxidic and sulfided Mo/C catalysts. The Mo $3d_{3/2}$ and $3d_{5/2}$ binding energies remained constant over the whole Mo loading range considered (232.5 and 235.7 eV for the oxidic catalysts and 229.3 and 232.5 for the sulfided catalysts) and correspond closely to the values reported for MoO_3 and MoS_2 model compounds (12). In Fig. 1 typical XPS spectra are shown. Clearly, in the oxidic state only Mo(VI) is observed. Computer curve fitting of the Mo 3d signal for the sulfided samples is shown, indicating the presence of only one type of Mo phase with parameters identical to MoS_2. The Mo-over-C photoelectron intensity ratios were used to measure the degree of dispersion of the Mo phase on the support. Theoretical intensity ratio's were calculated according to the catalyst model described by Kerkhof and Moulijn (13), assuming that the Mo phase is exclusively present as isolated or polymerized monolayer species. It is worth mentioning

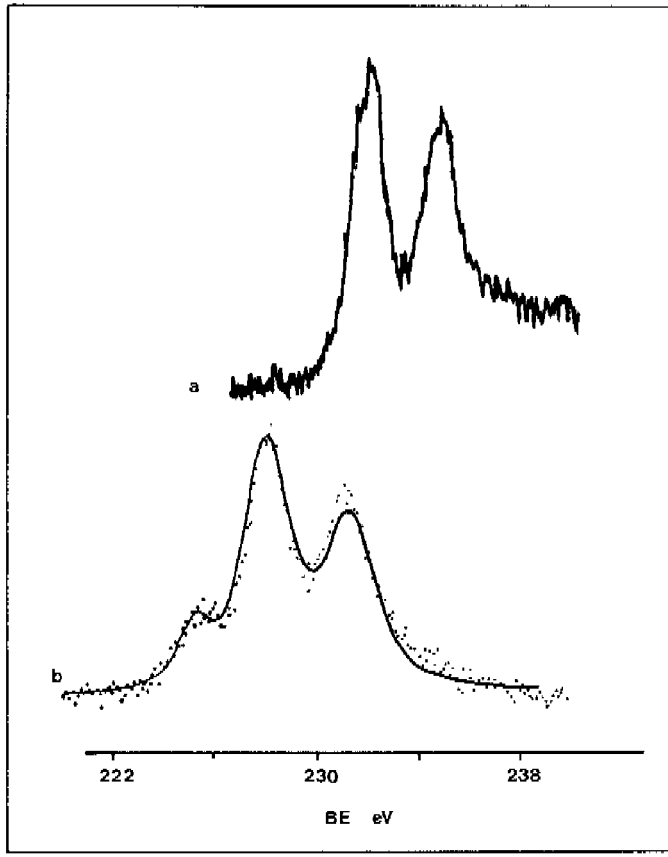

Fig. 1 Typical Mo $3d_{5/2,3/2}$ XPS photoelectron signals of activated carbon supported molybdenum catalysts in the oxidic state (a) and in the sulfided state (b).

Table 1 : XPS and chemical sulfur analysis results of Mo/C catalysts

catalyst composition	Oxidic state		Sulfide state (a)			
		Mo particle size		Mo particle size		chemical sulfur analysis
wt% Mo	$\frac{I_{Mo}}{I_C}$	(nm)	$\frac{I_{Mo}}{I_C}$	(nm)	$\frac{S}{Mo}$	$\frac{S}{Mo}$
1.3% Mo	0.014	-	-	-	-	-
3.0% Mo	0.040	-	0.027	1.2	1.69	1.68
4.8% Mo	0.052	<1.0	0.047	1.1	1.71	1.76
7.0% Mo	0.073	<1.0	0.061	1.8	1.90	-
9.9% Mo	0.117	<1.0	0.088	1.8	1.95	-
14.1% Mo	0.147	1.4	0.099	3.2	1.99	-

(a) XPS data according to (4).

that the average pore wall thickness of the support (0.89 nm) is considerably smaller than the escape depth of the C 1s and Mo 3d photoelectrons through carbon material (1.35 and 1.4 nm respectively (14)). In this respect XPS can be considered as a bulk technique, able to detect signals of underlying support layers (or pores). In Fig. 2 the experimentally determined XPS intensity ratios are plotted against catalyst composition for both oxidic and sulfided samples together with the theoretical ratio predicted for the monolayer type active phase dispersion.

In the oxidic state the Mo phase appears to be monolayer-like dispersed up to approximately 3 wt% Mo. The observed deviation from linearity above about 3 wt% Mo points to the formation of small three-dimensional particles. Calculations according to the model of Kerkhof and Moulijn (13) show that the average thickness of these particles is smaller than 1.0 nm for the 4.8-, 7.0-, and 9.9 wt% Mo samples and equal to 1.4 nm for the 14.1 wt% Mo sample, demonstrating that the Mo dispersion is high in all samples.

Clearly, during the sulfidation procedure applied, some particle growth takes place as can be concluded from the

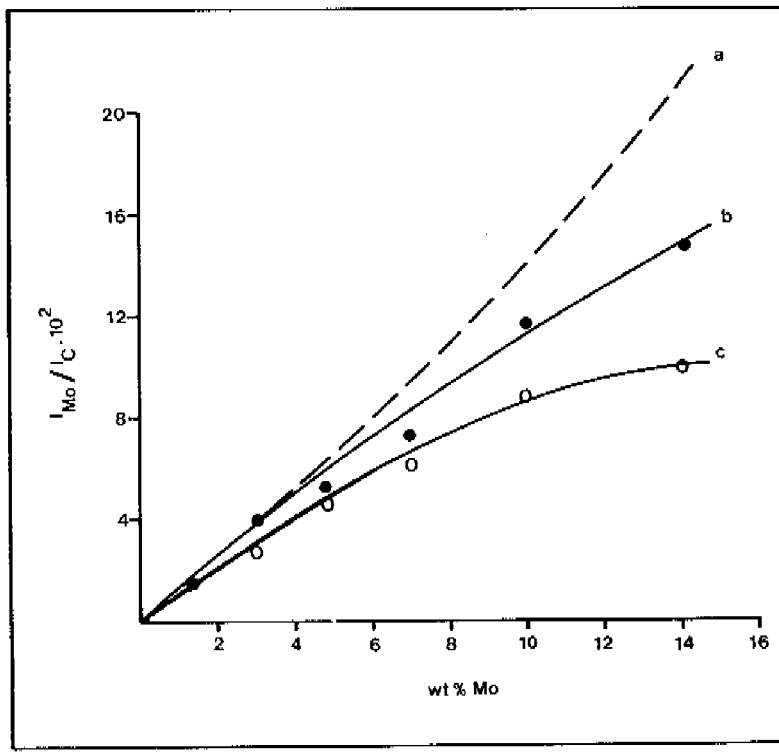

Fig. 2 Experimentally determined Mo-to-C XPS intensity ratios versus wt% Mo of Mo/C catalysts for :
(a) monolayer-like catalysts
(b) oxidic catalysts
(c) sulfided catalysts

lower XPS intensity ratios of the sulfided samples compared to the oxidic samples. As can be seen from Table 1, particle sizes increase up to 3.2 nm with increasing Mo loading. The sulfur over Mo stoichiometries calculated (14) from the relative XPS intensity ratios, were found to be high, especially at the low Mo loadings. However, as shown in Table 1, after subtraction of the amount of elemental sulfur (I_S/I_C = 0.003) observed after sulfidation of the carbon support itself, the S/Mo ratios are slightly below 2 (3.0, 4.8 wt% Mo) or nearly equal to 2 (7.0, 9.9, 14.1 wt% Mo). Evidently, for the low Mo loadings, these S/Mo ratios are subjected to a rather large uncertainty due to the low signal intensities and the relatively large correction for the amount of elemental sulfur. Also included in Table 1 are the S/Mo stoichiometries calculated from the chemical sulfur analysis. Again the amount of sulfur retained on the pure carbon support (0.6 wt% S) as determined in a separate experiment was subtracted. The S/Mo ratios so obtained are close to the ones measured by means of XPS.

In Fig. 3, the TPS patterns recorded for the Mo (9.9)/C sample and the pure carbon support sample, are given. At room temperature the carbon support adsorbs 0.38×10^{-3} mol H_2S per g carbon (1.2 wt% S), half of which is desorbed immediately after the temperature is increased. Thus about 0.6 wt% S (0.19×10^{-3} mol H_2S per g carbon) is retained on the carbon support, which is in perfect agreement with the chemical sulfur analysis results. In the case of the Mo (9.9)/C catalyst, sulfidation starts already at room temperature. During the isothermal stage 2.28 mol H_2S are consumed per mol Mo, although clearly part of the H_2S consumed is just adsorbed on the support. During the temperature increase three processes can be discerned, viz.:

- H_2S desorption (0.04 mol H_2S/mol Mo) from the carrier at low temperatures,
- Further sulfidation of the catalyst in the temperature region from room temperature up to approximately 570 K as was

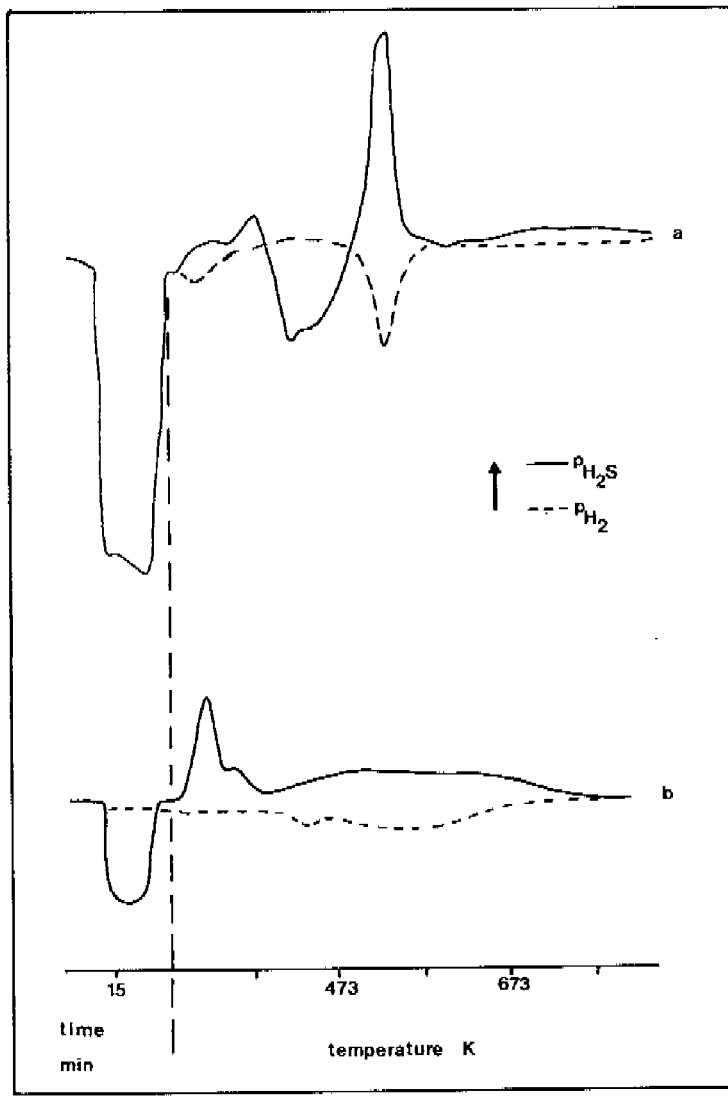

Fig. 3 TPS patterns of a 9.9 wt% Mo/C sample (a) and the pure activated carbon (Norit RX3 extra) (b).

noticed from the H_2O production and H_2S consumption (0.60 mol H_2S/mol Mo),

- H_2S production (0.72 mol H_2S/mol Mo) at approximately 530 K coupled with a H_2 consumption (1.03 mol H_2/mol Mo).

The final H_2S balance thus reached is 2.12 mol H_2S/mol Mo. If one subtracts the amount of H_2S still adsorbed by the pure support at high temperatures (0.19×10^{-3} mol H_2S/g carbon), a H_2S/Mo ratio of 2.0 is obtained. This agrees very well with the XPS results. It is noted that sulfidation is complete at approximately 570 K, since no variation in H_2S, H_2 or H_2O is observed at higher temperatures. Interestingly, up to the highest temperature recorded, no gasification to CH_4 or CO of the carbon support was observed, demonstrating that MoS_2 is not a catalyst for gasification of the activated carbon support.

DISCUSSION

The XPS data show that in the oxidic Mo/C catalysts the Mo phase is very highly dispersed, either in the form of isolated molybdate ions or two-dimensional polymolybdate patches (up to 3 wt% Mo) or as small three-dimensional particles (above 3 wt% Mo). From these results it appears that the carbon surface has approximately 0.17 relatively strong adsorption sites per nm^2 surface area, (corresponding to 3 wt% Mo) able to chemisorb the Mo ions present in the impregnation solution . This result was confirmed by an experiment in which the amount of Mo chemisorbed on the support surface was measured by passing an aqueous solution containing 1 wt% ammoniumheptamolybdate over a bed of the carbon support particles for a sufficiently long period. It appeared that in this way 2.8 wt% Mo could be chemisorbed on the carbon surface, in close agreement with the value mentioned above. The finding that the pH of the effluent solution increased during chemisorption from 5 (pH of the

ammoniumheptamolybdate solution) to 7, indicates that adsorption of the molybdate species occurs due to the electrostatic attraction between the positively charged carbon surface and the molybdate anions. This type of interaction is consistent with the work of D'Aniello (15) and Wang (16), from which it was concluded that the adsorption is dictated by the extent of surface charging. This adsorption-interaction process and the part which oxygen functional groups play in it, is discussed in more detail elsewhere (17). At support surface loadings higher than 0.17 Mo at/nm^2 (>3 wt% Mo) small three-dimensional particles are formed, indicating that with the presently applied solution pH the chemisorption sites on the carbon surface are saturated.

During sulfiding some sintering of the active phase takes place, even at the low Mo loadings where small three-dimensional sulfide particles are formed. Clearly, this observation points to a certain mobility of the Mo phase during sulfiding, indicating that no strong interactions between the active phase and the support (as encountered for the alumina-supported systems) are present, not even at low Mo surface loadings. Nonetheless the carbon surface stabilizes the small sulfide particles sufficiently since no bulky sulfide particles are observed. Probably, most of the sintering will take place during the actual sulfiding (O for S substitution) of the catalyst, since then at least part of the bridging oxygen atoms between support and active phase are replaced by sulfur atoms. The sulfidation process of Mo/C catalysts can be described in analogy with the sulfidation Mo/Al_2O_3 catalysts (11). Low-temperature sulfiding occurs through simple O-S substitution reactions on the Mo(VI) ion. No overall H_2 consumption is observed since the net reaction is $Mo(VI) - O^{2-} + H_2S \rightarrow Mo(VI) - S^{2-} + H_2O$. Reduction of Mo(VI) to Mo(IV) takes place through rupture of Mo(VI) sulfur bonds under formation of elemental sulfur. Again no H_2 is consumed. The elemental sulfur produced

adsorbs on the support surface and is reduced with H_2 to H_2S at 530 K resulting in the sharp H_2S production and H_2 consumption peaks in the TPS patterns. The quantitative TPS results are in good accordance with this model for the sulfidation. The amount of H_2S produced around 530 K may seem somewhat low (0.72 H_2S versus 1.03 H_2), but it should be realized that the recorded change in H_2S concentration may be the sum of a negative (consumption) and a positive (production) contribution. And in the range 400-570 K a negative and a positive H_2S contribution clearly overlap (cf. Fig. 3). As found by means of XPS and total sulfur analysis measurements, the S/Mo ratio of the final sulfided state of the Mo phase is very close to MoS_2.

It is interesting to compare our findings of the Mo/C catalysts with those reported for the Mo/Al_2O_3 system. There is consensus of opinion that in the oxidic precursor state up to high surface loadings, Mo is deposited on the alumina surface as a monolayer of (poly)molybdate ions (16). This is in contrast to the Mo/C carbon system where above 0.17 Mo at/nm^2 already small three-dimensional particles are present. The structure of sulfided Mo/Al_2O_3 catalysts has been much debated. Recently, however, EXAFS (18), IR (19), XPS (20), Raman (21) and TPS (11) measurements produced evidence that the Mo phase is present as a MoS_2-like "two-dimensional" single slab structure. The present study shows that small three-dimensional MoS_2 particles are present in the sulfided Mo/C catalyst systems. Furthermore, Arnoldy et al. (11) showed that for a series of Mo/Al_2O_3 catalysts two sulfiding regions could be discerned, viz. a low temperature sulfiding region similar to that in the Mo/C system and a high temperature sulfiding region (above 550 K up to more than 1000 K) which is completely missing in the Mo/C TPS patterns. In addition, it was shown that the high temperature sulfiding was more important at low Mo loadings, whereas with increasing Mo loading the low temperature sulfiding gained in importance. These observations were explained in terms of

heterogeneity of the interaction between the Mo(VI) ions in an oxidic surrounding with the Al_2O_3 support. Increased interaction with the support (low Mo loadings) increases the sulfidation temperature. Clearly, these strong interactions of the active phase with the support are not present in the carbon-supported catalysts of this study, thus unhampered formation of MoS_2 particles takes place at low temperatures. It becomes clear from these results that different Mo-sulfide structures are formed on alumina and carbon supports due to differences in interaction between the MoS_2 phase and the support surfaces, viz. a single slab monolayer strongly interacting with the support on alumina, and small three-dimensional particles essentially free of interaction with the support on carbon.

The question remains how to explain the difference in HDS activity observed for these two Mo sulfide phases (4) on the basis of their different configurations. Or stated otherwise, since carbon-supported catalysts -due to the inert character of the carbon carrier- exhibit identical catalytic features as unsupported sulfides (22), how can one understand that the interaction with the alumina support lowers the HDS activity of deposited Mo-sulfide? Unfortunately, detailed information on the nature of the interaction between MoS_2 and alumina is difficult to derive and as a consequence still lacking. Although it is generally accepted that Mo-O-Al bridging structures exist and are responsible for the strong interaction in sulfided Mo/Al_2O_3 catalysts, the relative abundance of these species in sulfided Mo/Al_2O_3 remains much debated. Massoth (23) concluded that each Mo atom was bonded with an oxygen of the Al_2O_3 substrate. Schrader and Cheng (21) obtained consistent results with the Massoth model by means of in situ Raman spectroscopy measurements. Arnoldy et al. (11), on the basis of TPS experiments on Mo/Al_2O_3 catalysts pointed to the possibility of Mo-O-Al bridges to the MoS_2 phase, albeit that the Mo-O interaction was not given the credit of a full bond.

EXAFS results (18) on the other hand demonstrated that the interactions between the MoS_2 phase and the alumina support take place via Mo-S-Al bridges, with only a small amount of Mo-O-Al bridges (less than 10% of all Mo atoms). Finally Candia et al. (24) suggested that preferentially the Mo edge atoms are bonded to the alumina support by oxygen-metal linkages, due to the more reactive nature of the Mo edge plane compared to basal plane atoms.

The net effect of the strong interaction with the alumina will be a nearly optimal dispersion of the Mo-sulfide phase, but also a charging of the Mo atom through the Mo-O-Al linkages. This will most probably lead to a polarization of the metal-sulfur bond increasing its bond strength. Now, it has been shown that changes in metal sulfur bonds largely influence the catalytic activity. Pecoraro and Chianelli (25) have derived that in order to achieve highly active HDS catalysts the metal-sulfur bond strength should be intermediate, allowing both S vacancy formation as well as metal-sulfur bond formation through adsorption of the S-containing molecule on an exposed metal atom. In this respect, the Mo-sulfur bond strength of pure MoS_2 appeared to be higher than the required optimal range. Based on theoretical considerations Harris and Chianelli (26) suggested that more active catalysts should have a high degree of metal-sulfur covalent bond strength. And finally, using carbon-supported transition metal catalysts it has been shown (22) that the lower the charge on the metal atom of the sulfide, the higher the HDS activity was. It may be clear from the above results that the strong interactions with alumina will have a negative effect on the HDS activity of the deposited Mo sulfide. Due to the absence of such strong support interactions when using carbon as a support material, higher HDS activities are obtained for Mo/C catalysts compared to Mo/Al_2O_3 systems. Based on the foregoing findings it may be argued that it is possible to increase the HDS activity of alumina-supported catalysts by

eliminating or reducing the strong support interactions. This may be accomplished by increasing the sulfiding temperature such that the Mo-O-Al bonds responsible for the interaction are sulfided and/or broken. This has been studied by Candia et al. (24) for Co promoted Mo/Al_2O_3 catalysts. They observed that a Co-Mo-S phase (refered to as type I) interacting with the alumina support was present after relatively low sulfiding temperatures and that this type I phase could be transformed by increasing the sulfiding temperature in a type II Co-Mo-S phase which is essentially free of interactions with the alumina, and has a much higher HDS activity.

REFERENCES

1. de Beer, V.H.J., Duchet, J.C., and Prins, R., J. Catal. 72, 369 (1981).
2. Duchet, J.C., van Oers, E.M., de Beer, V.H.J., and Prins, R., J. Catal. 80, 386 (1983).
3. Vissers, J.P.R., Lensing, T.J., Mercx, F.P.M., de Beer, V.H.J., and Prins, R., in "Hydrogen as an Energy Carrier" (G. Imarisio, and A.S. Strub, Eds.) p. 479, D.Reidel, Dordrecht, 1983.
4. Vissers, J.P.R., Bachelier, J., ten Doeschate, H.J.M., Duchet, J.C., de Beer, V.H.J., and Prins, R., in "8th Int. Congr. Catalysis", Berlin 1984, Verlag Chemie : Weinheim, p. II-387, 1984.
5. Voorhies, J.D., US patent 4.082.652 (1978).
6. Stevens, G.C., and Edmonds, T., in "Preparation of Catalysts II", (B. Delmon, P. Grange, P. Jacobs, and G. Poncelet, Eds.) p. 507, Elsevier, Amsterdam, 1979.
7. Gavin, D.G., and Jones, M.A., UK Patent Application GB 20456478A (1979). European Patent Application EP 0.024.109 A1 (1980).
8. Bridgewater, A.J., Burch, R., Mitchell, P.C.H., Appl.

Catal. 80, 386 (1983).
9. Topsøe, H., Bull. Soc. Chim. Belg., 93, 783 (1984).
10. Konings, A.J.A., van Doorn, A.M., Koningsberger, D.C., de Beer, V.H.J., Farragher, A.L., and Schuit, G.C.A., J. Catal. 54, 1 (1978).
11. Arnoldy, P., van den Heijkant, J.A.M., de Bok, G.D., and Moulijn, J.A., J. Catal., accepted for publication.
12. Mullenberg, G.E., (Ed.), "Handbook of X-ray photoelectron spectroscopy", Perkin-Elmer Press, 1978.
13. Kerkhof, F.P.J.M., and Moulijn, J.A., J. of Phys. Chem., 83, 1612 (1979).
14. Penn, D.R., J. Electron Spectrosc., 9, 29 (1976).
15. D'Aniello Jr, M.J., J. Catal. 69, 9 (1981).
16. Wang, L., and Hall, K.W., J. Catal. 77, 232 (1982).
17. Vissers, J.P.R., Bouwens, S.M.A.M., de Beer, V.H.J., and Prins, R., to be published, chapter 6 of this thesis.
18. Clausen, B.S., Topsøe, H., Candia, R., Villadsen, J., Lengeler, B., Als-Nielsen, J., and Christensen, F., J. Phys. Chem., 85, 3868 (1981).
19. Topsøe, N.Y., J. Catal. 64, 235 (1980).
20. Grimblot, J., Dufresne, P., Gengembre, L., and Bonnelle, J.P., Bull. Soc. Chim. Belg., 90, 1261 (1981).
21. Schrader, G.L., and Cheng, C.P., J. Catal. 80, 369 (1983).
22. Vissers, J.P.R., Groot, C.K., van Oers, E.M., de Beer, V.H.J., and Prins, R., Bull. Soc. Chim. Belg., 93, 813 (1984) chapter 5 of this thesis.
23. Massoth, F.E., J. Catal, 36, 164 (1975).
24. Candia, R., Sorensen, O., Villadsen, J., Topsøe, N.-Y., Clausen, B.S., and Topsøe, H., Bull. Soc. Chim. Belg., 93, 763 (1984).
25. Pecoraro, T.A., and Chianelli, R.R., J. Catal. 67, 430 (1981).
26. Harris, S., and Chianelli, R.R., J. Catal. 86, 400 (1984).

CHAPTER 4

CARBON-SUPPORTED COBALT SULFIDE CATALYSTS : STRUCTURAL ASPECTS AND THE ROLE OF CO IN SULFIDED Co-Mo CATALYSTS.

ABSTRACT

The thiophene hydrodesulfurization activities of cobalt sulfide catalysts supported on activated carbon were measured in a flow microreactor operating at atmospheric pressure. The cobalt content was varied between 1.3 and 13.3 wt% Co and the oxidic precursor catalysts were dried according to three different procedures. Structural characteristics and degree of Co phase dispersion in both the oxidic precursor and the sulfided state of the catalysts were obtained by means of X-ray photoelectron spectroscopy (XPS). Catalyst sulfiding was studied via temperature programmed sulfidation (TPS).

The oxidic cobalt phase present in the precursor catalysts was found to be inhomogeneuously dispersed over the carbon carrier surface. Dispersion decreased significantly with increasing catalyst drying temperature and during catalyst sulfidation. Under the TPS conditions applied, complete sulfidation of the oxidic precursor catalysts was achieved at temperatures below 570 K. XPS results pointed to the presence of a Co_9S_8-like species in the sulfided catalysts. However, sulfur was found to be in excess of the amount necessary to produce stoichiometric Co_9S_8.

The catalysts demonstrated very high hydrodesulfurization activities which were by far superior to those of corresponding carbon- or alumina-supported molybdenum catalysts. Comparison of the activity of carbon-supported Co-Mo with that of optimally dispersed cobalt sulfide on

carbon, demonstrates that the so-called promotor effect in sulfided Co-Mo catalysts is primarily caused by the exceptionally high catalytic activity of cobalt sites and shows that the role of MoS_2 in these catalysts is mainly to function as a support for optimally dispersed cobalt ions.

INTRODUCTION

The increasing need for efficient removal of sulfur, nitrogen and metal contaminants from various petroleum and coal feedstocks has been a continuous drive for the development of the so-called hydrotreating catalysts. Industrially, these catalysts consist of molybdenum or tungsten sulfide promoted by cobalt or nickel, supported on a high surface area alumina. Numerous efforts aiming to clarify the structure and related HDS activity of these complicated catalyst systems, resulted in different structural models, in which especially the role and the chemical state of the Co or Ni promotor ions in the sulfided catalysts remained much debated. Evidence was found by different authors for the presence of Co metal (1,2), $CoMo_2S_4$ (3), $CoAl_2O_4$ (4), Co_9S_8 (5), Co edge intercalated in between the MoS_2 layers (6,7), and a Co-Mo-S phase with Co ocupying edge positions in the MoS_2-like structures (8).

Different explanations have been suggested in the literature to describe the observed catalytic synergy in Co-Mo catalysts in terms of the variety of chemical structures proposed for the promotor ions. It was thought that the promotor ions would stabilize the Mo oxo-sulfo monolayer as proposed by Schuit et al. (4). In the model described by Voorhoeve (6) and by Farragher and Cossee (7) it was assumed that the pseudo-intercalated promotor ions in between successive layers of MoS_2 or WS_2 brought about a reorganization of the WS_2 or MoS_2 surface resulting in an increase of active sites for hydrogenation and HDS reactions. Yet in another model proposed by Delmon and

coworkers Co_9S_8 and MoS_2 exist in close interaction with each other. In this "remote control model" H_2 is dissociatively adsorbed on Co sulfide and subsequently transferred to the MoS_2 surface where it reacts with adsorbed S-containing molecules (9,10). However, Topsøe and coworkers clearly demonstrated that the HDS activity was closely related with the presence of a distinct Co-Mo-S phase, containing Co atoms at the edges of MoS_2 like structures. Although the nature of the active sites present in this Co-Mo-S was observed to be different from that in unpromoted MoS_2 (11,12), it has not been established whether the Co atoms are the active sites or whether the neighboring Mo atoms also play a direct role in the HDS reaction (13).

All the theories mentioned above assume no appreciable HDS activity for the promotor sulfide phase itself. Recently, the correctness of this presupposition was, however, questioned by de Beer c.s. (14,15) on the basis of high thiophene hydrodesulfurization activities measured for carbon-supported Co and Ni sulfide catalysts. They concluded that the possibility of Co or Ni sulfide acting as catalysts instead of promotors for the MoS_2 phase deserves more attention. Therefore the present study attempts to further elucidate some aspects concerning the preparation, structure and related HDS activity of carbon-supported Co catalysts. Comparison with results obtained for Co-Mo promoted catalysts provides further insight into the nature of the active sites for hydrodesulfurization in these promoted catalysts. Structural information on the catalyst system was derived from X-ray photoelectron spectroscopy (XPS) and temperature programmed sulfidation (TPS).

EXPERIMENTAL

Catalyst preparation

The carrier used was a Norit activated carbon (RX 3 extra) with a surface area of 1190 m^2/g and pore volume of 1.0 ml/g. This support was washed by the manufacturer with HCl in order to reduce the impurity content (e.g. wt% Fe = 0.011, wt% PO_4^{3-} = 0.026). It was used as received. A series of Co catalysts (1.3 - 13.3 wt% Co) was prepared by pore volume impregnation of the carrier with aqueous solutions of $Co(NO_3)2.6H_2O$ (Merck, "for analysis"). In order to study the influence of the drying procedure the impregnated catalysts were subdivided into three portions each of which was dried according to a different procedure :

1. at 293 K above P_2O_5 (about 2 weeks were needed)
2. at 293 K above P_2O_5 (same as procedure 1), followed by heating in air at 383 K overnight
3. starting at 293 K and slowly (2 h) raising the temperature up to 383 K where it was kept overnight.

With reference to these drying procedures, catalyst samples will be denoted as Co(x)/C(293 K), Co(x)/C(293-383 K), or Co(x)/C(383 K). In this notation (x) represents the wt% Co, which was checked by means of atomic absorption spectroscopy using a Perkin-Elmer 300 AAS spectrometer.

Co promoted carbon-supported Mo catalysts (2.1 wt% Co - 6.7 wt% Mo and 3.1 wt% Co - 8.0 wt% Mo) were prepared by a two-step pore volume impregnation procedure. The Mo phase was introduced first using an aqueous solution of ammoniumheptamolybdate. Subsequently, the samples were dried at 383 K for 16 h. Appropriate amounts of Co in the form of cobalt nitrate were added to the Mo/C catalysts by impregnation, followed by drying at 383 K in air. Precursor catalyst compositions were checked by means of atomic absorption spectroscopy.

Sulfidation and catalytic activity measurement

Catalyst samples (0.2 g) were sulfided in situ in a mixture of purified H_2 and H_2S (10 mol% H_2S, flowrate 60

ml/min). The following temperature program was applied : 10 min at 293 K, linear increase to 673 K in 1 h, and 2 h at 673 K. After sulfidation, the reaction mixture consisting of 6.2 mol% thiophene in hydrogen was introduced at a flowrate of 50 ml/min. The temperature and pressure were 673 K and 1 atm respectively. The reaction products were analyzed by on-line gas chromatography. The reaction constants for HDS and hydrogenation and the HDS activity per mol Co (QTOF or Quasi Turn Over Frequency value) were calculated using conversions measured after 2 h run time and assuming first order reaction in thiophene HDS and in the consecutive butene hydrogenation.

X-ray photoelectron spectroscopy

XPS spectra of the oxidic Co/C sample were recorded on a Physical Electronics 550 XPS/AES spectrometer equipped with a Mg anode and a double pass cylindrical mirror analyzer operating at a pass energy of 25 eV. The samples were pressed in a stainless grid. The measuring temperature was 293 K and the pressure did not exceed 5.10^{-8} torr. Spectra of the sulfided samples were recorded on a AES ES 200 spectrometer equipped with a Mg anode and a spherical analyzer operating at 50 eV pass energy. In order to avoid contact of the sulfided catalysts with air, a special sulfiding reactor was used (16) which allowed transfer of the samples to a N_2 flushed glove box attached to the XPS apparatus without exposure to air. After sulfiding, carried out as described above, the samples were flushed with purified He for 15 min at 673 K, subsequently cooled to room temperature in 0.5 h, and finally transferred into the glove box. The measuring temperature was 283 K and pressure better than 1.10^{-8} torr. All spectra (precursor and sulfided samples) were recorded in steps of 0.1 eV and the C 1s signal of the support (284.6 eV) was used as internal standard for binding energy calibration.

Temperature programmed sulfiding

TPS was carried out in the apparatus described in detail elsewhere (17). A catalyst charge of 45 mg was sulfided using a mixture of H_2S, H_2 and Ar (molar ratio 3.3 : 28.1 : 68.8) with a flowrate of 11 x 10^{-6} mol/s at atmospheric pressure. Product analysis during sulfidation was accomplished by means of a mass spectrometer which monitored almost continuously the peak intensities of H_2O, H_2S and Ar. After removal of H_2O and H_2S from the gas mixture the H_2 concentration was measured using a thermal conductivity detector. The sulfidation was carried out as follows : The catalyst was subjected to the sulfiding mixture for 0.5 h at room temperature, thereafter, the temperature was increased up to 1270 K at a rate of 10 K/min followed by an isothermal stage at 1270 K (30 min).

RESULTS

Catalytic properties

Catalytic properties measured for the Co/C samples, the Co-Mo/C catalysts and a commercial Co-Mo/Al_2O_3 catalyst (Ketjen, 124-1.5E, 4% Co O - 12% MoO_3) are given in Table 1. The HDS activity of the carbon support itself was below the detection limit. The rate constants for thiophene HDS of the Co/C samples are represented graphically in Fig. 1 and compared to corresponding activities for Mo/C catalysts (18). An increase in HDS activity is observed for the cobalt catalysts up to approximately 7 wt% Co irrespective of the drying procedure applied. Further increase of the Co content slightly decreases the activity for the 293-383 K and 383 K dried samples, while a further improvement in activity is noticed for the 293 K dried

Table 1 : Catalytic properties of sulfided Co and Co-Mo catalysts.

Catalyst composition (wt%)		Activity results								
		$k_{HDS} \times 10^3$ (m^3/kg.s)			QTOF* $\times 10^3$ (mol thiophene/mol Co.s)			$k_{HYD} \times 10^3$ (m^3/kg.s)		
Co	Mo	**293 K	293-383 K	383 K	293 K	293-383 K	383 K	293 K	293-383 K	383 K
1.31	-	4.5	4.3	3.8	22.6	21.6	19.3	4.2	4.4	3.8
3.86	-	8.1	7.3	6.2	13.8	12.4	10.6	8.7	7.4	6.6
7.06	-	10.0	8.6	7.9	9.4	8.1	7.4	13.1	9.7	8.7
10.05	-	10.8	8.7	7.7	7.1	5.7	5.1	10.9	10.0	10.2
13.34	-	10.7	8.1	7.6	5.3	4.0	3.7	10.7	8.6	10.6
2.1	6.7			12.2			38			14.2
3.1	8.0			17.7			38			22.5
3.1	8.0***			4.1			8.7			3.8

* QTOF stands for Quasi Turn-Over Frequency

** refers to drying temperature (see experimental section)

*** alumina-supported Co-Mo (Ketjen, 124-1.5E)

samples. In general, over the entire Co loading range studied the Co/C (293 K) catalysts are more active than the Co/C (293-383 K) samples, which in turn are more active than the Co/C (383 K) catalysts.

The hydrogenation activity of the Co/C catalysts behaves similar as the HDS activity. The calculated k_{HYD}/k_{HDS} ratios are nearly equal to 1 for all catalysts, except for the high Co content 383 K dried samples, which show a slightly higher hydrogenation activity.

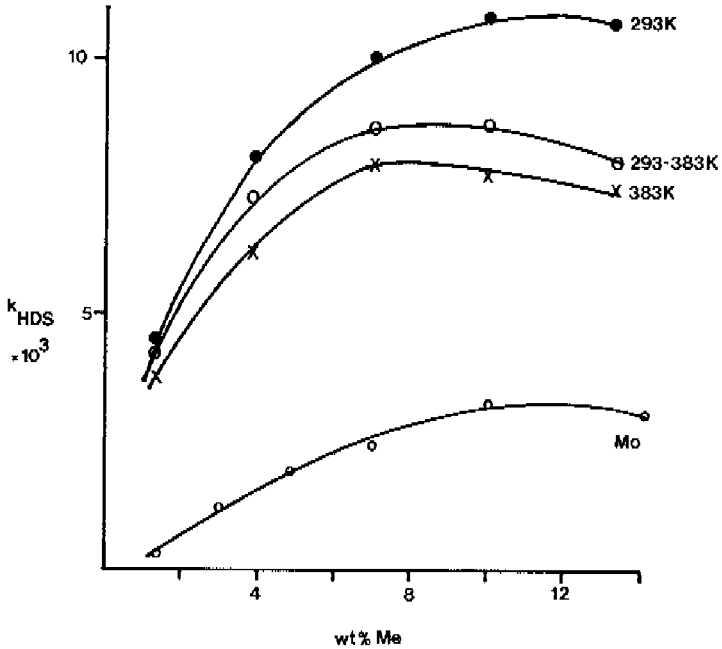

Fig. 1 Thiophene HDS reaction rate constants (k_{HDS}, $m^3/kg.s$) for carbon-supported Co sulfide catalysts dried according to different procedures (see experimental section). The activity of corresponding carbon-supported Mo sulfide catalysts (18) are included for comparison.

Structure of Co phase in oxidic and sulfided catalysts

XPS spectra were recorded for the entire Co loading range of the Co/C (293-383 K) catalysts, whereas the influence of the drying procedure on the XPS characteristics was studied only for the highest Co content samples. Whatever the drying procedure applied or the Co content of the catalyst, a typical spectrum of Co 2p as presented in Fig. 2a is

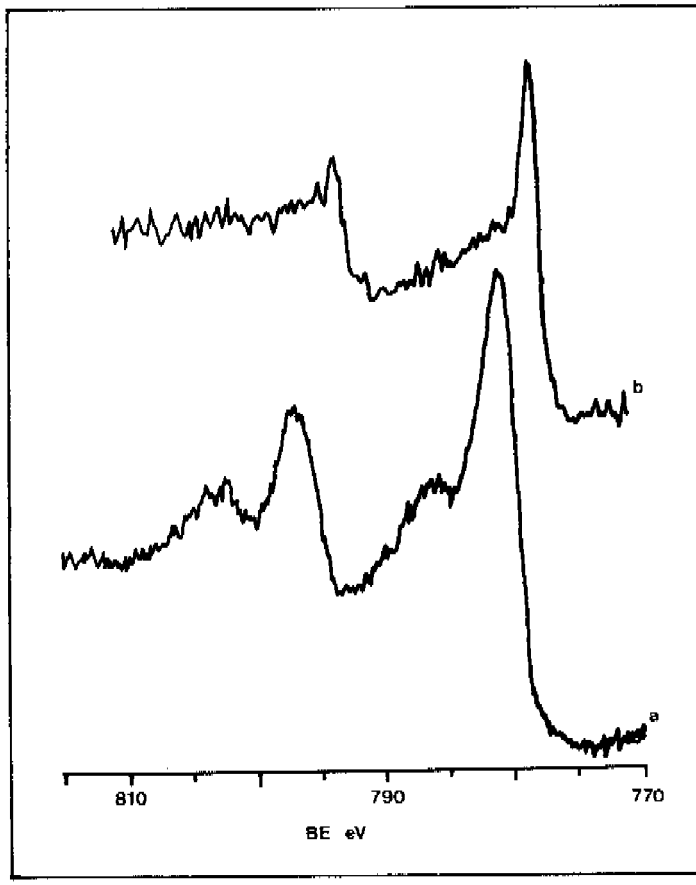

Fig. 2 Typical Co $2p_{3/2,1/2}$ XPS spectra of oxidic precursor Co/C catalysts (a) and sulfided Co/C catalysts (b).

observed for all oxidic catalysts. This spectrum which has been corrected for X-ray satellites ($K'_{\alpha\ 3,4}$), shows the main 2p signals at 781.3 and 797.1 ± 0.1 eV and the rather pronounced shake-up satellite lines shifted approximately 5.5 eV towards higher binding energy. From the intensities of the N 1s and Co 2p photoelectron signals measured for the samples with the highest Co content a N/Co atomic ratio of 1.7 could be calculated for the 293 K dried catalyst and a ratio of 1 for the 293-383 K and 383 K dried samples, by using the electron escape depths published by Penn (19) and the cross sections published by Scofield (20).

After sulfidation, in all samples the Co phase has the spectral characteristics presented in Fig. 2b. The binding energies measured for the Co 2p signals were 778.2 and 793.3 eV ± 0.2 eV. The S 2p peak binding energy varied between 162.7 and 162.8 eV. Accordingly, the difference in binding energy between the Co $2p_{3/2}$ peak and the S 2p peak is 615.5 ± 0.2 eV. This value is slightly lower than the values 615.7-616.2 eV measured by Alstrup et al. (21) for the Co_9S_8 reference compound. From the experimental Co 2p and S 2p intensity ratios, atomic sulfur-to-cobalt ratios were calculated, taking into account differences between sulfur and cobalt with respect to the mean free path of electrons through cobalt sulfide particles (19), cross-section (20), and detector efficiency (22). After subtraction of the amount of elemental sulfur formed during sulfidation of the carbon support itself (I_S/I_C = 0.003), S/Co ratios ranging from 1.3 to 1.5 were obtained for the catalyst samples. These values exceed the stoichiometric sulfur-to-cobalt ratio of Co_9S_8 (0.89), indicating an excess of sulfur. In Fig. 3 a typical S 2p signal of the catalysts is presented. Besides the contribution of S^{2-} (162.7 eV), sulfur species with binding energies located around 167 eV (probably representing oxidized sulfur species) seem to be present.

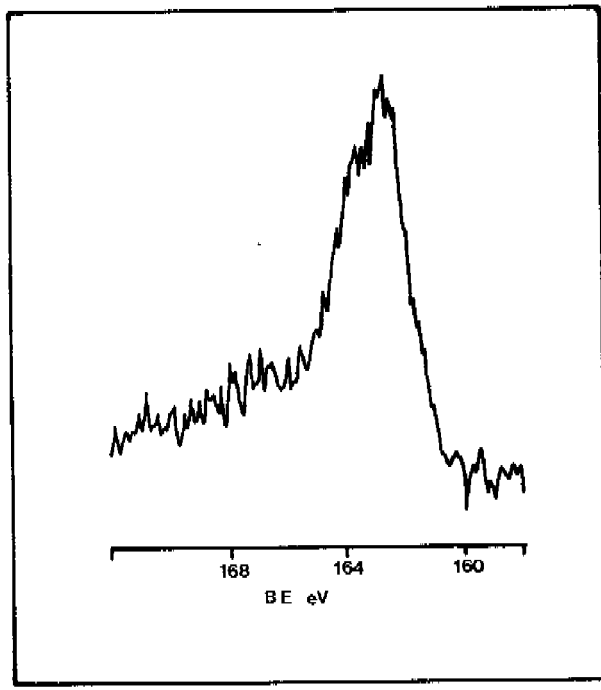

Fig. 3 Typical S $2p_{3/2,1/2}$ XPS spectrum of sulfided Co/C catalysts.

Repartition of the oxidic and sulfided Co phase on the carbon surface

Besides structural information, quantitative XPS enables one to obtain information on the state of dispersion of the cobalt phase deposited on the carbon surface. A model described by Kerkhof and Moulijn (22) was used for this purpose. In order to determine the dispersion, the experimental Co 2p/C 1s intensity ratio is compared with the

theoretical value predicted by the Kerkhof-Moulijn model which assumes monolayer coverage of the carrier surface by the deposited catalytic phase. The theoretical values were calculated using Scofield's cross sections (20), assuming the detector efficiency to depend on the reciprocal value of the electron kinetic energy (22), and using the electron mean free paths according to Penn (19). In Table 2 the experimental and theoretical intensity ratios are collected. The following features can be discerned :

- The experimental intensity ratios for the 293-383 K dried catalysts in the oxidic state are in excess of the theoretical values especially at low Co loadings.
- The intensity ratios of the sulfided catalysts are clearly lower than those of the corresponding oxidic samples.
- Up to approximately 7 wt% Co an increase in the intensity ratio of oxidic and sulfided Co(x)/C(293-383 K) samples is observed. At higher Co loadings no increase of importance is noticed.
- The drying procedure influences the intensity ratio. In the oxidic state the 293 K and 383 K dried Co(13.3)/C samples have a lower intensity ratio than the 293-383 K dried sample, while in the sulfided state the sequence is 293 K>293-383 K>383 K.

Table 2 : Quantitative XPS results of Co/C catalysts

Catalyst wt% Co	drying temperature (K)	$[I_{Co}/I_C]_{exp}$ oxidic	sulfided	$[I_{Co}/I_C]^*_{monolayer}$
1.31	293-383	0.11	0.042	0.069
3.89	"	0.71	0.31	0.21
7.06	"	0.85	0.43	0.40
10.05	"	0.85	0.40	0.60
13.34	"	0.91	0.48	0.84
13.34	293	0.71	0.57	0.84
13.34	383	0.63	0.43	0.84

* calculated according to (22)

In the calculation of the theoretical Co-to-C intensity ratio uniform monolayer coverage (optimal dispersion) of the carbon surface by the Co phase has been assumed, and therefore these ratios must be considered as the maximum values which can be reached for homogeneous samples at a given Co content. Since the experimentally determined intensity ratios are higher than the theoretical ones it is concluded that the deposited Co phase is not uniformly deposited on the support surface, and that a considerable enrichment of the Co in the pores located at the outer side of the support graines has occured. This certainty applies to the Co(x)/C(293-383 K) catalyst series and most likely also to the Co(13.3)/C(293 K) and Co(13.3)/C(383 K) samples.

Sulfidation of Co/C catalysts

In Fig. 4 the TPS pattern of the Co(13.3)/C (293-383 K) catalyst is shown. No qualitative nor quantitative differences were observed in these TPS patterns when a different drying procedure (293 K or 383 K) was applied to the catalysts. The TPS pattern of the carbon support itself showed only a minor adsorption of H_2S at room temperature (0.38 mol H_2S per g support) of which half was desorbed as soon as the temperature was increased (23). In case of the Co/C catalysts a considerable H_2S consumption is observed at room temperature. Per mol Co 0.65 mol H_2S is consumed. With increasing temperature an additional consumption of 1.19 mol H_2S per mol Co takes place. At the end of this stage (473 K) the total amount of H_2S consumed is 1.84 mol per mol Co. Finally between 473 K and 573 K a sharp H_2S production peak coupled to a H_2 consumption is observed (0.54 mol H_2S and 0.66 mol H_2 per mol Co). Sulfidation is complete at this stage (573 K) and corresponds to a total uptake of 1.3 mol H_2S and 0.66 mol H_2 per mol Co. If one subtracts the amount of H_2S still adsorbed by the pure carbon support at high temperatures (0.19×10^{-3} mol H_2S/g

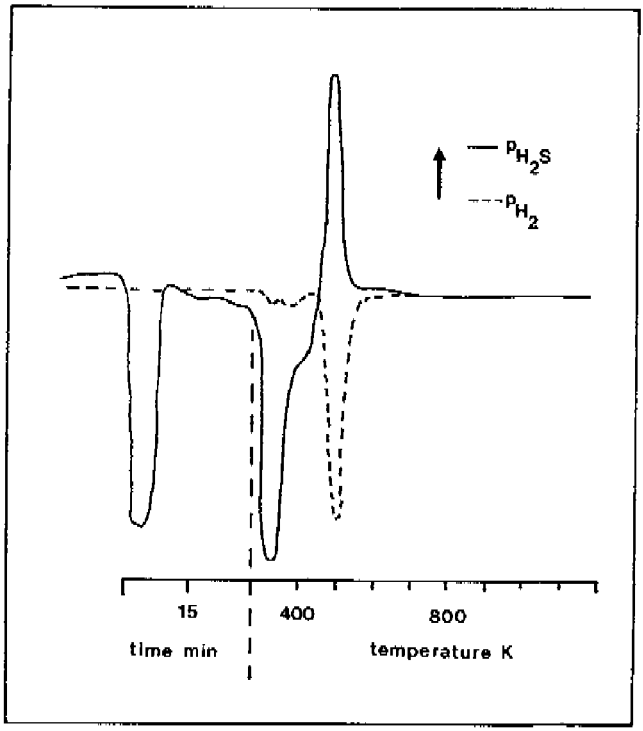

Fig. 4 TPS patterns of Co(13.3)/C (293-383 K) catalyst.

carbon) as was measured in a separate experiment (23), a H_2S/Co ratio of 1.23 is obtained. Note that the H_2S consumption corresponds very closely to the atomic S/Co ratio determined by means of XPS.

DISCUSSION

Morphology of carbon-supported cobalt catalysts

The typical XPS spectrum of the oxidic catalysts cannot be matched with that of CoO or Co_3O_4 reference compounds (24) (difference in sattelite characteristics, and in Co $2p_{3/2}$ B.E. which is 780 eV for both Co oxides). Instead, the high Co 2p binding energy and the nitrogen-to-cobalt atomic ratio suggest that the cobalt is present as a mixed nitrate-oxide compound, the nitrate content being dependent on the drying procedure applied. Increasing the drying temperature to 383 K leads to a lower nitrate content. This is in accordance with the finding that gradual heating of the catalyst led to evolution of nitrous oxides starting at 353 K (25). Similar observations were made by Groot et al. (26) who studied Fe/C catalysts. They concluded that iron nitrate (partially) decomposed during drying at 293 K and that the decomposition products are not (completely) desorbed from the carbon surface leading to iron (III) oxide particles interacting with nitrate anions.

As can be judged from the high XPS Co-to-C intensity ratios, the oxidic cobalt phase is inhomogeneously dispersed on the carrier surface yielding a considerable enrichment of Co at the outer surface of the support grains. This effect is probably less pronounced in the 293 K dried samples (lower XPS intensity ratio). For the 383 K dried sample the low XPS intensity ratio must be related to severe sintering of the Co particles. Again, similar effects were observed for the iron on carbon catalysts (26), namely inhomogeneous dispersion and sintering of the oxidic iron particles with increasing drying temperature.

It is obvious from the above results that the interaction between the oxidic Co phase and the carbon surface is very weak. This can be explained as follows. Due to the slightly acidic nature (pH=5.25) of the Co-nitrate

impregnation solution the carbon surface becomes partly protonated. Because of electrostatic repulsion, therefore, no adsorption of Co^{2+} ions will take place during impregnation. We checked this by passing an aqueous cobalt nitrate (2 wt%) solution at a flowrate of 60 ml/min over a column of carbon support particles while constantly monitoring the pH of the effluent solution. For the first 180 ml of solution a pH increase from 5.25 to almost 7 was registrated, indicating that the carbon surface becomes protonated. Thereafter, the pH decreases slowly towards its original value. By means of atomic adsorption spectroscopy it was determined that only a negligible amount of Co (0.1 wt%) was chemisorbed on the support particles.

These results agree with the findings of D'Aniello (27), who studied the adsorption of Co anions [$Co(CN_6)^{3-}$, $CoOx_3^{3-}$ and $Co(EDTA)^-$] on alumina. He suggested that the adsorption was an electrostatic process, the Co anions being adsorbed only on a positively charged surface. In view of these results, increasing the pH of the cobalt nitrate solution should result in more homogeneously dispersed catalysts. This is however, hampered by the precipitation of $Co(OH)_2$ around pH=7. On the other hand, impregnation with $Co(NH_3)_6^{2+}$ in ammoniacal solution seems worth trying.

In the sulfidation patterns of the precursor Co/C catalysts three regions can be observed : a room temperature sulfiding region, low-temperature sulfiding up to around 470 K and H_2S production around 530 K. It is interesting to compare our TPS results with those obtained for Co/Al_2O_3 catalysts (28). Sulfiding of Co/Al_2O_3 catalysts occurs both in a so-called low-temperature (up to 750 K) and in a high-temperature (750-1200 K) region, and proceeds via O-S exchange reactions. The (oxy-) sulfides formed by O-S exchange might reduce via cleavage of Co-S bonds resulting in the formation of elemental sulfur. This sulfur is easily reduced by H_2 under production of H_2S in a fast consecutive reaction catalyzed by Co. As a result no sharp H_2S

production peak was observed in the TPS patterns of Co/Al_2O_3 catalysts. From a comparison of our Co/C results with those obtained for Co/Al_2O_3 it is concluded that :

- Strong cobalt-support interactions are absent in Co/C catalysts (because no high temperature peaks are present) and consequently sulfidation is fast and complete at 570 K.
- Sulfidation of Co/C catalysts proceeds via O-S exchange reactions similar as observed for Co/Al_2O_3 catalysts. But since the sulfidation reactions take place at rather low temperatures the elemental sulfur produced is accumulated and not reduced to H_2S until the temperature is raised to about 500 K.

Upon sulfidation sintering of the Co phase takes place. This has also been reported for Mo (23) and Fe (26) based catalysts using the same carbon support, and reflects the rather weak interaction of the carbon surface with the deposited metal ions. In the final sulfided state catalyst dispersion seems to be better for the 293 K dried samples than for the 293-383 K and the 383 K dried samples. In accordance herewith, the thiophene HDS activities of the catalysts decrease with the drying procedure in the following order : 293 K > 293-383 K > 383 K.

Co/C catalysts show very high HDS activities compared to conventional alumina-supported systems (see Table 1). In view of this high HDS activity it is important to get some insight into the structure of the Co sulfide phase present on the carbon support. It has been stated (29) on the basis of thermodynamical considerations, that Co_9S_8 is the predominant phase present after sulfidation of unsupported Co catalysts. Due to the weak interaction with the carbon support the Co phase in Co/C catalysts will resemble very much to the Co phase in unsupported catalysts. This strongly suggests that Co_9S_8 should form upon sulfidation of Co/C catalysts. On the other hand it has been shown (13) that the activity per surface cobalt atom for unsupported Co_9S_8 is at

least 30 times lower than the activity per cobalt atom for Co/C catalysts. In this respect Mössbauer results (13) of a sulfided 1% Co/C catalyst indicated the presence of Co in different surroundings which correspond, however, close to those observed for the various bulk Co sulfides. Although it is difficult to assign the Co 2p XPS spectral features to a specific Co sulfide, the measured line shapes and binding energies of the Co 2p signals of the Co/C catalysts seem to point to the presence of a Co_9S_8-like species. The S 2p lines are consistent with S^{2-}-species although the line width (FWHM = 2.6 eV) points to the presence of other S species. Remarkably high S/Co ratios, as measured by XPS and TPS, are obtained for the catalysts. This result remains intriguing in view of the TPS findings which demonstrate that the catalyst can dispose of excess sulfur by H_2S production (sharp H_2S production peak in TPS at 530 K which temperature is well below the actual sulfidation temperature). Similar observations were made for Fe/C catalysts (26) where XPS pointed to the presence of FeS, while S/Fe ratios reached values well above 2. In view of the fact that Co catalyzes sulfur reduction (28) it seems likely that the excess sulfur (with respect to stoichiometric Co_9S_8) produced during sulfidation is deposited on the carbon surface and resists conversion to H_2S. In this respect it has been shown that microporous materials especially microporous carbons are known catalysts for the oxidation of H_2S to elemental sulfur, and that they can adsorb considerable amounts of this elemental sulfur produced (30-32). Due to the fact that sulfur is trapped in the micropores of the substrate it resists evaporation and reduction to H_2S by H_2. For instance, it has been shown (32) that even at 623 K 0.25 g sulfur could be adsorbed per g carbon on an activated charcoal having a micropore volume of 0.45 ml/g (the micropore volume of the Norit RX 3 extra carbon is 0.50 ml/g). Sulfur was found to be chemisorbed at the carbon surface, especially at

temperatures above 673 K (33). This sulfur desorbs as CS_2 and H_2S only when the carbon is heated in nitrogen up to 1270 K. In this respect, the broad XPS sulfur signal might indicate the presence of sulfur species with a higher valence state than 2- (binding energy of S^0 = 164 eV) representing deposited sulfur polymers in the micropores of the carbon support.

Catalytic properties of cobalt sulfide

Until recently, cobalt sulfide was believed to possess only poor HDS properties. In contradiction herewith, de Beer c.s. (14,15) prepared highly active carbon-supported cobalt catalysts giving cobalt sulfide the full credit of an outstanding HDS catalyst. They argued that the so-called synergetic effect of Co-Mo catalysts could be due to the activity of cobalt rather than molybdenum. In this respect molybdenum sulfide should be regarded as a "support" for the cobalt phase, enabling optimal dispersion of the Co phase.

The intrinsic HDS activity of optimal dispersed cobalt sulfide can be estimated from the present results. This has been done in Fig. 5 where reciprocal QTOF values of the low loading catalysts are plotted versus mol% Me. For comparison the corresponding values of Mo/C catalysts (18) prepared on the same carbon support are included. The reason for plotting the reciprocal QTOF values along the vertical axis is that in this way straight lines are obtained which can be easily extrapolated. If instead QTOF values were plotted, hyperbolic curves are obtained which are difficult to extrapolate. The intercept obtained after extrapolation to 0 mol% Me (see Fig. 5) gives a fair indication of the catalytic activity of 100% or atomically dispersed metal sulfide. In fact the QTOF (Quasi Turn-Over Frequency) value is the product of the actual turn-over frequency of the active sites (mol thiophene converted per site per second) multiplied by the fraction of atoms which

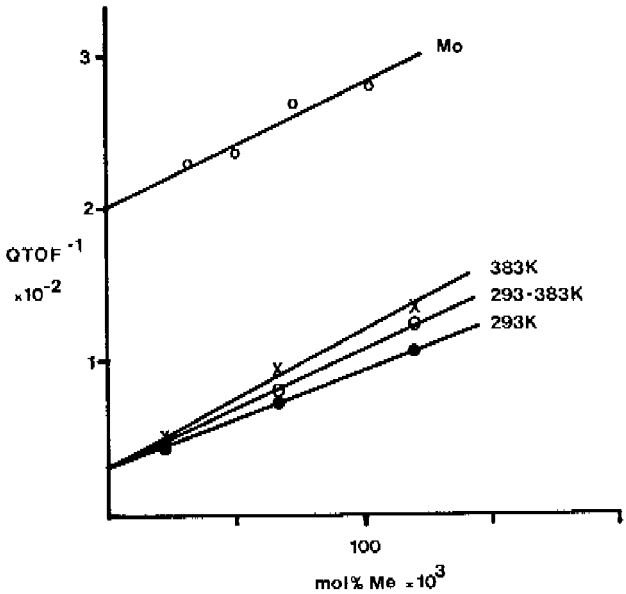

Fig. 5 Reciprocal QTOF values versus mol% Me for carbon-supported Co sulfide catalysts dried according to different procedures (see experimental section) and corresponding carbon-supported Mo sulfide catalysts (18).

are located at the surface (which is commonly referred to as the dispersion of the catalyst) multiplied by the fraction of surface atoms which are the actually active sites. By extrapolation to 0 mol% metal the dispersion factor is eliminated. Hence, the extrapolated value represents the HDS activity per metal surface atom which in fact is a minimum value for the actual turn-over frequency. For the Co/C catalysts dried according to the different procedures

the same intercept is found, as is to be expected since they all contain the same cobalt sulfide phase (only the dispersion is different). In this way we obtained intrinsic HDS activities of 5 x 10^{-3} mol thiophene converted per mol molybdenum per second and 33 x 10^{-3} mol/mol.s for cobalt, or nearly a seven-fold higher activity for cobalt sulfide than for molybdenum sulfide.

The question remains, however, whether the high HDS activity observed for cobalt can explain the so-called promotor effect in Co-Mo catalysts. For this purpose the two Co-Mo/C catalysts were prepared and evaluated for their thiophene HDS activity. These catalysts have Co/Mo atomic ratios of 0.51 (2.1% Co - 6.7% Mo) and 0.63 (3.1% Co - 8.0% Mo), corresponding to catalyst compositions which show a distinct promotion effect (according to (15) the maximum activity for carbon-supported catalysts is obtained at Co/Mo ratios around 0.6). Upon addition of cobalt to Mo/C catalysts an increase in the thiophene HDS rate constant was observed from 2.5 x 10^{-3} to 12.2 x 10^{-3} (2.1% Co - 6.7% Mo) and from 2.8 x 10^{-3} to 17.7 x 10^{-3} (3.1% Co - 8.0% Mo). According to the findings of Topsøe and coworkers (8,11,12,13), the Co-Mo/C catalysts should contain large amounts of the typical Co-Mo-S phase. If the activity of these catalysts is expressed per mol Co present, nearly the same activity (38 x 10^{-3} mol/mol.s) as that mentioned above for optimally dispersed cobalt sulfide is obtained (cf. Table 1). Hence, these results strongly suggest that the activity of highly dispersed cobalt can explain the observed promotion effect of Co-Mo/C catalysts. The observed k_{HYD}/k_{HDS} ratios of the Co-Mo/C catalysts (1.3 and 1.2) which is very close to that observed for the Co/C catalysts (1.0) corroborate this findings. Furthermore, it folows from the above that MoS_2 should be regarded as a support for the catalytically active Co species, the beneficial property being that it allows atomic (100%) dispersion of cobalt, a property which is clearly not fulfilled by the carbon

support.

It is interesting to compare these findings with the results obtained by Topsøe and coworkers (8,12,13) describing the Co-Mo-S model. As in the case of alumina-supported catalysts, Mössbauer studies (13) have shown that Co-Mo-S is present in sulfided Co-Mo/C catalysts and that catalytic activity could be related to the amount of Co-Mo-S. The salient findings of these Mössbauer studies are that the basic structure of the Co-Mo-S phase consists of MoS_2 with cobalt atoms atomically dispersed at the edge planes and that the active sites are most likely located on the Co atoms, although the neighbouring Mo atoms may also play an active role in the HDS process.

Our results prove, for the first time, that the active sites for hydrodesulfurization of thiophene in Co-Mo catalysts are definitely located on the Co atoms, excluding a major contribution to the HDS activity of neighbouring Mo atoms. Furthermore, they corroborate on the atomic dispersion of cobalt through interaction with MoS_2. In this respect, it becomes clear that the role of MoS_2 is of secondary importance (improved dispersion) since the intrinsic activity of the surface Co atoms in sulfided Co/C catalysts equals that in Co-Mo/C catalysts. Moreover, it may be argued that, if cobalt sulfide catalysts can be prepared on a carbon support which has surface properties such as to create a high degree of Co dispersion at relatively high Co loadings, one can dispose of the expensive MoS_2 "support".

A final remark concerns the Co-Mo/Al_2O_3 catalyst. As can be seen in Table 1 the activity of this catalyst is much lower than that of the corresponding (3.1% Co - 8.0% Mo) Co-Mo/C catalyst, suggesting that a strong interaction with the alumina support lowers the HDS activity of the Co-Mo-S phase. In this respect, it has been shown (34) that the intrinsic activity (per Co atom present as Co-Mo-S) is increased considerably when Co-Mo/Al_2O_3 catalysts were

sulfided at temperatures above 873 K instead of 673 K. It was suggested that in the high temperature sulfided catalysts the Co-Mo-S phase-alumina support interactions were less important. Hence, as can be concluded from the results presented in this study, the beneficial properties of using carbon as a support material is that the most active type of Co-Mo-S phase is present in the catalysts.

REFERENCES

1. Okamoto, Y., Nakano, H., Shimokawa, J., Imanaka, T., and Teranishi, S., J. Catal. 50, 447 (1977).
2. Brinen, J.S., and Armstrong, W.D., J. Catal. 54, 57 (1978).
3. Lo Jacono, M., Verbeek, J.L., and Schuit, G.C.A., J. Catal. 29, 463 (1973).
4. Gates, B.C., Katzer, J.R., and Schuit, G.C.A., in "Chemistry of Catalytic Processes", chapter 5. Mc Graw-Hill, New York, 1979.
5. Delmon, B., in "Proceedings, Climax Third Intern. Conf. on Chemistry and Uses of Molybdenum, Ann Arbor, 1979", (H.F. Barry and P.C.H. Mitchell, Eds.), p. 73. Climax Molybdenum Company, Ann Arbor, Michigan, 1979.
6. Voorhoeve, R.J.H., and Stuiver, J.C.M., J. Catal. 23, 243 (1971).
7. Farragher, A.L., and Cossee, P., in "Proceedings of the 5th International Congress on Catalysis, Palm Beach, 1972", (J.W. Hightower, Ed.) p. 1301, North Holland, Amsterdam, 1973.
8. Topsøe, H., Clausen, B.S., Candia, R., Wivel, C., and Mørup, S., J. Catal. 68, 433 (1981).
9. Delmon, B., Bull. Soc. Chim. Belg. 88, 1 (1979).
10. Pirotte, D., Zabala, J.M., Grange, P., and Delmon, B., Bull. Soc. Chim. Belg. 90, 1239 (1981).
11. Wivel, C., Candia, R., Clausen, B.S., Mørup, S., and

Topsøe, H., J. Catal. 68, 453 (1981).

12. Candia, R., Clausen, B.S., Bartholdy, J., Topsøe, N., Lengeler, B., and Topsøe, H., in "Proceedings of 8th International Congress on Catalysis, Berlin, 1984", p. II-375, Verlag Chemie, Weinheim, 1984.
13. Topsøe, H., Bull. Soc. Chim. Belg. 93, 775 (1984).
14. de Beer, V.H.J., Duchet, J.C., and Prins, R., J. Catal. 72, 369 (1981).
15. Duchet, J.C., van Oers, E.M., de Beer, V.H.J., and Prins, R., J. Catal. 80, 386 (1983).
16. Konings, A.J.A., van Doorn, A.M., Koningsberger, D.C., de Beer, V.H.J., Farragher, D.C., and Schuit, G.C.A., J. Catal. 54, 1 (1978).
17. Arnoldy, P., van den Heykant, J.A.M., de Bok, G.D., and Moulijn, J.A., J. Catal. accepted for publication.
18. Vissers, J.P.R., Bachelier, J., Ten Doeschate, H.J.M., Duchet, J.C., de Beer, V.H.J., and Prins, R., in "Proceedings of 8th International Congress on Catalysis, Berlin,1984", p. II-387, Verlag Chemie, Weinheim, 1984.
19. Penn, D.R., J. Elect. Spectrosc. 9, 29 (1976).
20. Scofield, J.H., J. Elect. Spectrosc. 8, 129 (1976).
21. Alstrup, I., Chorkendorff, I., Candia, R., Clausen, B.S., and Topsøe, H., J. Catal. 77, 397 (1982).
22. Kerkhof, F.P.J.M., and Moulijn, J.A., J. Phys. Chem. 83, 1612 (1979).
23. Vissers, J.P.R., de Beer, V.H.J., and Prins, R., J. Catal. to be published, chapter 3 of this thesis.
24. Wagner, C.D., Riggs, W.M., Mouder, J.E., and Muilenberg, G.E., "Handbook of X-ray Photoelectron Spectroscopy", Perkin Elmer Corporation, 1979.
25. Mercx, F.P.M., unpublished results.
26. Groot, C.K., Van der Kraan, A.M., de Beer, V.H.J., and Prins, R., Bull. Soc. Chim. Belg. 93, 707 (1984).
27. D'Aniello Jr., M.J., J. Catal. 69,9 (1981).
28. Arnoldy, P., de Booys, J.L., Scheffer, B., and Moulijn, J.A., to be published.

29. Pecoraro, T.A., and Chianelli, R.R., J. Catal. 67, 430 (1981).
30. Gmelins Handbuch der Anorganischen Chemie, 9(A3), 617 (1953).
31. Steijns, M., and Mars, P., J. Catal. 35, 11 (1974).
32. Steijns, M., and Mars, P., J. Colloid Interface Sci. 57, 175 (1976).
33. Wibaut,J.P., and van der Kam, E.J., Rec. Trav. Chim. Pays Bas 49, 121 (1930).
34. Candia, R., Sorensen, O., Villadsen, J., Topsøe, N.-Y., Clausen, B.S., and Topsøe, H., Bull. Soc. Chim. Belg. 93, 763 (1984).

CHAPTER 5

CARBON SUPPORTED TRANSITION METAL SULFIDES.

ABSTRACT

First, second and third row transition metal sulfides ranging from group VI to group VIII c, supported on activated carbon were evaluated for their ability to catalyze the hydrodesulfurization of thiophene at atmospheric pressure. X-ray photoelectron spectroscopy was used to measure the chemical state and to obtain an indication of the dispersion of the supported sulfide particles. Second and third row elements display volcano curves with catalytic activity varying over more than an order of magnitude and maxima occuring at Rh in the second and Ir in the third row. First row elements show a twin-shaped pattern with maximum activity located at Cr and Co. The resemblance of these experimental activity trends with those previously reported for unsupported transition metal sulfides demonstrate the advantage of carbon supports in studies on the intrinsic catalytic properties of small sulfide particles. A correlation between the catalytic activity of second and third row elements and the shift in XPS binding energies between metal and metal sulfide phases was found. Superior catalysts have low binding energy shifts and preserve a high degree of metal character under sulfiding conditions.

INTRODUCTION

row transition metal sulfides Pecoraro and Chianelli (1) demonstrated that the dibenzothiophene HDS activity measured at 673 K and 31 bar was related to the position of the metal in the periodic table. Typical volcano type plots with periodic position were obtained for second and third row elements with maxima occuring near Ru and Os. First row transition metal sulfides were found to be relatively inactive. However, these results were in striking contrast to reported thiophene (2) and dibenzothiophene (3) HDS activities measured at 623 K, 1 bar and 513 K, 1 bar respectively, for alumina-supported transition metal sulfides. No systematic variation in HDS activity with periodic position was observed. Cr, Co, Mo, Ru, Pd and especially Pt were mentioned to be the most active metals. The discrepancy between the above findings with unsupported and alumina supported sulfide catalysts might be due to the reactivity of the alumina support towards the transition metals, as well as to differences in textural properties between the unsupported metal sulfides. Recently, carbon materials have received increased attention as supports for catalyst systems. On carbon carriers higher active phase efficiences can be obtained than on alumina supports because unfavourable strong metal-support interactions are avoided, while none the less high active phase dispersions are obtained. Another advantage claimed for the carbon supported catalysts is that fundamental properties of well dispersed supported particles can be studied (4).

The present paper comprises the results of a systematic study on the catalytic HDS activities of transition metal (ranging from group VI to group VIII c) sulfides supported on activated carbon. Information on the structure of the sulfided catalyst systems is obtained by XPS. A general comparison with the data reported for unsupported and alumina supported transition metals sulfides is included.

EXPERIMENTAL

Catalysts

The catalysts were prepared by pore volume impregnation of a Norit activated carbon (RX3 extra, surface area 1190 m^2/g, pore volume 1.03 ml/g) with appropriate solutions of transition metal salts. In order to adequately compare the different catalysts, the concentration of the metal salt solutions was adjusted in such a way as obtain a final metal (Me) loading of 0.5 Me atoms per nm^2 support surface area. Because of the differences in atomic weight, the weight percentage of active metal therefore ranges from 4.9% (Cr) to 16.3% (Pt) in the different catalyst samples. The first two columns of Table 1 present the catalyst samples prepared and the precursor salts (chemical pure grades) used. For uniformity purposes the chloride precursor metal salt was chosen in most cases and aqueous solutions were used for the majority of the impregnations. Exceptions were Ru, Pd (concentrated HCl solutions).

Activity measurements

Catalyst samples (200 mg, 0.2-0.5 mm particle size) were presulfided in situ in a H_2S/H_2 gasflow (10 mol% H_2S, 60 ml/min) with the following temperature program : 6 K/min increase from 293 K to 673 K and 2 h at 673 K. Following the sulfidation the gasflow was switched to the reaction mixture : a 6.2 vol% thiophene in H_2 gasflow. The flowrate was 50 ml/min, reaction temperature 673 K and pressure 1 bar. Thiophene conversion was measured at different time intervals by on-line gas chromatography. First order rate constants for both thiophene HDS and the consecutive butene hydrogenation were calculated after a 2 h run as described elsewhere (4).

XPS analysis

XPS spectra of the sulfided catalysts were recorded on an AEI ES 200 spectrometer. After sulfidation of the catalysts according to the procedure described above, they were purged with purified He for 1/4 h at 673 K and subsequently within 0.5 h cooled to room temperature in flowing He. A special reactor (5) was used which allowed transfer of the samples to a dry N_2-flushed glove box attached to the XPS apparatus, without exposure to air. Samples were mounted on the specimen holder by means of double sided adhesive tape. Carbon (1s), metal (2p,3d or 4f) and sulfur (2p) signals were recorded in steps of 0.1 eV (second and third row metal sulfide catalysts) or 0.2 eV (first row metal sulfides). Scan times were varied according to the intensity of the signals. The C 1s peak was used as internal standard (284.6 eV) for binding energy calibration.

RESULTS

In Table 1 the raw conversion data, as well as the rate constants for the hydrodesulfurization and hydrogenation calculated after 2 h run time are collected. Since deactivation after 2 h run time is estimated to be less than 1% thiophene conversion decrease per hour, the activity data reported in Table 1 are taken from reasonable stabilized catalysts. Plotting the catalyst activity against the position of the metal in the periodic table yields typical volcano type curves for second and third row elements (cf. Fig. 1). Second and third row elements of the same group have about the same HDS activity. Furthermore the volcano type plots show some asymmetry due to a more pronounced decline in activity at the right side (Pt, Pd) of the curves. Maximum activity is located at Rh and Ir. HDS activity for first row transition metal sulfides shows a

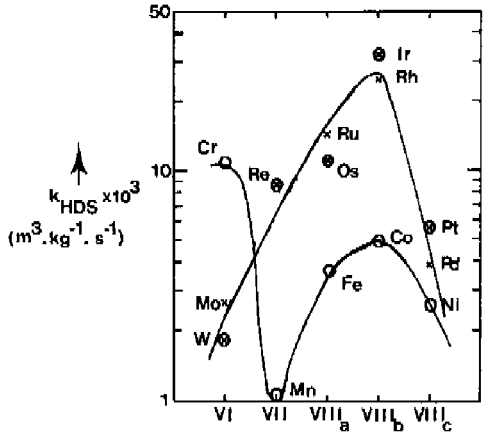

Fig. 1 Periodic trends for the rates of HDS Me/C catalysts.

Table I : Activity measurements of Me/C catalysts

Catalyst	Precursor metal salt	Thiophene conversion (%)	k_{HDS} x 10^3 (m^3/kg.s)	k_{HDS} x 10^3 (m^3/kg.s)
4.9% Cr/C	$Cr(NO_3)_3.9H_2O$	68	10.8	48.2
5.2% Mn/C	$MnCl_2.4H_2O$	<1	<0.1	-
5.3% Fe/C	$FeCl_3.6H_2O$	33	3.8	7.5
5.6% Co/C	$CoCl_2.2H_2O$	40	4.9	4.5
5.6% Ni/C	$NiCl_2.6H_2O$	24	2.6	4.0
8.8% Mo/C	$(NH_4)_6Mo_7O_{24}.4H_2O$	35	3.7	8.0
9.2% Ru/C	$RuCl_3$	78	14.6	26.3
9.3% Rh/C	$RhCl_3.xH_2O$	92	23.9	112.1
9.6% Pd/C	$PdCl_2$	34	3.9	14.3
15.9% W/C	$(NH_4)_2W_4O_{13}.8H_2O$	17	1.8	12.5
15.7% Re/C	NH_4ReO_4	61	8.9	10.9
16.0% Os/C	$OsCl_3$	66	10.3	38.9
16.1% Ir/C	$H_2IrCl_6.xH_2O$	96	31.6	320.3
16.3% Pt/C	$H_2PtCl_6.6H_2O$	44	5.6	47.5

twin-shaped pattern, with Fe, Co and Ni following approximately a similar curve as the second and third row elements but a factor 2-6 lower in activity. Mn had very low activity, while surprisingly Cr was the most active first row element and the only first row transition metal sulfide that had a higher activity than the corresponding second and third row sulfides.

The butene hydrogenation capability of the carbon supported transition metal sulfides behaves analogous to the HDS activity ; volcano type plots for second and third row sulfides, with maxima located at Ir and Rh, and a twin-shaped curve for the first row elements with Cr and Fe as the most active catalysts. In general, the hydrogenation activity increases from first to second to third row elements.

In Table 2 XPS data of the catalyst samples are presented, while in Fig. 2 the 2p, 3d and 4f metals photoelectron signals are shown, arranged in first (2p), second (3d) and third (4f) row elements. Because of the wide range in transition metal sulfide binding energies, spectra are plotted relative to the corresponding binding energies of the metals. The sulfidation procedure applied clearly converts the precursor metal salts into their metal sulfide form. No chlorine of the precursor salts was retained on the sulfided catalysts. The measured metal binding energies indicate that the following metal sulfides were mainly present : Cr_2S_3, MnS, FeS, Co_9S_8, Ni_3S_2, MoS_2, Rh_2S_3, PdS, WS_2, ReS_2, PtS (6-8). No XPS literature data could be found on Ru, Ir or Os sulfides. However, since the measured binding energies are about 1.0 eV (Ru, Ir) higher in energy than those of the corresponding metals, it is evident that also Ru and Ir are in a positive valence state coordinated by S ligands. The major part of the S 2p peak arises from the presence of S^{2-} sulfide ions coordinated to the metal ions ; but there is also a contribution from elemental sulfur (164.0 eV) which is produced during sulfidation.

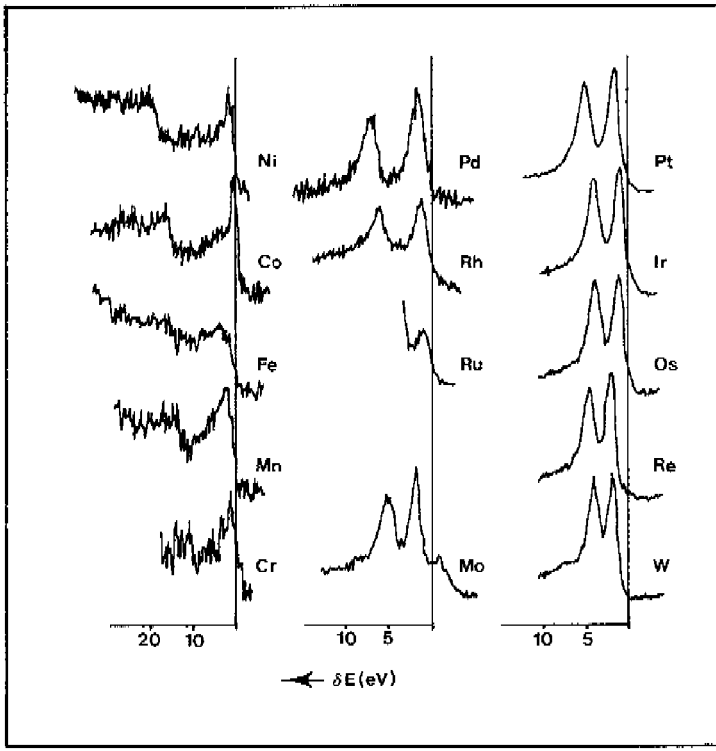

Fig. 2 XPS spectra of sulfided Me/C catalysts plotted relative to the metal binding energies. For Ru only the $3d_{5/2}$ line was resolved from the C 1s signal and for the Os catalyst an arbitrary shift of 1 eV relative to the metal B.E. was chosen.

Except for the case of Fe this S^0 contribution is small. The measured S/Me ratios (Table 2), corrected for the amount of sulfur formed in a blank experiment with the pure carbon support, are fairly close to the stoichiometries expected for most of the stable sulfides, although the elemental sulfur produced by the catalysts is included in the measured

Table 2 : XPS results of Me/C catalysts

Catalyst	Metal binding energies	S 2p binding energies	$\frac{I_{Me}}{I_C}$	$\frac{I_S}{I_{Me}}$	Particle size (nm)	$\frac{S^*}{Me}$	phases present after sulfidation
Cr	575.1/584.4	162.3	0.147	0.238	0.5	1.6	Cr_2S_3
Mn	640.7/652.0	161.2	0.186	0.192	0.5	1.4	MnS
Fe	710.0/723.4	162.7	0.131	0.239	1.5	2.6	FeS_x+S^0
Co	778.2/793.4	162.8	0.204	0.086	1.0	1.1	Co_9S_8
Ni	853.2/870.8	162.8	0.225	0.092	0.5	0.94	Ni_3S_2
Mo	229.3/232.4	162.8	0.078	0.342	2.0	1.9	MoS_2
Ru**	281.0/ -	163.3	-	-	-	-	RuS_x
Rh	308.2/312.9	163.2	0.094	0.179	2.5	1.5	Rh_2S_3
Pd	336.4/341.6	162.9	0.111	0.097	2.5	0.93	PdS
W	32.8/ 34.9	162.9	0.136	0.425	-	2.5	WS_2
Re	42.3/ 44.6	163.0	0.081	0.301	2.0	2.0	ReS_2
Os	51.5/ 54.1	163.2	0.215	0.113	-	0.82	OsS_x
Ir	61.6/ 64.5	163.1	0.231	0.180	-	1.5	IrS_x(no Ir^0)
Pt	72.5/ 75.8	163.4	0.087	0.146	3.5	1.3	PtS

* λ_{Me}/λ_S calculated according to
$\lambda_{Me}/\lambda_S = \varepsilon_{Me}/\varepsilon_S\,[(\ln\varepsilon_S - 2.3)/(\ln\varepsilon_{Me} - 2.3)]$

** Due to the vicinity of the C 1s peak no peak areas could be calculated for Ru.

ratios. Mostly this contribution will be small except for Fe. A shoulder in the S 2p signal located around 169 eV (SO_4^{2-}) was observed only for Cr, Fe and Co, pointing to the reactive nature of these sulfides towards traces of oxygen still present in the glove box. To obtain an indication on the dispersion of the catalysts we have used XPS intensities to calculate the particle sizes. The calculations were carried out according to the catalyst model described by Kerkhof and Moulijn (9). For the third row, Os and Ir sulfides the experimental metal over carbon intensity ratios were larger than the theoretical values predicted for monolayer coverage. It is very probable that the distribution of the sulfide phase on the carbon support is not uniform due to an enrichment of this phase at the outer surface of the support graines. As a consequence no particle sizes could be calculated for these catalysts. For

Pt, Re, first and second row elements, particle sizes could be calculated. Since almost no information is available on electron mean free paths (λ) through transition metal sulfides, we estimated λ on the basis of photoelectron kinetic energy : $\lambda \sim E_{kin}^{0.75}$ (10). Although, the particles of the first row metal sulfide catalysts were found to be smaller (average 1.0 nm) than the second and third row metal sulfide particles (average 2.5 nm), all sulfide catalysts seemed well dispersed. In view of the difficulties in XPS particle size determination of the present catalysts the reported data should be considered as indications rather than absolute values. Absolute particle sizes can only be obtained in combination with complementary techniques such as high resolution transmission electron microscopy or selective gas chemisorption. When the HDS activities are normalized for the calculated particle sizes the periodic trends for HDS changes only slightly (cf. Fig. 3).

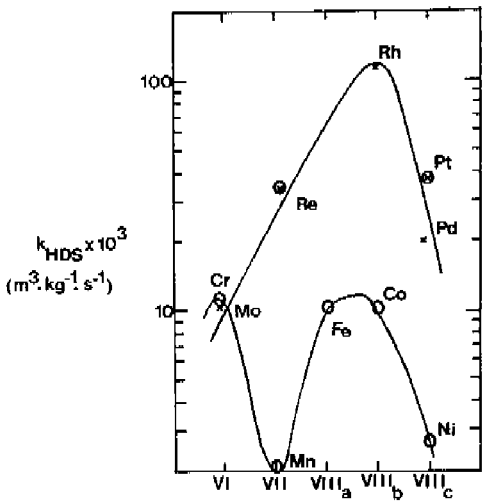

Fig. 3 Periodic trends for the rates of thiophene HDS of Me/C catalysts, normalized on 0.5 nm particle size (100% dispersion).

DISCUSSION

Since the XPS metal peak positions and the major sulfur peaks were close to those of the corresponding stable sulfides we conclude that, during the sulfidation procedure applied, the metal salts are completely converted to the metal sulfides. The relative HDS activities of the carbon supported sulfide (Me/C) catalysts correlate very well with those reported for the unsupported sulfides (1), although completely different test conditions were applied ; high pressure (31 bar) HDS of dibenzothiophene at 673 K for the unsupported systems and atmospheric thiophene (673 K) HDS for the Me/C catalysts. Especially for the second and third row elements, where the typical volcano curves with periodic position were obtained, the similarity is striking. This once more, strongly suggests that the HDS activity of Me/C catalysts is related to the presence of metal sulfides formed on the carbon and not of metal carbides nor metal intercalates. Differences in periodic HDS activity trends between the unsupported sulfides and Me/C catalysts are the locations of the maxima at Rh and Ir for the Me/C systems instead of Ru and Os for the unsupported catalysts and the slight asymmetry in the volcano curves for the Me/C catalysts. In general for the first row elements the same features were found as for the unsupported systems, viz. maximum and lowest activity for Cr and Mn respectively. Fe, Co and Ni sulfide catalysts supported on carbon showed, however, an appreciable HDS activity whereas the unsupported systems were relatively inactive. In this respect it must be mentioned that Pecoraro and Chianelli (1) have used unsupported first row sulfides having low surface areas. As a consequence the activities of these sulfides are probably underestimated relative to those of the second and third row elements. On the other hand, when corrected for particle size the activity of the first row Me/C catalysts decreases relative to second and third row elements (cf. Fig. 3).

We conclude that the results obtained with the sulfided Me/C catalysts confirm the earlier reported (1) conclusion concerning the unsupported sulfides : viz. the primary effect in HDS by transition metal sulfides is the "electronic" effect which is related to the position of the element in the periodic table. This implies that the crystal structure of the sulfides is of secondary importance, and thus that HDS activity is not related to sulfides having a layered structure. In fact it may be argued that transition metal sulfides function as the well known Birch reductor system in organic chemistry : organic molecules are reduced in potassium or sodium in liquid ammonia by electrons and are subsequently protonated. The same might hold for the reduction of sulfur and nitrogen containing molecules in HDS and HDN reactions, since transition metal sulfides in their substoichiometric state, as present under working conditions are good conductors and their surface is full of SH groups which supply protons.

At this point we want to emphasize the relative ease with which the results on the carbon-supported sulfide catalysts were obtained. Nothing more than a simple pore volume impregnation with the appropriate metal salt solution, followed by drying and sulfidation of the catalyst precursor was involved. This advantage will become even more apparent when promoting effects are studied, for the preparation of unsupported promoted transition metal sulfides causes severe problems with proper mixing of the two elements and obtaining samples with reasonable surface areas.

It is tempting to relate the observed periodic trends for HDS to some chemical or physical parameter. In a recent study Harris and Chianelli (11,12) compared X molecular orbital calculations of MeS_6^{n-} complexes with catalytic properties for HDS. They identified that the orbital occupation of the highest occupied molecular orbital (HOMO) together with the metal-sulfur covalent bond strength were important factors which determine catalytic activity. They

suggested that binding of an organic sulfur molecule with its ring sulfur atom to an exposed metal atom (active site) depends on the ability of the metal to bond covalently with sulfur through combined sigma and p interactions. It is interesting to note that these theoretical calculations indicate that maximum activity is located at Rh and that the volcano plots are asymmetric. These features are strikingly well reproduced in our experimental results.

For the second and third row elements we are able to relate the experimental HDS activities with the observed chemical shift of the metal sulfides. Recall Fig. 2, where the metal photoelectron signals of the catalysts are plotted relative to their corresponding metal binding energies. It is this core level shift, δE, of the $3d_{5/2}$ or $4f_{7/2}$ photoelectrons of the metal sulfide relative to their metal valence state which shows a remarkable correlation with the catalytic activities of the corresponding sulfides as is shown in Fig. 4. Highly active sulfides have small chemical shifts. Only ReS_2 forms an exception.

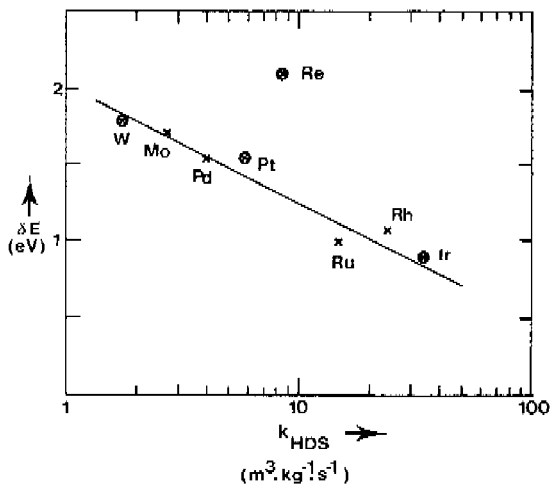

Fig. 4 Correlation between the chemical shift (δE) and HDS activity for second and third row Me/C catalysts.

The question arises why this correlation holds. In order to answer this we have to consider the origin of the core level shift. In metal sulfides the metal and sulfur orbitals combine to form a valence electron distribution which is such that there is a small positive charge on the metal atom. As a result all inner core levels of the metal atom will experience a small energy shift proportional to the charge on the metal atom. Low chemical shifts will be obtained for those transition metal sulfide catalysts which have removed as much sulfur ligands as possible, creating a sulfur deficient highly reduced sulfide, and for those where the valence electrons in the metal sulfur molecular orbitals maintain their metal character. It may be clear from these observations that highly active transition metal sulfides preserve their metallic character in the sulfide phase under reaction conditions. These conclusions agree very well with the theoretical calculations of Harris and Chianelli (11,12). For the second row elements the number of d electrons in the HOMO is highest for Ru and Rh sulfides because only the $2t_{2g}$ level is occupied in a low spin configuration, whereas for Pd sulfide the $3e_g$ level is occupied. Looking at the charge distributions of these antibonding energy levels it can be seen that in the $2t_{2g}$ level the electrons are localized primarily on the metal atom (69% for Ru) while the $3e_g$ level is quite diffuse. Therefore, sulfides with high occupancy of the $2t_{2g}$ level will have low chemical shifts, while occupation of the $3e_g$ level will increase the chemical shift of the sulfide. Highly active catalysts have high occupancy of the $2t_{2g}$ level, while less active sulfides have the $3e_g$ level occupied, which is completely consistent with the predicted chemical shift-activity relation. Also the finding that the more active catalysts have covalent metal-sulfur bonds is compatible with our results, since increased covalency or metal sulfur d-p mixing is equal to increased metal character of the electrons in the bonding energy levels.

It is challenging to incorporate the above findings in an explanation of the observed differences in the catalytic activity of alumina and carbon supported transition metal sulfides. It is well known that alumina interacts strongly with the deposited sulfide phases probably through interactions of oxygen anions with the transition metal cations. This will cause an extra charging of the transition metal since oxygen is a harder ligand than sulfur with less covalent character. Based on the above discussion it must be concluded that the activity of alumina supported catalysts will be lower than those of the corresponding Me/C catalysts, and this is indeed what the experimental results show. (4,13). The alumina support-metal sulfide interaction seems to be largest for second and third row group VIII a, b elements since especially their activity is lowered considerably relative to the carbon supported or unsupported catalysts.

CONCLUSIONS

- By means of XPS analysis it is demonstrated that, under the conditions applied, sulfiding of the activated carbon supported transition metal chloride, nitrate or oxide catalysts used in this study results in the formation of a transition metal sulfide phase.

- It is clearly established that, nothwithstanding differences in testing conditions, the relative HDS activities of these carbon supported sulfide catalysts, are very much the same as the relative HDS activities measured by Pecoraro and Chianelli (1) for unsupported sulfides. In both cases typical volcano shaped curves were obtained for the second and third row metal sulfides while first row elements show a twin-shaped curve. This implies that small sulfide particles deposited on a carbon surface evidently

have the same catalytic properties for HDS reactions than bulky unsupported particles.

- For second and third row sulfides HDS activity is found to correlate with the chemical shift between metal and metal sulfide. This indicates that high activity catalysts preserve best their metallic character either through sulfur deficiency and/or high metal character of the valence molecular orbitals.

REFERENCES

1. Pecoraro, T.A., and Chianelli, R.R., J.Catal., 67 430 (1981).
2. Wakabayashi, K., and Orito, Y., in Report of the Government Chemical Industrial Research Institute, Tokyo, 66, 382 (1971).
3. Dhainut, E., Charcosset, H., Gachet, C., and Mourgues, L., Appl. Cat. 2, 75 (1982).
4. Duchet, J.C., Van Oers, E.M., de Beer, V.H.J., and Prins, R., J. Catal. 80, 386 (1983).
5. Konings, A.J.A., van Doorn, A.M., Koningsberger, D.C., de Beer, V.H.J., Farragher, A.L., and Schuit, G.C.A., J. Catal. 54, 1 (1978).
6. Wagner, C.D., Riggs, W.M., Mouder, J.E., and Muilenberg, G.E., "Handbook of X-ray Photoelectron Spectroscopy", Perkin-Elmer Press (1978).
7. Wang, T., Vasquez, A., Kato, A., and Schmidt, L.D., J. Catal. 78, 306 (1982).
8. Alstrup, I., Chorkendorff, I., Candia, R., Clausen, B.S., and Topsøe, H., J. Catal. 77, 396 (1982).
9. Kerkhof, F.P.J.M., and Moulijn, J.A. J. Phys. Chem., 83, 1612 (1979).
10. Szajman, J., Liesegang, J., Jenkin, J.G., and Leckey, R.C.G., J. of Elect. Spec. and Rel. Phen. 23, 97

(1981)

11. Harris, S., and Chianelli, R.R., J. Catal. 86, 400 (1984).
12. Harris, S., Chem. Phys. 67, 229 (1982).
13. Vissers, J.P.R., Bachelier, J., Ten Doeschate, H.J.M., Duchet, J.C., de Beer, V.H.J., and Prins, R., in Proceedings of 8th International Congress on Catalysis, Berlin, 1984, Verlag Chemie, Weinheim, P. II-387, 1984.

CHAPTER 6

THE ROLE OF THE CARBON SURFACE OXYGEN FUNCTIONALITY ON THE DISPERSION OF CARBON BLACK-SUPPORTED MOLYBDENUM CATALYSTS.

ABSTRACT

Four carbon black samples differing in surface area, pH and surface properties (oxygen functionality) were pore volume impregnated with aqueous molybdate solutions as to achieve a Mo loading of 0.5 Mo atoms per nm^2 support surface area. Dispersion measurements obtained by means of X-ray photoelectron spectroscopy, dynamic oxygen chemisorption and transmission electron microscopy, indicated the presence of highly dispersed molybdate in all precursor samples, which upon sulfidation was converted into molybdenum sulfide with a particle size varying between 3.5 and 13.5 nm dependant on the type of carbon black support. To explain these dispersion differences the interaction between molybdate ions and the carbon surface was studied by means of FTIR and XPS. No major changes were observed in the oxygen functionality of the carbon black upon loading with molybdate. Some minor changes were, however, observed by means of FTIR which could point to a chemical reaction between an aryl ether functional group and the molybdate ions.

INTRODUCTION

Refining of oil fractions often involves conversion of the hydrocarbon fraction to different forms. In one such conversion, hydrodesulfurization, the concentration of sulfur components in the hydrocarbon feedstock is reduced so that, when the product is eventually combusted, less sulfur

oxides will form, and hence enviromental pollution will be reduced. To this is added that it is very often desirable to remove sulfur in order to prevent poisoning of downstream catalysts. Hydrodesulfurization (HDS) has been carried out succesfully on an industrial scale for decades, over catalysts comprising Mo or W sulfide promoted with Co or Ni sulfide, supported on a porous alumina carrier. The increased world wide industrial application supplies a continuous drive to a better understanding of these complex catalyst system and to search for improved catalytic ensembles. In this respect it has been shown that carbon-supported catalysts, under the reaction conditions applied, showed higher HDS activities [1,2], coupled to lower coking propensities [3,4] than alumina-supported systems. Moreover, the carbon-supported transition metal valuables can be easily recovered from spent catalysts by burning off the carbon carrier. These interesting properties of carbon-supported sulfide catalysts were the outset of research, aimed at elucidating the structure and related HDS activity of these catalyst systems [2,4-10].

The present paper focusses on the interaction of the carbon surface with initially deposited molybdate ions, which forms the precursor state of the catalyst. It presents a contribution to the unraveling of the role that carbon surface oxygen functionality might play with respect to the dispersion of the precursor catalyst and of the dispersion of the actuallly active state of the catalyst obtained after sulfidation. While on the commercially applied alumina support the exposed surface hydroxyl groups serve as adsorption sites for the molybdate ions in a condensation reaction [11], a more complex situation is encountered in case of carbon-supported catalysts due to the variety of oxygen functional groups present on the carbon surface. In addition, a sharp distinction among the different functional groups cannot be made since they electronically interact with each other through the aromatic

carbon substrate. In this study Fourier transform infrared spectroscopy (FTIR), X-ray photoelectron spectroscopy (XPS) and thermo gravimetric analysis are used to measure the amount and relative concentration of the various oxygen functional groups. The dispersion of the deposited molybdenum phase was considered of primary importance. Therefore, quantitative XPS intensity analysis of the Mo and C photoelectron signals, selective dynamic oxygen chemisorption (DOC) on the Mo-sulfide phase, and transmission electron microscopy (TEM) analysis, were used to study the dispersion. Four types of carbon blacks differing in surface area and oxygen functionality were applied as carrier materials. The use of carbon blacks was based upon the following considerations :

(i) Scattering in the FTIR spectra is kept to a minimum since the size of the carbon black particles (13-30 nm) although fused into larger aggregates (500 μ nm), is significantly smaller than the infrared wavelengths of interest (2.5-20 μ m) [12]. This allows the measurement of accurate and reproducible spectra.

(ii) Carbon blacks are used as substrate particles in the preparation of carbon black composite materials which are considered to be promising materials for their use as supports for hydrodesulfurization catalysts [10].

EXPERIMENTAL

Catalyst preparation

Four commercial carbon blacks were used as support material : Monarch 700, 1100, 1300, and Ketjen EC, the properties of which are collected in Table 1. The carbon blacks were impregnated (pore volume impregnation) with aqueous solutions of ammonium heptamolybdate (Merck, min 99%). Since the main concern of this study is to evaluate

Table 1 : Carbon black properties

sample	d* (nm)	S_{BET} (m^2/g)	pore volume (ml/g)	pH**
Monarch 700	18	300	1.9	8
Monarch 1100	14	240	1.4	7
Monarch 1300	13	560	1.7	2.5
Ketjen EC	30	1010	4.4	9.5

* mean diameter of the primary carbon black particles, according to the manufacturer.

** according to the manufacturer.

the interaction of the carbon surface with the Mo phase, the catalysts were prepared in such a way that the support surface loading (approximately 0.5 Mo atoms per nm^2 support surface area) was kept constant. Although this results in catalysts with different wt% Mo, it allows a fair comparison to be made among the different carrier surfaces with respect to their ability to disperse the Mo phase. After impregnation the catalysts were dried starting at room temperature and slowly increasing (about 3 hr) up to 383 K where they were kept overnight.

Conversion of the oxidic precursor catalysts into their catalytically active sulfided state was accomplished by sulfiding in a H_2S/H_2 flow (10 mol% H_2S, total flow rate 60 ml/min) using the following temperature program : linear increase (6 K/min) from room temperature up to 673 K and holding at this temperature for two additional hours.

Fourier transform infrared spectroscopy (FTIR)

FTIR spectra were obtained with a Bruker IFS 113v, single beam Fourier-transform spectrophotometer using a globar (SiC) as infrared source and a HgCdTe detector operating at liquid nitrogen temperature. In view of the reactivity and absorption capacity of carbon surfaces, care was taken to avoid artefacts in the spectra that result from

contamination. Spectra were recorded of the pure carbon blacks as well as of the precursor catalysts, in order to detect possible changes in the spectral characteristics arising from molybdate deposition. Prior to FTIR measurement the samples were dried at 393 K overnight in air, together with the KBr reference material. KBr pellets used for FTIR analysis contained 0.25 or 0.125 mg carbon black or catalyst dispersed in 125 mg KBr. These dispersions were prepared from a ground and homogenized standard sample (0.50 mg carbon or catalyst per 125 mg KBr) via dilution and homogenization (grinding in an agate mortar for 10 min). Disks (13 mm) were pressed at 10,000 kg/cm^2 in vacuum (10 torr) and mounted in the evacuated sample compartment of the spectrophotometer. A blank KBr (Merck, "Uvasol fur Spectroscopie") disk was used as a reference. Typically, 512 scans were run in both the reference and sample beams at a resolution of 4 cm^{-1}. The transmission spectra of the samples were obtained by dividing each data point of the spectra by the corresponding data point of the reference KBr spectrum. Spectra were recorded in duplo.

X-ray photoelectron spectroscopy (XPS)

XPS spectra of the carbons and precursor catalysts were recorded on a Physical Electronics 550 XPS/AES spectrometer equipped with a magnesium X-ray source (E=1253.6 eV) and a double pass cylindrical mirror analyzer. The powdered samples were pressed on a stainless steel grid which was mounted on top of the specimen holder. Spectra were recorded in steps of 0.05 eV. The pressure did not exceed 5 x 10^{-8} torr and the temperature was approximately 298 K. Spectra of the sulfided catalysts were recorded on an AEI ES 200 spectrometer equipped with a purified N_2 flushed glove box attached to the XPS introduction chamber. After sulfidation, as described above, the catalyst samples were purged with purified He for 15 min at 673 K and subsequently

cooled within 30 min to room temperature in flowing He. A special reactor [13] allowed transfer of the sulfided samples to the XPS apparatus, without exposure to the air. Samples were mounted on the specimen holder by means of double sided adhesive tape. Spectra were recorded at 283 K in steps of 0.1 eV. The C 1s peak (284.6 eV) was used as internal standard for binding energy calibration.

Dynamic oxygen chemisorption (DOC)

After in situ sulfiding of the samples according to the procedure previously described, the oxygen chemisorption of the pure sulfided carbon black supports and the sulfided catalyst samples was measured at 333 K by injecting 2.19 ml pulses of a 5.20 % O_2/He mixture at 3 min intervals into the carrier gas flow. When effluent O_2 peaks had increased to constant size (less than 1% difference between two successive peaks) the total O_2 uptake was calculated.

Transmission electron microscopy (TEM)

TEM measurements were carried on a Jeol 200 CX top entry stage microscope. Photographs were taken at different magnifications up to 630,000 times. Further enlargements were made photographically. Samples were prepared by applying a slurry of the sulfided catalysts in alcohol on to a carbon coated copper grid, and evaporating the alcohol.

Thermo gravimetrical analysis (TGA)

Weight loss of carbon samples upon heating in a N_2 atmosphere were determined in a Mettler thermobalance up to temperatures of 1173 K.

RESULTS

Dispersion of precursor and sulfided catalysts

The dispersion of the molybdenum phase was measured by means of XPS in case of the precursor catalysts and via XPS, DOC and TEM measurements in case of the sulfided catalysts. Molybdenum particle size can be determined from the Mo/C photoelectron intensity ratio as outlined by Kerkhof and Moulijn [14]. In their model the catalyst is thought to consist of sheets of support with cubic active phase crystallites of dimension c deposited on both sides. The thickness of the sheets (t) is estimated from the density (ρ) and the surface area (s) of the support : $t = 2(\rho s)^{-1}$. It is assumed that the electrons leave the sample in a direction perpendicular to the surface and that a Lambert-Beer type law is valid. Theoretical intensity ratios can be calculated for monolayer dispersion of the Mo phase on the different supports, taking into account the photoelectron transparancy of the support sheets. Deviation of the experimentally found Mo 3d/C 1s intensity ratio from the calculated monolayer ratio, indicates the presence of crystallites, the average size (c) of which can be calculated according to :

$$\frac{[I_{Mo}/I_C]_{exp}}{[I_{Mo}/I_C]_{mono}} = \lambda / c \, [1 - \exp(-c/\lambda)]$$

with c = crystallite size

λ = escape depth of Mo 3d electrons through the Mo oxide (precursor catalyst) or Mo sulfide phase (sulfided catalysts)

In Table 2 the quantitative XPS data of the precursor and sulfided catalysts are collected. It can be seen that for the precursor catalysts the particle sizes are small.

Table 2 : Quantitative XPS data of carbon black-supported Mo catalysts

support	wt% Mo	theoretical I_{Mo}/I_C for monolayer coverage	oxidic state		sulfided state	
			$[I_{Mo}/I_C]_{exp}$	Mo particle size (nm)	$[I_{Mo}/I_C]_{exp}$	Mo particle size (nm)
Monarch 700	1.45	0.033	0.027	0.6	0.010	9.5
Monarch 1100	1.70	0.033	0.026	0.7	0.014	3.8
Monarch 1300	4.06	0.057	0.050	0.4	0.025	3.5
Ketjen EC	7.08	0.099	0.067	1.2	0.013	13.5

Especially the Monarch 1300-supported catalyst is nearly monolayer-like dispersed. The catalyst based on Ketjen EC contains slightly larger particles. Upon sulfidation considerable particle growth takes place. Ketjen EC is found to contain large sulfide particles, while the smallest sulfide particles are present on Monarch 1300.

The dispersions obtained by means of XPS are only reliable if the deposited particles are homogeneously distributed on the support surface area. If on the other hand the Mo phase is inhomogeneously dispersed on the carbon surface, the experimental Mo/C intensity ratios cannot be used for comparison with the theoretical monolayer ones to predict Mo particle sizes since the monolayer ratio assumes deposition of Mo on the entire surface area of the carbon. For instance when Mo is deposited preferentially on the outer surface of the support grains, the Mo XPS signal will be overestimated relative to the C signal and a too low particle size will be calculated. In order to get an indication of the degree of homogeneity of the samples, dispersions of the sulfided catalysts were determined using dynamic oxygen chemisorption (DOC) which measures the amount of oxygen chemisorbed on the molybdenum sulfide surface [2,15-16]. Being a gas pulse technique, DOC is insensitive to the distribution of the particles on the

Table 3 : Dynamic oxygen chemisorption on carbon black-supported Mo sulfide catalysts.

support	wt% Mo	total oxygen uptake (mol O/g cat x 10^4)	oxygen uptake of the support (mol O/g support x 10^4)	oxygen uptake of Mo-sulfide (mol O/g cat x 10^4)	$\frac{O}{Mo}$
ionarch 700	1.45	0.54	0.19	0.35	0.23
ionarch 1100	1.70	0.86	0.37	0.50	0.28
ionarch 1300	4.06	1.97	0.49	1.51	0.36
etjen EC	7.08	1.48	0.83	0.74	0.10

support. Hence, comparison of the dispersion data derived by means of XPS and DOC gives an indication of the homogeneity of the sample. In Table 3 the DOC results of the sulfided catalysts are collected. The values have been corrected for the oxygen uptake of the carbon black supports, which were determined in separate experiments. The O/Mo ratios are a measure for the dispersion of the catalyst, viz., the higher this ratio, the higher catalyst dispersion. As can be judged from these O/Mo ratios, a clear dispersion difference is noticed among the catalysts. Very interestingly, the DOC dispersions correlate with those measured by means of XPS. This is graphically depicted in Fig. 1, where $(O/Mo)^{-1}$ values are plotted against XPS particle size. From the linear correlation it appears that the Mo sulfide phase is indeed homogeneously dispersed on the carbon surface. Hence, the calculated XPS particle sizes can be considered as being reliable.

As a last check on the dispersion of the catalysts we performed TEM measurements of the sulfided Monarch 1300 and Ketjen EC catalysts, being the catalysts with the highest and lowest dispersion, respectively. In case of the Monarch 1300-supported catalyst no particle contours could be discerned in the micrographs, while for the Ketjen EC-supported catalyst large particles were observed.

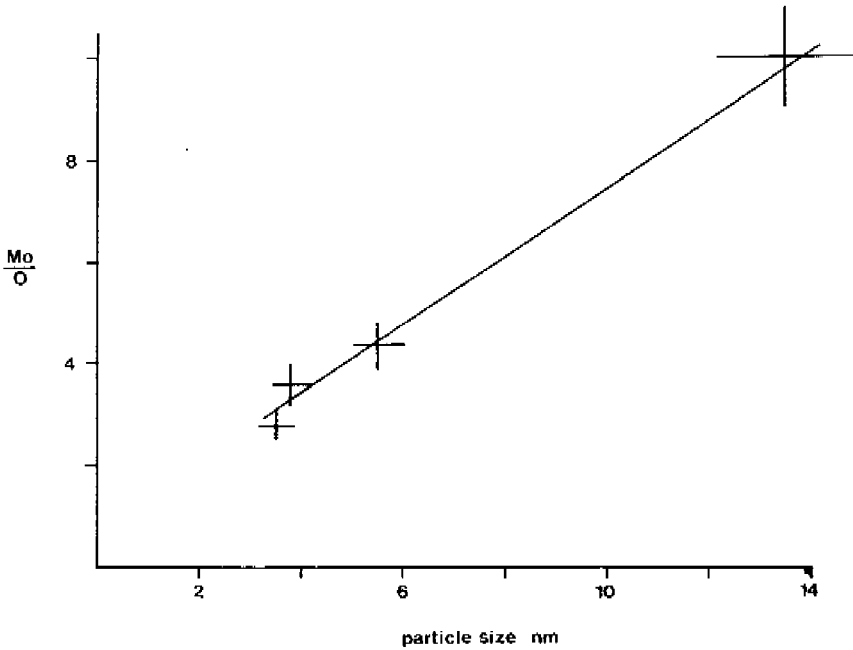

Fig. 1 DOC Mo/O ratios versus XPS particle size for sulfided carbon black-supported Mo sulfide catalysts. The estimated accuracy of the measurements is indicated.

Figures 2 and 3 are typical micrographs of Mo-sulfide particles on Ketjen EC support, taken at different magnifications. Figure 2 shows the presence of large particles (d = 10-40 nm), while Fig. 3 shows a high resolution micrograph of a typical particle. The overall hexagonal symmetry of MoS_2 is clearly observed. Furthermore, the graphitic layers of the carbon support can be noticed, and also lattice fringes in the particle approximately 0.32 nm apart can be observed. These very probably correspond to different layers of Mo atoms in MoS_2 viewed perpendicular to the basal planes.

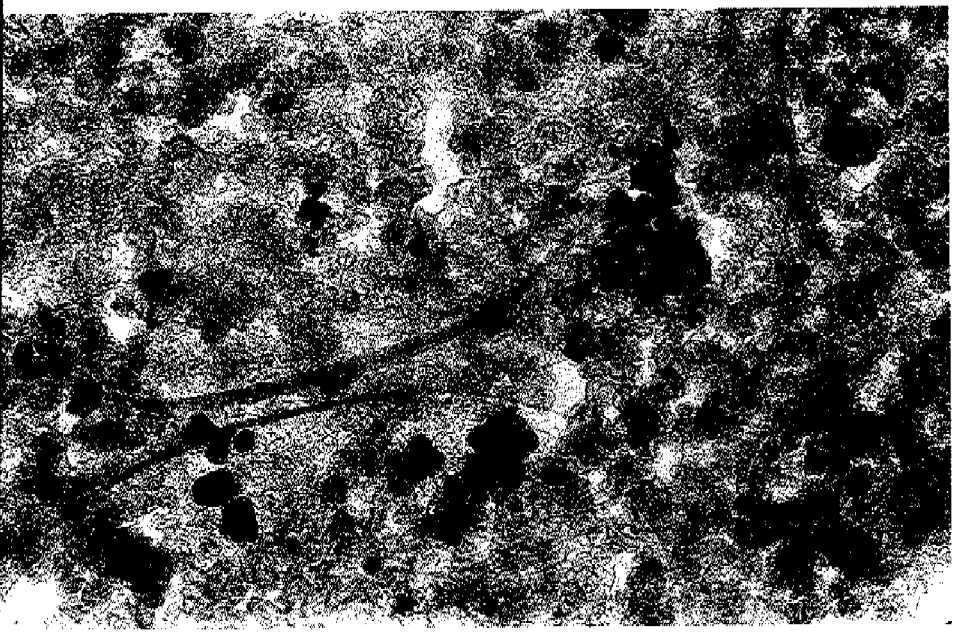

Fig. 2 Electron micrograph of sulfided Mo/Ketjen EC catalyst (mag. 64000 x).

Fig. 3 Electron micrograph of sulfided Mo/Ketjen EC catalyst (mag. 1008000 x) showing a MoS_2 crystallite.

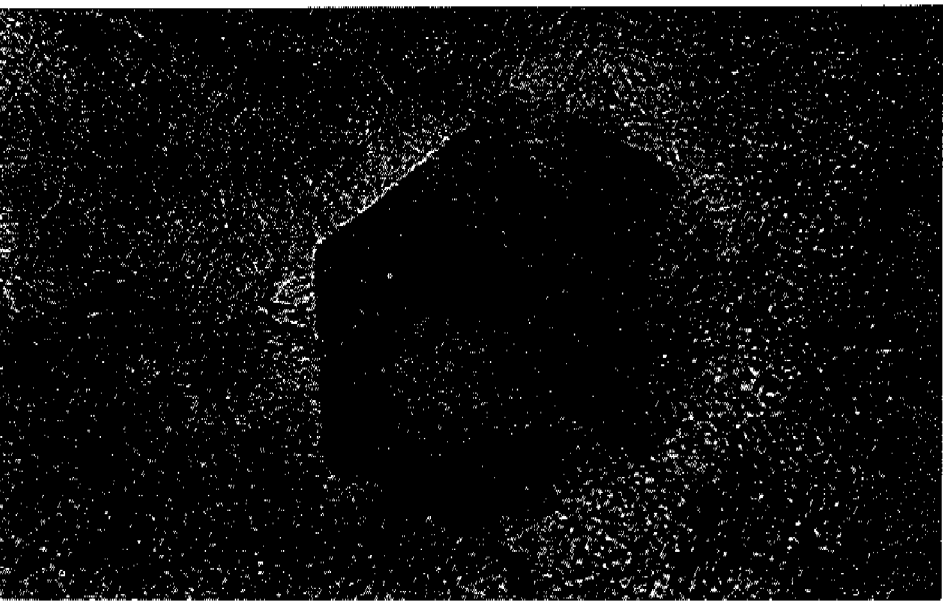

Surface oxygen functionality on carbon black supports

A measure of the total amount of oxygen functionality on the carbon black supports was made by means of thermo gravimetrical analysis (TGA). In Fig. 4 the TGA curves are depicted. For Monarch 1300 considerable weight loss is noticed, although a large part (approximately 8 wt%) seems to be due to water evaporation from the pores. Ketjen EC has a very low oxygen functionality as can be judged from the low weight loss. This finding was confirmed by element analysis (combustion method) which indicated 97.1% C ; 0.9% H ; 1.0% N and 1.0% O for Ketjen EC.

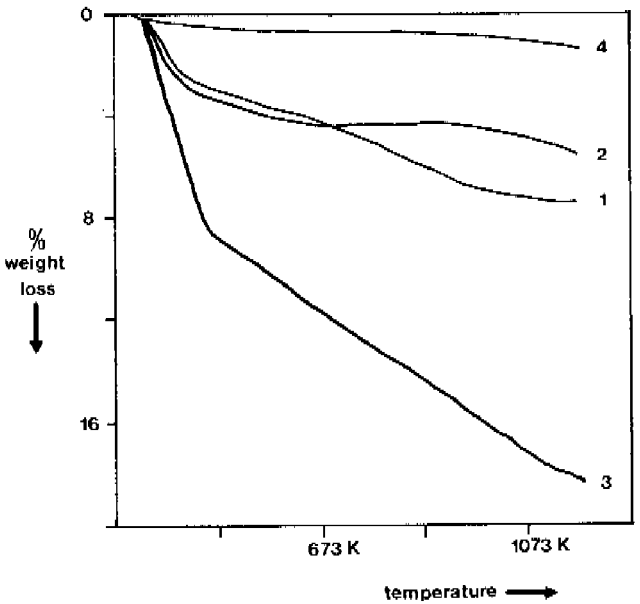

Fig. 4 Weight loss of carbon black supports upon heating in N_2 (TGA).
(1) Monarch 700 ; (2) Monarch 1100 ; (3) Monarch 1300 ; (4) Ketjen EC.

The Fourier transform infrared absorbance spectra of the carbon blacks are presented in Fig. 5. The spectra consist of small signals in the 800-1800 cm^{-1} region superimposed upon a broad background which is almost a linear function of the wavenumber. This background should be attributed to the intrinsic absorption of the particular carbon black rather than to scattering [12]. Furhtermore, the apparant background of the different samples obeys Beer's law in the concentration range studied. Unlike in other studies [12,17] no moisture peaks were detected in the 3200-3600 cm^{-1} region. In order to extract the spectral features superimposed on the absorption background a linear baseline with endpoints at 1800 and 800 cm^{-1} was substracted. The resultant spectra are shown in Fig. 6. Two bands are observed, centered at 1720 cm^{-1} and 1600 cm^{-1}, and a broad envelope ranging from 1000 to 1500 cm^{-1}. These bands in the resolved spectra also obey Beer's law in that the magnitude of the absorbance (peakheight) is linear with the concentration of carbon black in the sample (0.25 or 0.125 mg carbon black per 125 mg KBr).

An obvious feature of the spectra is that the bands are all very broad, which is probably due to the range of different electronic enviroments of a given functional group. Remarkably, the spectral features of Ketjen EC are the most intense in spite of its low amount of functional groups. In the literature [12,17,18] the observed bands are related to the following absorption phenomena :

- 1720 cm^{-1} : C=O stretching frequencies of lactone, aldehyde and most probably carboxylic acid,
- 1600 cm^{-1} : skeletal modes of the aromatic carbon structure, enhanced by the presence of surface oxygen groups,
- 1000-1500 cm^{-1} : C-O stretching frequencies of carboxylic acid, phenol, ethers, etc. and to bulk absorption processes of the carbon black.

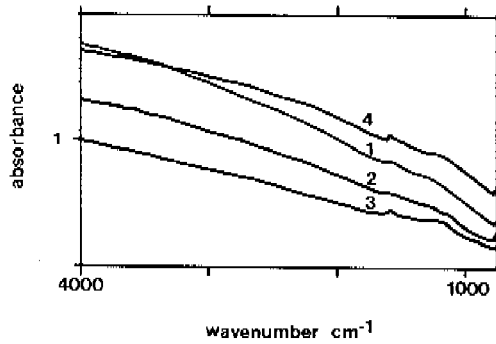

Fig. 5 FTIR spectra of carbonblack samples.
(1) Monarch 700 ; (2) Monarch 1100 ; (3) Monarch 1300 ; (4) Ketjen EC.

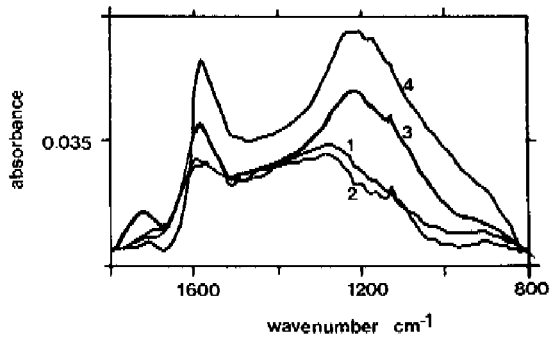

Fig. 6 Baseline resolved carbon black FTIR spectra in the 1800-800 cm^{-1} range.
(1) Monarch 700 ; (2) Monarch 1100 ; (3) Monarch 1300 ; (4) Ketjen EC.

In view of these assignments the following conclusions can be drawn concerning the different carbon blacks :

- Ketjen EC seems to have a specific carbon structure, different fron other carbon blacks, which demonstrates high IR absorption in spite of a very low content of oxygen functional groups. Perhaps the highly graphitic character, the electrical conductivity nature or the hollow shell particle structure [19], determine these spectral features.
- The intensity of the spectral features of Monarch 1300, 1100 and 700 are proportional to the amount of oxygen functionality.
- Monarch 1300 has a high content of carboxyl groups (intense 1720 cm^{-1} band) which is consistent with the low pH value of this black (pH=2.5) and the considerable weight loss in the low (<700 K) temperature region of the TGA pattern, which is associated with the decomposition of carboxyl groups into CO_2.

The C 1s XPS spectra of Monarch 1300 and Ketjen EC carbon blacks are presented in Fig. 7. Extensive studies [20-24] on the C 1s core level binding energy shifts of a wide range of compounds have demonstrated that these shifts tend to occur in groups. The following shifts in binding energy for carbon-oxygen structures have been observed : C-O, ΔE = + 1.6 eV ; C=O, ΔE = + 3.0 eV, and COO, ΔE = + 4.0 - 4.5 eV, all relative to an aromatic carbon atom not attached to oxygen, having a binding energy of 284.6 eV.

The overall C 1s signals of Monarch 1300 and Ketjen EC are very much alike, showing typical asymmetric tail structures on the high binding energy side. Apart from the contribution arising from the carbon-oxygen structures, electron excitation [25] or interband transitions have been reported to contribute to the tail structure. Monarch 1300 has the most intense satellite structures which is consistent with its high amount of oxygen functionality.

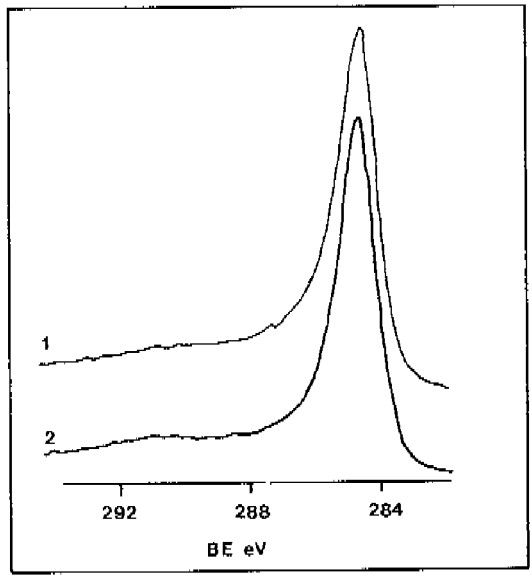

Fig. 7 C 1s photoelectron signals of Monarch 1300 (1) and Ketjen EC (2) carbon black.

Changes in oxygen functionality on carbon black supports after catalyst impregnation

In order to determine the changes in the FTIR absorbance spectra of the impregnated precursor catalysts compared to the pure carbon blacks, the spectra recorded for the catalysts were substracted by means of the computer from those recorded for the unloaded carbon blacks. In Fig. 8 the difference spectra (0.25 mg sample per 125 mg KBr) are presented for the Ketjen EC, Monarch 1100 and Monarch 1300 samples. The difference spectra were found to be reproducible. Generally speaking, no large differences in spectral characteristics of the precursor catalysts compared to the pure supports could be noticed, indicating that no

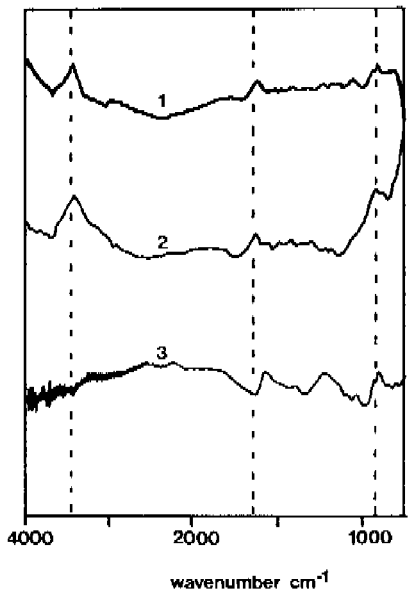

Fig. 8 FTIR difference spectra : ammoniumheptamolybdate (aqueous solutions) impregnated carbon black minus unloaded carbon blacks.
(1) Monarch 1100 ; (2) Monarch 1300 ; (3) Ketjen EC.

large variations in the carbon surface oxygen functionality occurs upon impregnation with molybdate ions. However, the following features can be discerned from Fig. 8 :

- For all samples studied a negative peak is present in the difference spectra around 1700 cm^{-1} while a positive peak seems to be present around 1600 cm^{-1}. This points to a shift of the 1600 cm^{-1} band in the catalysts relative to the unloaded carbon blacks.
- For all samples a positive peak is present around 900 cm^{-1}.
- For the Monarch 1100 and Monarch 1300 samples a positive

peak appears around 3400-3450 cm^{-1} in the difference spectra.

The normalized difference spectra (precursor catalyst minus pure support) of the C 1s photoelectron signal for the Monarch 1300 and Ketjen EC sample show no noticeable difference in the tail structure of the C 1s peak of the precursor catalysts compared to the unloaded supports. This implies that XPS detects no major changes in the carbon surface oxygen functionality of the carbon blacks upon addition with molybdate ions.

DISCUSSION

It has been shown that the dispersion of carbon-supported particles largely depends on the surface properties of the carbon substrate. Walker and co-workers [26,27] observed a distinct difference in size distribution of platinum particles supported on a graphitized carbon black subjected to varying levels of carbon burn-off. Dispersion was found to increase with the extent of prior gasification of the carbon support. They proposed that the effect of gasification increased the heterogeneity of the carbon surface which raised the potential energy barrier for platinum diffusion. Interestingly, the active carbon surface atoms appeared to influence metal dispersion rather than the oxygen functionality. In a comparative study on the properties of iron-based catalysts supported on different types of carbon substrates Groot et al. [28] observed a distinct variation in dispersion of the iron sulfide particles, the general trend being that on the more inert support the lowest degree of dispersion was obtained. Ehrburger et al. [29] observed that the surface area of iron phthalocyanine particles deposited on carbon substrates was higher on a heterogeneous carbon having both basal and edge planes at its surface than on a homogeneous carbon, the

surface of which was composed only of basal planes. Furthermore, they concluded that the oxygen complexes associated with the edge carbon atoms act as anchoring sites for the iron phthalocyanine particles and ensure a higher state of dispersion. Finally, it was recognized by Vissers et al. [10] that molybdenum sulfide was better dispersed on an activated carbon support than on the more inert carbon black composite supports. A number of oxidative treatments which resulted in an increase in the concentration of oxygen functional groups, applied to a carbon composite support, resulted in a higher activity of the catalyst compared to that of the untreated carbon-supported catalyst.

The available evidence indicates that two aspects of the carbon surface, namely the concentration of active carbon surface atoms and the presence of oxygen functional groups can have an important influence on the catalytic properties of carbon-supported catalysts. The active carbon surface atoms are made up of defects, dislocations or discontinuities in the carbon layers creating edge atoms with a high tendency to chemisorb other elements such as oxygen and hydrogen to form functional groups. These active carbon atoms or the oxygen groups could serve as anchor sites for the catalytic metal ions added to the carbon. Upon activation or oxidation of the carbon the amount of active carbon surface and as a consequence the amount of oxygen functionality increases and an improvement in active phase dispersion is observed.

In the present study an attempt was made to describe the interaction of molybdate ions with carbon black surfaces. From the dispersion measurements it became clear that the molybdate ions were highly dispersed on the carbon surfaces which indicates the existence of a sufficiently strong interaction between both phases. However, upon sulfidation particle growth took place especially for the Ketjen EC supported sample, which suggests that the interaction is insufficient to maintain a high degree of dispersion during

sulfiding and reaction conditions. This situation is clearly different from that observed for alumina-supported catalysts where upon sulfidation the Mo oxide monolayer formed after impregnation and calcination is converted into a "single slab" Mo sulfide layer without loss of dispersion loss [30,31].

Comparison of the TGA results with the dispersion measurements indicates that dispersion is best for carbon blacks with high oxygen functionality, suggesting that oxygen functionality is an important factor which controls the interaction between Mo and the carbon support. Our attempts to unravel the role of the oxygen functionality were based on the supposition that, if a chemical reaction takes place between the molybdate ions and a specific oxygen group, a change in the spectral characteristics of the impregnated compared to the unloaded carbon blacks will become apparant. XPS measurements, however, indicated nearly identical spectra for the precursor catalysts and the unloaded carbon blacks. The FTIR measurements, however, indicated some minor differences. The appearance of the 900 cm^{-1} band in the IR spectra of the precursor catalysts can be ascribed to Mo=O vibrations, which is consistent with the spectrum of ammoniumheptamolybdate described in the literature [32]. Evidently, this band provides no information on a possible interaction between molybdate and the carbon surface. On the other hand the appearance of 3400 cm^{-1} band and the shift of the 1600 cm^{-1} band of the precursor catalysts relative to the unloaded carbon blacks supply some evidence of a possible interaction between both phases. Before interpreting these results the significance of the spectral differences presented in Fig. 8 need to be discussed. There is little doubt about the reliability of the 3400 cm^{-1} band for several reasons. Firstly, the reproducibility of this band as measured in duplo experiments was very satisfactory. Secondly identical spectral features (except for the magnitude) were observed

for this band at the two different sample concentrations (0.125 and 0.25 mg sample per 125 mg KBr). And thirdly, the absorbance of this band (approximately 0.03 absorbance units) is well above the limits of detectability which is ± 0.005 absorbance units according to Mosher and Prest [12], and lower than ± 0.01 absorbance units according to our duplo measurements. The shift of the 1600 cm^{-1} band is clearly less pronounced ; although the reproducibility was found to be satisfactory even in the different sample concentrations, the absorbance of this band in the difference spectra (± 0.01 absorbance units) (Fig. 8) is at the limit of detectability. Furthermore, this shift can also be caused by a Christiansen effect [33,34] if the particles (fused conglomerates of the primary carbon black particles) of the precursor catalysts and unloaded carbon black differ considerably in size.

Keeping in mind the above considerations concerning the reliability of the difference spectra, the following suggestions regarding the interaction of molybdate with the carbon black surfaces can be made. Consider first the shift of the 1600 cm^{-1} band. As was pointed out by Morterra and Low [18] via oxidation of a carbon with $^{16}O_2$ and $^{18}O_2$, the 1600 cm^{-1} band must be assigned to an aromatic C=C vibration. It was suggested that an oxidized layer which is mainly formed by ether-like bonds crosslinking the aromatic substrate gives the polyaromatic network enough dipole moment change during vibration to make the C=C mode IR active. In view of these results, our measurements indicate that deposition of molybdate on the carbon surface influences this C=C vibration, either indirectly by changing the properties of the ether-like bonds, or directly by deposition of the molybdate anions on the aromatic carbon surface. In the latter case the presence of oxygen functionality on the carbon surface is not required since the interaction is based on a weak electrostatic attraction between molybdate and the underlying aromatic substrate.

This in turn could explain the high dispersion of molybdate on the low oxygen content but highly graphitic Ketjen EC support. Furthermore, the possibility that such type of adsorption interaction does occur is corroborated by the finding that considerable sintering of the Mo phase takes place during sulfidation of all carbon black-supported catalysts due to the high mobility of this Mo phase at sulfiding temperatures.

However, in order to explain the difference in sintering behavior of the Mo phase among the different carbon black supported catalysts the presence of stronger interaction sites has to be assumed for the Monarch based samples. In this respect the 3400 cm^{-1} band which is present only for the Monarch samples and totally absent in case of the Ketjen EC sample might give an indication of the nature of the interaction. The appearance of the O-H stretch vibration in the precursor Monarch-supported catalysts cannot be caused by O-H groups linked to molybdate since then one would expect an intense 3400 cm^{-1} band in the spectra of the Ketjen EC based catalyst since this sample has the highest amount of Mo. Therefore, it is concluded that the 3400 cm^{-1} band must be attributed to the formation of O-H bonds on the carbon surface. The appearance of such bonds upon interaction of molybdate ions with the carbon surface functionality can be visualized as a reaction between a carbon surface aryl ether group and the molybdenum anions as depicted in Fig. 9.

In this mechanism C-O-Mo bridging bonds are formed which ensure a much stronger metal-support interaction. Hence, it is suggested that less sintering of the Mo phase will occur when such interaction sites are present. However, the stability of the ether bond which is known to react only with hot concentrated acids, questions such an interaction mechanism. On the other hand it would account for the proton consumption which has been observed during chemisorption of molybdate on activated carbon [7].

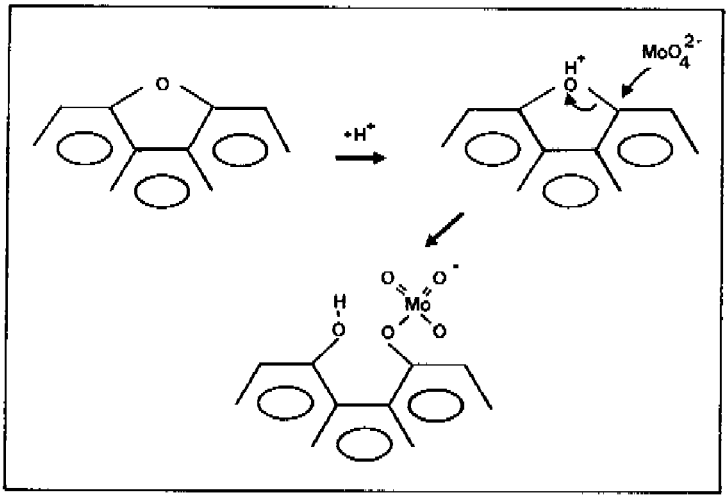

Fig. 9 Possible mechanism of the interactions between molybdenum anions and an ether-like carbon surface functional group.

Summarizing our results we can conclude that no major changes in the oxygen functionality of the carbon blacks occurs upon impregnation with molybdate ions. Only by means of FTIR some minor changes were observed which could point to a chemical reaction between aryl ether functional group and the molybdate ions. In view of these results it would be interesting to determine whether the active carbon surface atoms instead of the oxygen functionality determines the dispersion of carbon-supported sulfide catalysts.

REFERENCES

1. J.C. Duchet, E.M. van Oers, V.H.J, de Beer and R.Prins, J. Catal. 80, 386 (1983).
2. J.P.R. Vissers, J. Bachelier, H.J.M. ten Doeschate, J.C. Duchet, V.H.J. de Beer and R. Prins, Proc. 8th Int. Congr. on Catal., Berlin, Verlag Chemie : Weinheim, p. II-375 (1984).
3. A.W. Scaroni, Ph.D. Thesis, the Pennsylvania State University (1981).
4. V.H.J. de Beer, F.J. Derbyshire, C.K. Groot, R. Prins, A.W. Scaroni and J.M. Solar, Fuel 63, 1095 (1984).
5. J.P.R. Vissers, C.K. Groot, E.M. van Oers, V.H.J. de Beer and R. Prins, Bull. Soc. Chim. Belg. 93, 813 (1984).
6. C.K. Groot, A.M. van der Kraan, V.H.J. de Beer, and R. Prins, Bull. Soc. Chim. Belg. 93, 707 (1984).
7. J.P.R. Vissers, V.H.J. de Beer and R. Prins, J. Catal. to be published, chapter 3 of this thesis.
8. J.P.R. Vissers, F.P.M. Mercx, V.H.J. de Beer and R. Prins, J. Catal. to be published, chapter 4 of this thesis.
9. J.P.R. Vissers, T.J. Lensing, V.H.J. de Beer and R. Prins, Proc. Conf. Carbon, 16th, Univ. Calf. San Diego 607 (1983).
10. J.P.R. Vissers, T.J. Lensing, V.H.J. de Beer and R. Prins, Appl. Catal to be published, chapter 8 of this thesis.
11. B. Delmon and M. Houalla, Preparation of Catalysts II (Edited by B. Delmon, P. Grange, P. Jacobs and G. Poncelet), p. 439, Elsevier, Amsterdam (1979).
12. W.M. Prest, Jr. and R.A. Mosher, Colloids and Surfaces in Reprographic Technologies (Edited by M. Hair and M. Croucher), chapter 12, ASC Symposium Series, 225 (1982).
13. A.J.A. Konings, A.M. van Doorn, D.C. Koningsberger, V.H.J. de Beer, A.L. Farragher and G.C.A. Schuit, J.

Catal. 54, 1 (1979).
14. F.P.J.M. Kerkhof and J.A. Moulijn, J. Phys. Chem. 83, 1612 (1979).
15. S.J. Tauster and R.R. Chianelli, J. Catal. 63, 515 (1980).
16. J. Bachelier, J.C. Duchet and D. Cornet, J. Phys. Chem. 84, 1925 (1980).
17. J.M. O' Reilly and R.A. Mosher, Carbon 21, 47 (1983).
18. C. Morterra and M.J.D. Low, Spectroscopy Letters 15, 689 (1982).
19. W.F. Verhelst, A. Voet, P. Ehrburger, J.B. Donnet and K.G. Wolthuis, Rubber Chemistry and Technology 50, 735 (1977).
20. D.T. Clark and H.R. Thomas, J. Polymer Science 16, 791 (1978).
21. D.T. Clark and A. Dilks, J. Polymer Science 17, 957 (1979).
22. A. Ishitani, Carbon 19, 269 81981).
23. A. Grint and D.L. Perry, Proc. of the 15th London Carbon Graphite Conf., p. 125 (1982).
24. M.L. Deviney, R.N. King, S.F. Chappell and G.M. Gynn, Proc. of the 15th London Carbon Graphite Conf., p. 240 (1982).
25. J.M. Thomas, E.M. Evans, M. Barber and P. Swift, Trans. Faraday Soc. 67, 1815 (1971).
26. P. Ehrburger, O.P. Mahajan and P.L. Walker, Jr., J. Catal. 43, 61 (1976).
27. P. Ehrburger and P.L. Walker, Jr., J. Catal. 55, 63 (1978).
28. C.K. Groot, P.J.G.D. van de Gender, W.S. Niedzwiedz, A.M. van der Kraan, V.H.J. de Beer and R. Prins, Appl. Catal., to be published.
29. P. Ehrburger, A. Mongilardi and J. Lahaye, J. Catal. 91, 151 (1983).
30. B.S. Clausen, H. Topsøe, R. Candia, J. Villadsen, B. Lengeler, J. Als-Nielsen and F. Christensen, J. Phys.

Chem. 85, 3868 (1981).

31. J. Grimblot, P. Dufresne, L. Gengembre and J.P. Bonnelle, Bull. Soc. Chim. Belg. 90, 1261 (1981).
32. J. A. Gadsen, Infrared Spectra of Minerals and Related Inorganic Compounds, R.J. Acford Ltd, Chichester, Sussex (1975).
33. G. Duykaerts, the analyst 84, 201 (1959).
34. W.J. Potts, Jr., Chemical Infrared Spectroscopy, Wiley & Sons, New York, P. 137 (1963).

CHAPTER 7

INFLUENCE OF PHOSPHATE ON THE HDS ACTIVITY OF CARBON-SUPPORTED MOLYBDENUM SULFIDE CATALYSTS.

ABSTRACT

Activated carbon supports which contained various amounts of phosphate, were prepared via pore volume impregnation, drying and sulfiding with a constant amount of molybdenum sulfide common for industrial applications. The thiophene HDS activity of the catalysts was found to decrease drastically with increasing amount of phosphate present. Extraction results pointed to the formation of a 12-molybdophosphate species in the precursor catalysts. Upon sulfidation only MoS_2-like species could be detected in the catalysts, irrespective of the amount of 12-molybdophosphate present in the precursor catalysts. Dynamic oxygen chemisorption as well as quantitative XPS measurements indicated no variation in size of the MoS_2 particles for catalysts with different phosphate loadings. Thus, the poisoning effect of phosphate on the HDS activity of Mo/C catalysts cannot be explained in terms of dispersion variations or incomplete sulfidation. Hence, it is concluded that the 12-molybdophosphate complex acts as a precursor for a low activity species consisting of MoS_2 particles electronically influenced by phosphorus.

INTRODUCTION

Alumina-supported molybdenum oxide or sulfide catalysts and the cobalt or nickel promoted systems have been widely examined with respect to their hydrodesulfurization (HDS)

capabilities. Although these conventional catalytic ensembles are active and stable for hydrodesulfurization reactions, the future needs for a more efficient utilization of the various fossil fuel feedstocks require that catalysts of yet higher activities and stabilities are to be developed.

It was recognized in the past that phosphate added to the above described catalysts acts as a promotor for hydrodesulfurization (1-9), hydro- denitrogenation (2,4), and hydrodemetallization (5) reactions. Moreover, phosphorus also provides increased strength and heat stability of the alumina support (10,11). Originally, phosphoric acid was added to increase the solubility of the precursor metal salt in the impregnation solutions, the advantage being that with a single impregnation step, catalysts can be prepared with metal compositions common for industrial applications (2,3,12). Hence, the promotion effect of phosphate on the HDS activity of alumina-supported catalysts was explained in terms of a more uniform dispersion of the metal compounds on the support surface (2,3,7,8). In case the phosphate was incorporated into the alumina support prior to a conventional impregnation with a metal salt solution, the observed promotion effect is more difficult to explain. In this respect, it was suggested that the function of phosphate is to inhibit the formation of catalytically inactive nickel (cobalt) aluminate (13), or to affect the repartition of the molybdenum phase (6) in the catalysts.

In striking contradiction herewith, it was demonstrated that phosphate in carbon-supported molybdenum-based HDS catalysts should be regarded as a poison, able to drastically lower the HDS activity of the catalysts (14-16). This dual character of phosphorus is very intriguing, the more so because the chemistry by which it acts as a promotor on one hand, or as a poison on the other hand, has not been firmly established.

The present study aims to shed more light on this problem by evaluating the properties of phosphate containing, activated carbon-supported Mo catalysts. A series of catalysts samples with varying phosphate content and nearly constant Mo content were prepared and tested for their thiophene HDS activity. X-ray photoelectron spectroscopy, ^{31}P solid state NMR and dynamic oxygen chemisorption were used to characterize the catalysts.

EXPERIMENTAL

Catalyst preparation

The support used was an activated carbon (Norit RX3 extra, B.E.T. surface area 1190 m^2/g and pore volume 1.0 ml/g). Various amounts of phosphate were added by immersing the support in H_2O-H_3PO_4 solutions with different H_3PO_4 concentrations. After refluxing for 1 h, when most of the phosphate was chemisorbed by the carbon, the samples were filtered off and dried at 383 K. The phosphate content was determined according to a standard procedure (17).

Catalysts were prepared on the phosphate-containing carbon supports by pore volume impregnation using aqueous solutions of ammonium heptamolybdate such as to obtain a constant Mo loading of approximately 0.5 Mo at nm^{-2} (8.0 wt% Mo). The exact catalyst composition was checked by means of atomic absorption spectroscopy. After impregnation the catalysts were dried in air, starting at 293 K and increasing up to 383 K in 1.5 h where they were kept overnight. Catalysts are denoted as Mo-P(x)/C with x being the wt% of phophate in the catalysts.

Catalyst activity measurements

Activities for thiophene hydrodesulfurization (HDS) were

measured in a microflowreactor operating at 673 K and atmospheric pressure. The feed consisted of a 6.2 vol% thiophene in H_2 flow, the flowrate was 50 ml/min and the catalyst charge 200 mg. Data points were taken at different time intervals and analyzed by on-line gas chromatography. The conversion of thiophene after a 2 h run was taken to calculate the first order rate constant for hydrodesulfurization and the rate constant for the consecutive butene hydrogenation reaction (18). Prior to activity measurement the catalysts were presulfided in situ in a H_2S/H_2 flow (10 mol% H_2S, total flow rate 60 ml/min) using the following temperature program ; linear increase from 293 K to 673 K over 1 h, followed by an extended sulfiding at 673 K for 2 h.

Catalyst characterisation

Some catalyst samples were characterized using the following techniques :

(1) In situ dynamic oxygen chemisorption (DOC) was carried out in order to obtain a measure for the active surface area of sulfided catalysts as has been described elsewhere (19). After sulfidation according to the procedure described above the samples were purged in purified He (O_2 content $<< 10^{-3}$ ppm) for 15 min and subsequently cooled within 30 min to 333 K under flowing He. Oxygen chemisorption was measured at 333 K by injecting 2.19 ml pulses of a 5.2% O_2/He mixture, at 3 min intervals, into the He carrier gas flow. When effluent O_2 peaks had increased to constant size, the total O_2 uptake was calculated.

(2) XPS spectra of the oxidic samples were recorded on a Physical Electronics 550 XPS/AES spectrometer equipped with a magnesium X-ray source (E=1253.6 eV) and a double pass cylindrical mirror analyzer. The powdered samples were pressed on a stainless steel mesh which was mounted on top of the specimen holder. Spectra were recorded in steps of

0.05 eV. The pressure did not exceed 5 x 10^{-8} torr and temperature was approximately 293 K. Spectra of the sulfided samples were recorded on an AEI ES 200 spectrometer equipped with a purified N_2 flushed glove box attached to the XPS introduction chamber. After sulfidation according to the procedure described above the catalyst samples were purged with purified He for 15 min at 673 K and subsequently cooled within 30 min to room temperature in flowing He. A special reactor (20) allowed transfer of the sulfided samples to the XPS apparatus, without exposure to air. The samples were mounted on the specimen holder by means of double-sided adhesive tape. Spectra were recorded at 283 K in steps of 0.1 eV. The C 1s peak (284.6 eV) was used as internal standard for binding energy calibration.

(3) ^{31}P-solid state MAS NMR spectra were recorded on a Bruker CXP-300 spectrometer. Typically 0.12 g of sample was used, and 90 pulses were applied at 1214 MHz at 20 s intervals. 400 FID's were accumulated in 2 K data points zero-filled to 8 K, followed by Fourier transformation (line broadening 25 Hz). The chemical shift is measured with respect to 80% phosphoric acid. No crosspolarization was applied.

(4) Determination of the amount of extractable phosphate was carried out as follows : x g sample was refluxed for 1 h in a solution containing 10 times x ml H_2O and x ml concentrated HCl. After filtration, 10 ml of a standard (17) ammoniumheptamolybdate-ascorbic acid solution was added to the extract. In this way the blue molybdophosphate complex is formed, the concentration of which can be determined photometrically.

RESULTS

In Table 1 the catalyst compositions and the HDS activity test results are collected. It should be noticed that 0.026% PO_4^{3-} was present on the pure carbon support, in spite of the fact that it had been industrially washed with HCl. It is seen that by adding small amounts of phosphate, the HDS activity of the catalysts drops tremendously until ultimately in the highest phosphate content sample a 90% decrease in activity is measured. In agreement with previous publications (14-16), these results clearly show that phosphate, even when present in very small concentrations, has a severe poisoning effect on the thiophene HDS activity of Mo/C catalysts. The butene hydrogenation capability seems less affected by phosphate , only a decrease of about 40% is measured for the Mo-P(2.7)/C sample.

Table 1. Catalytic Properties of Mo-P(x)/C catalysts.

Catalyst composition		Activity		
		Hydrodesulfurization		Hydrogenation
wt% PO_4^{3-}	wt% Mo	$k_{HDS} \times 10^3$ (m^3/kg.s)	OTOF $\times 10^3$ $\frac{\text{mol thiophene}}{\text{mol Mo.s}}$	$k_{HYD} \times 10^3$ (m^3/kg.s)
0.02	7.83	2.7	3.7	8.0
0.10	8.33	2.4	3.1	7.6
0.17	8.06	2.0	2.6	7.0
0.28	8.46	1.8	2.2	5.9
0.47	8.80	1.3	1.6	5.2
0.66	9.20	1.1	1.3	4.5
2.7	7.40	0.3	0.4	5.2

At first it is important to establish whether in the precursor catalyst the molybdate ions interact with phosphate to form molybdophosphate species or whether molybdate and phosphate exist as separate phases on the

carbon surface. In order to distinguish among the two possibilities the amount of HCl extractable phosphate in the Mo-P(x)/C catalysts was determined. Phosphate which is present as a molybdophosphate complex is not extracted in this way (12,17). No phosphate could be extracted from the catalysts except for the Mo-P(2.7)/C sample where 2.08 wt% PO_4^{3-} was found to be extractable. On the basis of these experiments it becomes clear that a molybdophosphate is actually formed in the catalysts. The stoichiometry of this complex can be estimated from the extraction results of the Mo-P(2.7)/C sample, where it was found that 0.62 wt% PO_4^{3-} combine with 7.4 wt% Mo, or a Mo to P ratio of approximately 12. Interestingly, this value corresponds very closely with that of known molybdophosphate complexes $(PO_4Mo_{12}O_{36})^{3-}$. Furthermore, since no phosphate could be extracted unless it is in excess relative to the amount required to form the 12-molybdophosphate complex (Mo-P(2.7)/C), it can be concluded that the complex forming reaction is fast and complete.

The presence of this 12-molybdophosphate complex in the precursor catalysts was examined by means of ^{31}P-solid state NMR measurements. In Fig. 1 the spectra of the 12-molybdophosphoric acid $(H_3(PO_4Mo_{12}O_{36}).H_2O$ (Janssen Pharmaceutica) reference compound together with the P(3)/C (precursor sample for the Mo-P(2.7)/C sample) and Mo-P(2.7)/C samples are depicted. While the 12-molybdophosphoric acid shows a sharp peak around -2ppm, the P(3)/C sample has a rather broad signal around -4ppm. Upon addition of Mo (Mo-P(2.7)/C sample), the P signal, when compared to the signal of the unloaded support (P(3)/C), broadens and shows a slight shift towards a lower ppm value. Although these spectral changes are small, they are not conflicting with the formation of the 12-molybdophosphate complex since the latter spectrum can be understood to contain contributions of the 12-molybdophosphate complex and phosphate, deposited on the

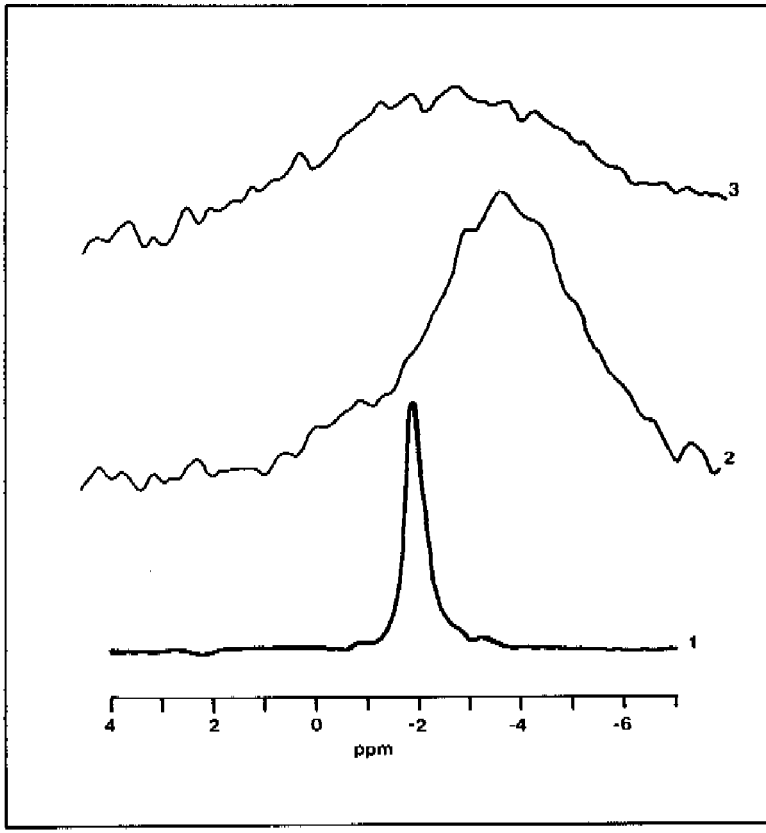

Fig. 1 ^{31}P-MAS-solid state NMR spectra of :
1 : 12-molybdophosphate acid
2 : P(3)/C
3 : precursor Mo-P(2.7)/C catalyst.

carbon surface. (It is to be noted that this sample contained excess phosphate).

In order to study the effect of phosphate addition on the properties of precursor and sulfided Mo/C catalysts a comparative XPS and DOC study was performed using the catalysts with the lowest and highest phosphate content as reference samples. The results are collected in Table 2. Surprisingly, the data obtained for both samples are essentially similar. Thus in the precursor state only highly dispersed Mo(VI) is present while the actually active sulfided state contains small MoS_2-like particles which according to the DOC results have a high fraction of active surface area. These results seem to be conflicting with the HDS activity data measured for these catalysts. Because the P 2p XPS signal was estimated to be very weak, no attempt was made to measure its intensity.

Table 2 : Catalyst characterization

	Mo(7.93) - P(0.02)/C	Mo(7.40) - P(2.7)/C
1. XPS		
a. oxidic state		
Mo $3d_{5/2,3/2}$ B.E. (eV)	232.5 235.7	232.6 235.8
I_{Mo}/I_C	0.095	0.086
particle size	<1.0 nm	<1.0 nm
b. sulfided state		
Mo $3d_{5/2,3/2}$ B.E. (eV)	229.3 232.4	229.3 232.4
S 2p B.E. (eV)	162.8	162.8
I_{Mo}/I_C	0.075	0.066
particle size	1.8 nm	2.0 nm
S/Mo atomic ratio	1.90	1.96
2. DOC		
O/Mo ratio	0.25	0.22

DISCUSSION

Precursor catalyst

The results of the extraction (and ^{31}P-solid state NMR) measurements show that the phosphate present on the carbon surface interacts with the molybdate ions and forms a 12-molybdophosphate complex, most likely according to the following reaction :

$$7\ PO_4^{3-} + 12(NH_4)_6\ Mo_7O_{24}.4H_2O + 72H^+ \longrightarrow$$
$$7\ (NH_4)_3[PO_4(Mo_{12}O_{36})].12H_2O + 51\ NH_4^+$$

Such a complex consists of four groups of three MoO_3 octahedra with the P atom located in the center of the complex, tetrahedrally surrounded by oxygen (21). Evidently, although our findings point to the formation of this particular complex, other types of molybdophosphate species cannot be fully excluded.

The presence of molybdophosphate complexes were not observed by means of XPS, the obvious reasons being :

- That no shift in Mo 3d binding energy is to be expected since Mo is octahedrally surrounded by oxygen in the molybdophosphate complex as well as in the isopolymolybdate structures.
- That the size of the molybdophosphate complex is comparable to that of the isopolymolybdate species (e.g. $Mo_7O_{24}^{6-}$).

Sulfided catalyst

Previously (15,16), we assumed that Mo-P(x)/C catalysts, due to the formation of molybdophosphate complexes, were difficult to sulfide or non-sulfidable at all. In this way, the low HDS activities of these catalysts could be

explained. Clearly, these assumptions must be rejected on the basis of the present XPS results. The XPS peak shapes, binding energies and S/Mo ratio prove that a MoS_2-like phase is present in both the low and the high phosphate content samples. Apparantly, P is not sulfided since the S/Mo ratio is remarkably close to 2 for the Mo-P(2.7)/C catalyst. Furthermore, quantitative XPS and oxygen chemisorption analysis do not show a difference in molybdenum sulfide particle size and amount of oxygen-detectable Mo surface sites between sulfided catalysts with low and high phosphate content. Yet, these catalysts demonstrate a tremendous difference in HDS activity. These puzzling results indicate that the poisoning effect of phosphate on the HDS activity of carbon-supported Mo catalysts is more complicated than thought before.

Evidently the low activity of the sulfided Mo-P(x)/C catalysts can only be explained if an intimite contact exists between the MoS_2 phase and the phosphate ions. In this respect it is logic to assume that the 12-molybdophosphate complex acts as a precursor for such a phase. In Fig. 2 the HDS activity expressed per mol Mo (QTOF value) is plotted versus the calculated relative amount of 12-molybdophosphate present in the precursor catalysts, assuming that a complete reaction takes place between the phosphate and molybdate ions to form the complex (in agreement with the extraction results). Interestingly, a linear relationship is observed, indicating that the HDS activity of Mo-P(x)/C catalysts can be described as the sum of two activities, namely :

$$QTOF\ (x10^3) = 3.7\ (1 - f_{MoP}) + 0.4\ f_{MoP}$$

with f_{MoP} being the fraction of Mo present in the 12-molybdophosphate configuration.

The above relationship contains some interesting features.

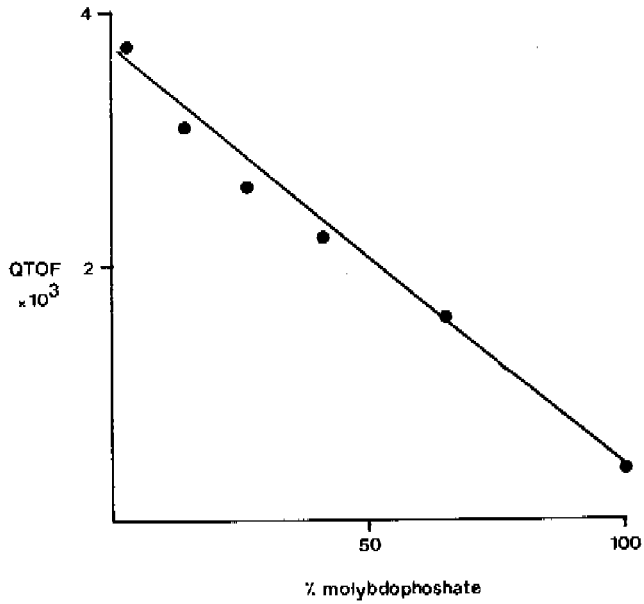

Fig. 2 Thiophene HDS activity per mol Mo (QTOF value expressed in mol thiophene per mol Mo per second) of sulfided Mo-P(x)/C catalysts as a function of Mo present in the precursor catalysts as 12-molybdophosphate.

Indeed, one has to keep in mind that the amount of 12-molybdophosphate is a characteristic of the oxidic precursor catalysts while the HDS activity is measured for the sulfided samples. Therefore, in view of the linear correlation it must be concluded that 1 phosphate molecule kills the activity of 12 MoS_2 units (QTOF value decreases from 3.7×10^{-3} to 0.4×10^{-3}). The observation of this 12 Mo to 1 P stoichiometry which apparantly also holds for the sulfided catalysts is intriguing in view of the fact that considerable sintering of the Mo phase occurs during conversion from precursor to sulfided state. Hence, this

suggests that during sulfidation of a 12-molybdophosphate, phophorus remains in contact with its surrounding Mo atoms.

Unfortunately, besides the indication of a 12 Mo to 1 P stoichiometry, it is not possible with the present results to obtain detailed information on the structure of the MoS_2-P species. More research efforts will also be needed to explain how P interacts with the surrounding MoS_2 phase, and as such decreases the capability for hydrodesulfurization. Evidently, based on the DOC results and the observation that small amounts of phosphate have a tremendous effect on the HDS activity of Mo/C catalysts, it is not likely that the poisoning effect of phosphate can be explained in terms of segregation of phosphate to the MoS_2 edge planes, physically blocking the active sites for the reactant molecules. Rather an interaction altering the electronic structure of the active sites has to be visualized. In this respect, P can be present either as a P^{3-} dopant in the MoS_2 phase or as phosphate in intimite contact with MoS_2. In the latter case, P-O-Mo bridging bonds might form on exposed Mo edge atoms, thus leading to a situation analogous to the Al-O-Mo bonds in sulfided Mo/Al_2O_3 catalysts. This strong metal-phosphate interaction might lower the HDS activity of the MoS_2 phase in a manner similar as the strong metal-alumina support interaction lowers the HDS activity of Mo/Al_2O_3 catalysts (23-25).

Finally, in view of the results obtained in this study, it is unlikely that in alumina-supported catalysts Mo-P species are formed, since this would lower the HDS activity of the catalyst instead of promoting it. The strong interaction of alumina with phosphate ions, resulting in the formation of $AlPO_4$ species (11,22), apparently prevents formation of such complexes on alumina. In this respect the addition of phosphate might prevent deposition of molybdate on the strong adsorption sites of the alumina surface. This could explain the promoting effect since strong metal-support interactions must be avoided in order to obtain highly

active catalysts (23-25).

CONCLUSIONS

The thiophene HDS activity of carbon-supported molybdenum sulfide catalysts decreases drastically upon addition of phosphate. It was shown that in the precursor catalysts a 12-molybdophosphate complex was formed via reactions of the phosphate with the impregnated molybdate ions. In the sulfided catalysts only well-dispersed MoS_2-like particles could be detected irrespective of phosphate content. It was suggested that the 12-molybdophosphate complex is a precursor for a MoS_2-P phase which has poor catalytic properties.

REFERENCES

1. Haresnape, J.N., and Morris, J.E., British Patent 701,217 (1953).
2. Colgan, J.D., and Chomitz, N., US Patent 3,287,280 (1966).
3. Mickelson, G.A., US Patent 3,749,663 , 3,755,196 , 3,755,150 , 3,755,148 , and 3,749,664 (1973).
4. Pine, L.A., US Patent 3,904,550 (1975).
5. Eberly, P.E. Jr, US Patent 4,003,828 (1977).
6. Chadwick, D., Aitchison, D.W., Badilla-Ohlbaum, R., and Josefsson L., in "Preparation of Catalysts III" (Poncelet, Grange and Jacobs, Eds.), elsevier, p. 323, 1982.
7. Millman, W.S., US Patent 4,392,985 (1983).
8. Wilson, G., and Kayamoto, M., US Patent 4,388,222 (1983).
9. Fitz, Jr., C.W., and Rase, H.F., Ind. Eng. Chem. Prod. Res. Dev. 22,40 (1983).

10. Hopkins, P.D., and Meyers, B.L., Ind. Eng. Chem. Prod. Res. Dev. 22,421 (1983).
11. Gishti, K., Iannibello, A., Marengo, S., Morelli, G., and Titarelli, P., Appl. Catal. 12,381 (1984).
12. "Aqueous Solutions of Molybdenum Compounds for Catalytic Applications", Bulletin Cdb-16 of the Molybdenum Climax Company, Connecticut (1973).
13. Hilfman, L., US Patent 3,617,528 (1971).
14. Voorhies, J.D., US Patent 4,082,652 (1978).
15. Duchet, J.C., Van Oers, E.M., de Beer, V.H.J., and Prins, R., J. Catal. 80, 386 (1983).
16. Vissers, J.P.R., Lensing, T.J., de Beer, V.H.J., and Prins, R., in "Proceedings of the 16th Biennial Conference on Carbon, San Diego,1983", p. 607 (1983).
17. Norit Testing Methods, Norit N.V., Amersfoort.
18. Van Sint Fiet, T.H.M., PhD Thesis, Eindhoven (1973).
19. Vissers, J.P.R., Bachelier, J., ten Doeschate, H.J.M., Duchet, J.C., de Beer, V.H.J., and Prins, R., in "Proceedings of the 8th International Congress on Catalysis, Berlin, 1984", Verlag Chemie, Weinheim, p. II-387, 1984.
20. Konings, A.J.A., van Doorn, A.M., Koningsberger, D.C., de Beer, V.H.J., Farragher, A.L., and Schuit, G.C.A., J. Catal. 54, 1 (1978).
21. Cotton, F.A., and Wilkinson, G., in "Advanced Inorganic Chemistry", p. 954, John Wiley, New-York, 1972, and references cited therein.
22. Haller, G., Mc Millan, B., and Brinen, J., Prepr. Am. Chem. Soc., Div. Pet. Chem. 29, 939 (1984).
23. Vissers, J.P.R., de Beer, V.H.J., and Prins, R., to be published, chapter 3 of this thesis.
24. Vissers, J.P.R., Groot, C.K., van Oers, E.M., de Beer, V.H.J., and Prins, R., Bull. Soc. Chim. Belg. 93, 813 (1984), chapter 5 of this thesis.
25. Candia, R., Sorensen, O., Villadsen. J., Topsøe, N.-Y., Clausen, B.S., and Topsøe, H., Bull. Soc. Chim. Belg. 93, 763 (1984).

CHAPTER 8

CARBON BLACK COMPOSITES AS CARRIER MATERIALS FOR SULFIDE CATALYSTS.

ABSTRACT.

Various carbon blacks, differing, amongst others, in particle size and surface area, were used to prepare carbon black composites by mixing the carbon particles with a polyfurfuryl alcohol binder and subsequently carbonizing the binder material at elevated temperatures. Textural properties of the composites were found to vary according to the carbon black substrate properties. The composites demonstrated promising textural properties (B.E.T. surface area ranging from 120-730 m^2/g ; % mesoporosity ranging from 50-90 %) for use as supports for sulfide catalysts. Mo sulfide catalysts were prepared on the composite supports and evaluated for their thiophene HDS activity at atmospheric pressure. Due to the inert character of the composite surface, sintering of the Mo-phase took place during sulfidation as was observed by X-ray photoelectron spectroscopy. Therefore, the composites were subjected to several oxidative treatments to increase their surface heterogeneity and thus their affinity towards the deposited Mo-phase. A HNO_3 treatment demonstrated the most promising results.

INTRODUCTION

Hydroprocessing of petroleum based feedstocks over catalysts such as cobalt sulfide promoted molybdenum sulfide

supported on porous Al_2O_3, has been carried out for over sixty years now. Such applications include sulfur removal (hydrodesulfurization (HDS)), nitrogen removal (hydrodenitrogenation), and product quality improvement (hydroconversion). In the future more and more conversion of heavy into light oil fractions will be needed in Western Europe to meet the surplus of heavy fractions. In order to meet these requirements, a new generation of transition metal sulfide catalysts are needed with higher activities, better selectivity to desired products, and greater resistance to poisons.

In this respect the use of carbon as a support is of particular interest, since recently (1,2,3) it was found that Mo-based carbon-supported catalysts had much higher HDS activities than the corresponding alumina-supported catalysts. Interestingly, when supported on carbon, the promotor Co and Ni sulfides showed higher (Co) or equal (Ni) HDS activities than Mo or W disulfide (4,5). Furthermore the application of carbon-supported sulfide catalysts for the conversion of residua (high in metal content), would make it possible to easily recover the transition metal valuables from spent catalysts by burning off the carbon carrier. In addition, it has been shown that carbon supports have lower coking propensities for anthracene than alumina supports (6). For alumina-supported Mo catalysts a correspondence between thiophene HDS activity and reactions which result in carbon deposition was observed (7). The rate of carbon deposition on carbon-supported catalysts appeared to be insensitive to the nature of the metal, whereas HDS activity was not. Consequently, it seemed possible to enhance HDS activity without an attendant increase in coking propensity. In this respect, carbon-supported catalysts should maintain their HDS activity over extended periods of operation.

However, most carbon materials have an important drawback in practicle applications, namely their pore structure

merely consists of micropores inaccessible for large sulfur-containing molecules present in industrial feedstocks. For most carbon materials enlarging the meso- and macropore structure will be at the expense of their mechanical properties, resulting in materials with poor crushing strength. One possible way to circumvent these problems is the use of carbon covered alumina (CCA) as support material (8), which is prepared by covering the Al_2O_3 surface with a thin layer of carbon (deposited via hydrocarbon pyrolyses) prior to impregnation of the transition metals.

In the present paper a completely different approach is presented , which describes the application of carbon black composite type carrier materials (denoted CBC) for HDS catalysts. These carbon materials which can be prepared relatively easily, have little microporosity and an extensive mesoporosity with a narrow and adjustable pore size distribution (9). The HDS performance of Mo sulfide catalysts supported on CBC supports is evaluated. In addition, various treatments were applied on the carbon supports in order to modify the carbon surface affinity towards the deposited active phase. Furthermore X-ray photoelectron spectroscopy was used to determine the degree of Mo dispersion in some Mo/CBC catalysts.

EXPERIMENTAL.

Preparation of carbon black composites.

CBC type supports were prepared according to a method described by Schmitt et al. (9). Partially polymerised furfurylalcohol (PFA) that was used as organic binder material was prepared as follows : a solution containing 200 ml furfurylalcohol, 200 ml H_2O and 1 ml concentrated H_2SO_4 was heated at 363 K for 10 min under stirring. A polymeric

phase (PFA) precipitates. Commercially (Cabot, Ketjen) available carbon blacks with different properties (Table 1) were selected as substrates. Preparation of carbon black composites was performed by dissolving 10 g of PFA in 100 ml of acetone. To this solution 40 - 60 g carbon black was added. After thorough mixing, the resulting composition was heated overnight at 383 K to volatize off the acetone present. The resulting carbonaceous body was heated (pyrolyzed) under flowing N_2 to 923 K in 1 h and kept at this temperature for an additional hour. In the following, the carbon black composites will be denoted by the type of carbon black and the ratio carbon black over binder which is given in parentheses, e.g. SAF-(4).

Table 1 : Properties of carbon blacks

carbon black	particle diameter* (nm)	pore volume (ml/g)	S_{BET} (m^2/g)
SAF	25	1.01	138
Monarch 1300	13	1.66	673
Monarch 1100	14	1.37	261
Monarch 700	18	1.9	202
Ketjen EC	30	4.4	1010

* according to the manufacturer.

Textural properties.

From the N_2 adsorption-desorption isotherms determined at 77 K on a Carlo-Erba sorptomatic 1800, the surface area and the pore size distribution were calculated by using the BET equation and the Kelvin equation respectively.

CBC treatments.

Four different treatments were applied :

1. HCl treatment : 5 g CBC was added to a solution of 15 ml concentrated HCl in 200 ml H_2O. After boiling for 1 h

the carbon was filtrated and subsequently washed with boiling H_2O until the effluent pH was about 7. The carbon was then dried overnight in air at 383 K.

2. $KMnO_4$ + H_2SO_4 treatment (10) : 10 g CBC was added to 100 ml aqueous solution containing 0.2 M $KMnO_4$ and 2 M H_2SO_4. After stirring for 25 min the carbon was filtrated and washed with cold and hot (363 K) H_2O until a pH of about 7 was reached. The carbon was subsequently dried overnight in air at 383 K.

3. Moist air treatment (11) : 5 g composite was placed in a quartz reactor and heated to 558 K. An air water-vapour mixture (total pressure 1 atm, p_{H_2O} = 17 torr), generated by bubbling air through distilled water maintained at 293 K, was passed through the carbon bed at 200 ml/min for 20 h.

4. HNO_3 treatment (11) : A suspension containing 5 g composite in 50 ml concentrated HNO_3 was heated to 353 K for a 10-12 h period. Thereafter the carbonaceous material was washed until neutral pH indication of the effluent wash water, and dried overnight in air at 383 K.

Catalyst preparation.

The various CBC samples were impregnated (pore volume impregnation) with an aqueous solution of ammonium heptamolybdate (Merck, min 99%). In order to compensate for variations in surface area of the various supports used, the concentration of ammonium heptamolybdate was adjusted in such a way that for each catalyst the support surface loading was approximately 0.5 Mo atoms per nm^2. After impregnation the samples were dried in air, starting at 293 K and slowly increrasing up to 383 K where they were kept overnight.

Activity measurements.

Catalysts (200 mg) were presulfided in situ in a H_2S/H_2 flow (10 mol% H_2S, total flow rate 60 ml/min) using the following temperature program : linear increase from 293 K to 673 K in 1 h and holding at this temperature for two additional hours. After sulfiding, a flow (50 ml/min) of thiophene (6.2 mol%) in H_2 was led over the catalyst at 673 K and atmospheric pressure. The conversion of thiophene to butane, butenes and H_2S measured after a 2 h run was taken to calculate the activity per mol Mo (QTOF = Quasi Turn-Over Frequency, expressed in mol thiophene converted per mol Mo per second).

XPS measurements

XPS spectra of the oxidic precursor samples were recorded on a Physical Electronics 550 XPS/AES spectrometer equipped with a magnesium X-ray source (E = 1253.6 eV) and a double pass cylindral mirror analyzer. The powdered samples were pressed on a stainless steel mesh which was mounted on top of the specimen holder. Spectra were recorded in steps of 0.05 eV. The pressure did not exceed 5×10^{-8} torr and temperature was approximately 293 K. Spectra of the sulfided samples were recorded on an AEI ES 200 spectrometer equipped with a dry N_2-flushed glove box attached to the XPS apparatus. After sulfidation according to the procedure described above, the catalysts were purged with purified He for 1/4 h at 673 K and subsequently cooled within 0.5 h to room temperature in flowing He. A special reactor (12) allowed transfer of the sulfided samples to the glove box, without exposure to air. The samples were mounted on the specimen holder by means of double-sided adhesive tape. Spectra were recorded at 283 K in steps of 0.1 eV.

RESULTS AND DISCUSSION.

Textural properties of CBC supports.

CBC support materials are formed by binding the carbon black particles together in packed relationship with a carbon binder (PFA). The use of such binder improves the mechanical properties of the final CBC material because pyrolyzed PFA is in fact a glassy carbon known for its outstanding mechanical properties (13). An important variable in the preparation is the filler (carbon black)-to-binder (PFA) ratio. Varying this ratio allows materials differing in surface area and pore size distribution to be obtained. A series of CBC's with the filler to binder ratio varying from 6 to 1 was prepared using the SAF carbon black. In Table 2 the textural properties are collected. Evidently, at the high SAF/PFA ratio the composite resembles very much the original carbon black, while with decreasing ratio the carbon molecular sieve character (13) (micropores) of the carbonized PFA becomes apparent. It is clear that although the SAF-(1) sample has a higher mechanical strength, the aim to produce

Table 2 : Properties of SAF composites

Surface area (m^2/g)	SAF-(6)*	SAF-(4)	SAF-(3)	SAF-(1)
S_{BET}	134	152	148	229
S micropores (r<1.5 nm)	54	76	81	170
S meso + macro pores (r>1.5 nm)	80	76	67	59

* numbers in parentheses represent carbon black over binder ratio's

a carbon support with extensive mesoporosity is obviously not met by this sample. Therefore in the present study filler to PFA ratios were kept between 6 and 4. As a result, the CBC texture is to a large extent dependent upon the original properties of the carbon black used, since the interstices in between the carbon black spheres form the pores of the CBC (9). Variation in carbon black sphere properties (see Table 1) will, thus lead to CBC's with different pore size distributions. In Table 3 the results obtained for the various CBC supports prepared are summarized, and in Fig. 1 the pore size distributions are presented. For comparison also a commercial Al_2O_3 support (Ketjen, grade B) and an activated carbon (Norit RO3) have been included. These results show that, depending on the carbon black substrate used, it is possible to prepare CBC type carrier materials with a largely varying texture. Very important in this respect is the carbon black sphere size (Table 1) which controls the pore size distribution in CBC's. Large carbon black spheres (SAF, Monarch 700) lead to a pore size distribution in the resulting CBC centered around larger pores, while small carbon black particles lead

Table 3 : Properties of composites

support	S_{BET} (m^2/g)	% surface area in meso- and macropores (r>1.5 nm)	pore volume (ml/g)
SAF-(4)*	152	50	0.78
Monarch 700-(4)	120	70	1.06
Monarch 1100-(4)	130	90	0.9
Monarch 1300-(6)	458	80	1.05
Ketjen EC-(5)	726	73	1.7
Al_2O_3 (Ketjen, grade B)	270	91	1.88
Norit RO3 active carbon	1050	25	0.75

* numbers in parentheses represent carbon black to binder ratio's

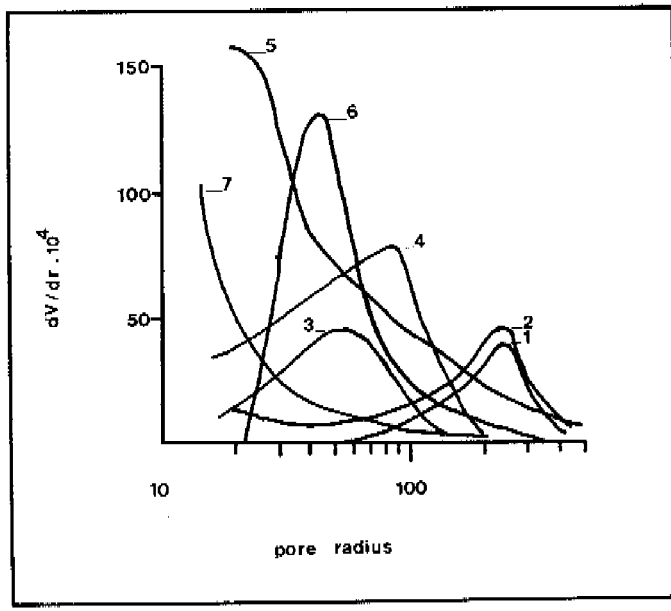

Fig. 1 Pore size distributions of carbon black composites.
1 : SAF-(4) 2 : Monarch 700-(4)
3 : Monarch 1100-(4) 4 : Monarch 1300-(6)
5 : Ketjen EC-(5) 6 : Y -Al_2O_3 grade B
7 : Norit RO3 activated carbon.

to CBC's with smaller pores (Monarch 1100, Monarch 1300). The CBC prepared using Ketjen EC carbon black is an exceptional sample, showing very high porosity due to the hollow shell structure (14) of the carbon black particles. These hollow shell particles form large cavities, but the pores are of the inkbottle type as was concluded from the hysteresis curve of the nitrogen adsorption-desorption isotherms.

In view of their use as supports for HDS catalysts, it is important to note that the composites indeed have much more favourable textural properties than activated carbon, i.e. most of the pores are in the transitional region since they arise from the geometrical outer surface of the carbon black particles, whereas the micropore region is most developed in the case of activated carbons. Furthermore, it seems possible to prepare composite carrier materials having bi-or trimodal pore size distribution by properly mixing carbon blacks with different particle sizes. Finally the mechanical strength of the CBC can be selected by varying the ratio filler (carbon black) over carbon-yielding binder (PFA).

Thiophene HDS activity of Mo/CBC catalysts.

The results of the thiophene activity tests are collected in Table 4. Thiophene, having small molecular dimensions, is able to penetrate in the major part of the pore system of the catalyst including most of its micropores. The reported activities should therefore be regarded as a measure of the

Table 4 : Thiophene HDS activity of Mo/CBC catalysts

catalyst*	catalyst activity $\times 10^3$ (mol thiophene/mol Mo.s)
1.1% Mo/SAP-(4)**	1.3
1.0% Mo/Monarch 700-(4)	1.0
0.8% Mo/Monarch 1100-(4)	1.0
2.4% Mo/Monarch 1300-(6)	1.7
4.7% Mo/Ketjen EC-(5)	2.5
2.1% Mo/Al_2O_3	0.5
7.4% Mo/Norit RO3	3.7

* wt% Mo was choosen in such a way as to obtain a surface loading of 0.5 Mo atoms/nm^2.

** cf. Tables 2 and 3.

intrinsic activity of the catalyst (related to the active phase dispersion), irrespective of the textural properties of the support. Evidently, the textural characteristics will be of prime importance when hydroprocessing of industrial feedstocks is concerned.

As shown in Table 4, Mo/CBC catalysts demonstrate intrinsic HDS activities varying between 1.0 and 2.5 x 10^{-3} mol thiophene converted per mol Mo per second ; values that are intermediate between the HDS activity reported for the corresponding alumina- and activated carbon-supported catalysts. These findings demonstrate once more that sulfides supported on carbon carriers are more effective in catalyzing the hydrogenolysis of sulfur-bearing molecules than the corresponding alumina-supported systems (1-5,8).

The observation that Mo/CBC catalysts are less active than the corresponding activated carbon supported catalysts deserves further attention. Due to the preparation method (pyrolysis at 923 K) , the surface of the composites has low oxygen functionality. This is demonstrated in Fig. 2 which shows the weight loss due to the evolution (as CO_2 and CO) of thermally unstable oxygen functional groups as determined by thermo gravimetric analysis (heat treatment in N_2 up to 1173 K). Since, for the pure carbon blacks (except Monarch 1300) no weight loss was recorded in the 873- 1173 K region, and pyrolysis of the composites was carried out at 923 K, it is evident that the weight loss observed for the CBC materials in the 873-1173 K temperature region (cf. Fig. 2) is due to further carbonization of the binder, instead of to loss of oxygen functionality at the carbon surface. This low oxygen content reflects the inert character of the carbon surface (15). As a consequence the precursor molybdate ions will be weakly bonded to the composite surface. In the oxidic precursor state the molybdenum phase might still be reasonably dispersed, but during sulfiding (up to 673 K) the Mo ions become mobile and will start migrating over the carbon surface to form rather large MoS_2

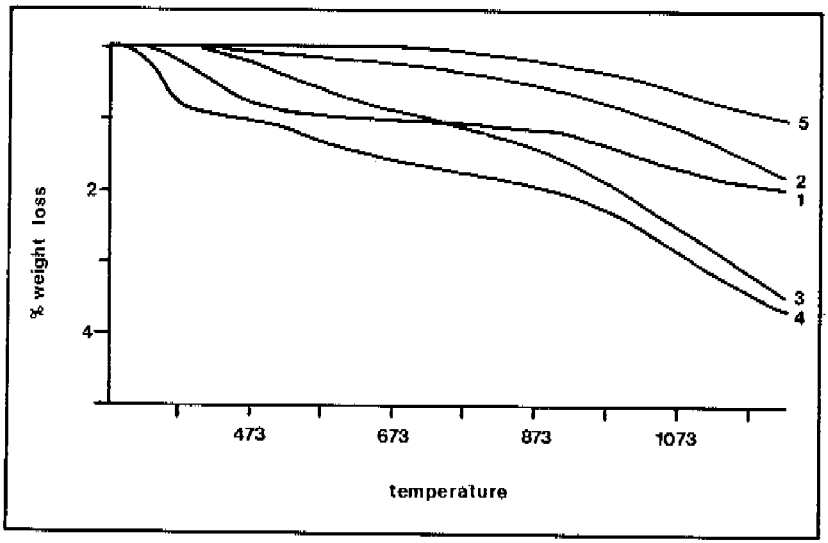

Fig. 2 Thermo gravimetric analysis of carbon black composites. Weight loss measured while heating the sample in N_2 up to 1173 K.

1 : SAF-(4) 2 : Monarch 700-(4)

3 : Monarch 1100-(4) 4 : Monarch 1300-(4)

5 : Ketjen EC-(5)

particles. The resulting low dispersion explains the differences in HDS activity between CBC and activated carbon based catalysts. In order to verify this sintering behaviour, XPS spectra were recorded before and after sulfidation for two Mo/CBC catalysts. The Mo 3d over C 1s signal intensity ratio was used to calculate particle sizes according to the catalyst model described by Kerkhof and Moulijn (16), using Scofield's cross section (17) and the electron escape depth according to Penn (18). As can be seen from Table 5 the particle sizes calculated for the

Table 5 : XPS results

Catalyst*	oxidic state		sulfided state	
	I_{Mo}/I_C	particle** size	I_{Mo}/I_C	particle** size
2.4% Mo/Monarch 1300-(4)***	0.0213	1.7nm	0.0110	5.5nm
4.7% Mo/Katjen EC-(5)	0.0364	2.0nm	0.0212	5.2nm

* wt% Mo was chosen in such a way as to obtain a surface loading of 0.5 Mo atoms /nm^2.

** λ of Mo electrons passing through the MoO_3 (MoS_2) phase was calculated (18) to be 1.5 nm (1.8 nm).

*** cf. Tables 2 and 3.

oxidic catalysts are about 2.0 nm while for the sulfided samples particle sizes of 5.5 and 5.2 nm were calculated. These values are a factor 3 larger than the corresponding particle sizes (below 1.0 nm and 1.8 nm respectively (3)) calculated for a 0.5 Mo atoms/nm^2 activated carbon supported catalyst, demonstrating the difference in dispersion of the catalysts supported on the two types of supports.

A considerable difference in catalytic activity was measured among the various CBC-supported catalysts (see Table 4). Interestingly, a correlation seems to exist between the HDS activity of the CBC-supported catalysts and the amount of porosity (BET surface area) of the supports. At present, we are not able to elucidate whether this correlation has a chemical or physical basis. A tentative explanation for the existence of the correlation may be that sintering of the molybdenum phase is hampered on the more ruggedly shaped carbon surfaces (corresponding to larger surface areas) due to the physical barrier of the carbon surface on a microscopic scale.

In an attempt to modify the surface affinity of the CBC carrier towards the active Mo phase, in order to limit

Table 6 : Thiophene HDS activity of modified composite supported catalysts.

catalyst*	catalyst activity (mol thiophene/mol Mo.s)
1.1% Mo/SAF-(4)**	1.3
1.1% Mo/SAF-(4) H_2SO_4-$KMnO_4$	1.2
1.1% Mo/SAF-(4) HCl	1.6
1.1% Mo/SAF-(4) steam	1.7
1.1% Mo/SAF-(4) HNO_3	2.2

* wt% Mo was choosen in such a way as to obtain a surface loading of 0.5 Mo atoms/nm^2.

** cf. Tables 2 and 3.

sintering at sulfidation and reaction conditions, different oxidative treatments were applied on the SAF composite and evaluated for their effect on the HDS activity of supported Mo. As can be seen in Table 6, the H_2SO_4-$KMnO_4$ treatment had a negative effect on catalytic activity, which is very likely due to the fact that the carrier was largely contaminated by Mn (24 wt%). All other treatments of the supports, especially the HNO_3 treatment which increased the oxygen functionality tremendously and is known to induce pits in the carbon surface (19), resulted in higher HDS activities of the catalysts. These observations suggest that the increase in oxygen functionality or surface heterogeneity, brought about by the oxidative treatments had a positive effect on both the extent and preservation of the active phase dispersion. This is in accordance with the findings of Walker c.s. 20 who observed a decrease in the average particle size of Pt particles deposited on an oxidized carbon support relative to the particle size measured on the unoxidized support. Ehrburger (21) observed a similar effect when depositing iron phtalocyanine on an oxidized and nonoxidized carbon black. The specific effect of oxygen functionality on Mo active phase dispersion will

be discussed elsewhere (15).

In conclusion, the present study has shown that by using carbonized polyfurfurylalcohol and carbon black particles carbon black composites can be prepared with pores predominantly in the transitional region. These CBC's have outstanding textural properties for use as supports for hydrotreating catalysts. Their surface however, appeared to be too inert to create and maintain a high degree of dispersion of the Mo phase under sulfiding and reaction conditions. Oxidative treatment of the support prior to impregnating of the active phase may overcome this drawback. Our work has thus shown that it is possible to prepare HDS catalysts based on carbon supports with the textural properties required and allowing a reasonable degree of dispersion of the active phase.

REFERENCES

1. J.L. Schmitt Jr. and G.A. Castellion, US patent 3,997,473 (1976).
2. J.C. Duchet, E.M. Van Oers, V.H.J. de Beer, and R. Prins , J. Catal., 80 (1983) 386.
3. J.P.R. Vissers, J. Bachelier, H.J.M. Ten Doeschate, J.C. Duchet, V.H.J. de Beer, and R. Prins, in Proceedings of 8th Int. Conf. Catal., Vol II, (1984) 387.
4. V.H.J. de Beer, J.C. Duchet, and R. Prins, J. Catal., 72 (1981) 369.
5. J.P.R. Vissers, F.P.M. Mercx, V.H.J. de Beer, and R. Prins, J. Catal., to be published, chapter 4 of this thesis.
6. A.W. Scaroni, PhD Thesis, Pennsylvania State University (1981).
7. V.H.J. de Beer, F.J. Derbyshire, C.K. Groot, R. Prins, A.W. Scaroni, and J.M. Solar, Fuel, 63 (1984) 1095.
8. J.P.R. Vissers, F.P.M. Mercx, S.M.A.M. Bouwens, V.H.J.

de Beer, and R. Prins, to be published, chapter 9 of this thesis.

9. J.L. Schmitt Jr., P.L. Walker Jr., and G.A. Castellion, US patent 3,978,000 (1976).
10. M. Fujikira and T. Osa, Progress in Batteries and Solar Cells, Vol 2, JEC Press. Inc. Cleveland (1979).
11. O.P. Mahajan, A. Younet, and P.L. Walker Jr., Separation Science and Technology, 13 (1978) 487.
12. A.J.A. Konings, A.M. van Doorn, D.C. Koningsberger, V.H.J. de Beer, A.L. Farragher, and G.C.A. Schuit, J. Catal., 54 (1978) 1.
13. P.L. Walker Jr., in "Proc. Fifth Industrial Conference on Carbon and Graphite", London, Soc. Chem. Ind., (1978) 427.
14. W.F. Verhelst, A. Voet, P. Ehrburger, J.B. Donnet, and K.G. Wolthuis, Rubber Chemistry and Technology, 50 (1977) 735.
15. J.P.R. Vissers, S.M.A.M. Bouwens, V.H.J. de Beer, and R. Prins, to be published, chapter 6 of this thesis.
16. F.P.J.M. Kerkhof and J.A. Moulijn, J. Phys. Chem., 83 (1979) 1612.
17. J.H. Scofield, J. Elect. Spect., 8 (1976) 129.
18. D.R. Penn, J. Elect. Spec. and Rel. Phen., 9 (1976) 29.
19. J.B. Donnet, Carbon, 20 (1982) 267.
20. P. Ehrburger and P.L. Walker Jr., J. Catal., 55 (1978) 63.
21. P. Ehrburger, A. Mongilardi, and J. Lahaye, J. Catal., 91 (1983) 151.

CHAPTER 9

CARBON-COVERED ALUMINA AS A SUPPORT FOR SULFIDE CATALYSTS.

ABSTRACT

Carbon-covered alumina carrier materials (10-35 weight % carbon deposited) were prepared via pyrolysis (873-973 K) of cyclohexene or ethene on the surface of a gamma-alumina, and evaluated for their use as supports for cobalt sulfide hydrodesulfurization catalysts. Promising textural properties were obtained for the samples prepared : B.E.T. surface areas up to 334 m^2/g, meso- and macropore surface areas reaching values of 190-270 m^2/g and narrow pore size distributions in the 2.5-10 nm pore radius range. XPS measurements showed that the alumina surface was not uniformly covered, probably due to diffusion limitations of the carbon forming hydrocarbons. The coverage could be improved (maximum value reached was 77%) by increasing the amount of carbon deposited as well as by an additional high temperature (1073 K) treatment. The thiophene hydrodesulfurization activity of Co sulfide supported on the prepared carbon-covered aluminas was found to increase linearly with increasing alumina surface coverage by carbon. A three-fold increase in activity compared to Co/Al_2O_3 catalysts was obtained, demonstrating the effective shielding by the carbon layer which reduces or eliminates the strong metal-alumina interactions. Oxidizing the carbon surface prior to the introduction of cobalt led to a further improvement of the catalytic activity.

INTRODUCTION

Alumina-supported sulfided cobalt molybdenum catalysts are currently used for hydrodesulfurization (HDS), hydrodenitrogenation (HDN), and several other important hydrotreating applications (1). Interest in these catalysts has increased dramatically in the last few years, not only because of their application in the production of synthetic fuels but also because of their importance in the treatment of heavy crude oil and resids. Most of the studies published in the literature concern the characterization of the structure of the metal sulfide or the precursor metal oxide phase in connection with the alumina carrier (2). Considerably less attention has been given to the impact that different support materials may exert on the metal sulfide characteristics. The exclusive use of alumina supports in hydrodesulfurization catalysts is intriguing because the reactive alumina surface causes unwanted metal oxide-support interactions which lower the HDS activity of the catalyst. Especially the promotor ions Co and Ni react upon calcination with the alumina support and occupy octahedral or tetrahedral sites in the external layers of the support or even form $CoAl_2O_4(NiAl_2O_4)$. Extensive studies by Burggraf et al. (3) resulted in a model which describes the competition between formation of a tetrahedral species, by diffusion of the metal ion into the Al_2O_3 spinel, and formation of an octahedral species at the support surface. Only at high wt% metal the corresponding metal oxide (NiO, Co_3O_4) is formed. It is evident that the poor HDS activity of sulfided Co- or Ni oxide/Al_2O_3 catalysts is at least partly due to the strong interaction between Co and Ni ions and the alumina support, as a result of which a considerable fraction of these cations is not accessible to the reactants. Also the morphology of the sulfide phase induced by interaction with the alumina support may be such that a low density of HDS sites with

poor turn-over frequency is attained at the surface of the metal sulfides. Such a situation has been observed for Mo sulfide/Al_2O_3 catalysts (4). Numerous studies have been carried out aimed at preparing more effective catalysts via reduction of the active phase-support interaction. Bachelier et al. (5) observed for NiO/Al_2O_3 catalysts that lowering of the calcination temperature as well as raising the sulfiding temperature led to higher thiophene conversions. The use of alumina doped with alkali earth cations as a support has been studied by Lycourghiotis et al. (6,7). Some regulation of the active phase-carrier interaction could be obtained with these doped supports, especially with dopes such as Be^{2+} and Mg^{2+} which inhibit the reaction between Co_3O_4 and Al_2O_3 to $CoAl_2O_4$ and the dissolution of Co^{2+} into the Al_2O_3 layers. However, to our knowledge no data have been reported which demonstrate that application of these doped supports results in higher HDS activities. In contrast herewith, substantially more active Co catalysts have been prepared on the less reactive SiO_2 support (8), and recently it has been shown that Co and Ni are even more active (Co) or equally active (Ni) than the corresponding Mo-based catalysts when they are supported on relatively inert carbon carriers (9,10). Thus, application of a material as inert as carbon offers the advantage that all transition metal compounds present in the precursor state will be quantitatively converted into their active sulfide form.

Most of the carbon materials applicable as support for HDS catalysts have, however, either extensive microporosity or have poor mechanical properties . For catalytic reactions involving large molecules the micropores are of little utility since part of the transition metals will be deposited in these pores, in effect, be wasted. Most mesoporous carbons on the other hand have either poor crushing strengths, low bulk densities or a too low surface area. One possibility to circumvent these drawbacks

consists in the application of carbon black composite carrier materials (11). Another approach is presented in this paper and is based on the covering of the Al_2O_3 surface with a thin layer of carbon prior to impregnation of the transition metals. In this way the favourable carbon surface properties (quantitative conversion of the precursor metal salts into their highly active sulfide form) are combined with the optimal textural and mechanical properties of the Al_2O_3 support. The present study reports the preparation and evaluation of these carbon-type supports denoted Carbon-covered Alumina (CCA). Attention will be paid to variations in textural properties and degree of alumina surface coverage with increasing carbon deposition, to the effect that different carbon forming hydrocarbons have on the above properties, and to the thiophene hydrodesulfurization activities of Co/CCA catalysts. Cobalt was chosen as active fase because the difference in HDS activity between Co/Al_2O_3 and Co/C catalysts is very large (Much larger than that for the corresponding Mo catalysts). Techniques used were ^{13}C solid state NMR, TGA, XPS, and HDS activity measurements.

EXPERIMENTAL

Preparation and pretreatments of the supports.

The method used to prepare the carbon-covered alumina supports was adopted from Youtsey et al. (12), and consisted in pyrolysing a hydrocarbon on the surface of a high surface area alumina. Two types of hydrocarbons were selected : cyclohexene (Fluka, purity > 99%) and ethene (Hoekloos, purity > 99%). Preparation consisted of heating 1.2 g of alumina (Ketjen, grade B) in a quartz reactor up to the reaction temperature at a heating rate of 10 K/min under continuous N_2 flow of 18 ml/min, and keeping at this

temperature for an additional 0.5 h. It was observed that identical results were obtained when the corresponding boehmite was applied as starting material, hence in most of the experiments boehmite was used. After preheating under N_2 the gas flow was switched to a mixture of N_2 and the hydrocarbon to be pyrolysed. Total flowrate was 20 ml/min. After completion of the reaction the samples were cooled to room temperature under flowing N_2. Different CCA samples were prepared, using the hydrocarbons mentioned above, by varying the hydrocarbon partial pressure, the pyrolysis temperature or the duration. In Table 1 the reaction conditions applied together with the resulting amount of carbon deposited, are listed. The samples will be denoted as C-x or E-x, indicating the type of hydrocarbon used (Cyclohexene or Ethene), and the amount of carbon deposited (x=weight percentage based on total weight of the CCA sample). Some cyclohexene type CCA samples were subjected

Table 1 : Preparation conditions of CCA samples

hydrocarbon used	hydrocarbon partial pressure (Torr)	pyrolysis temperature (K)	run time (h)	weight* percentage carbon (%)	notation**
cyclohexene	26	898	3.0	11	C-11
	76	873	6.0	20	C-20
	76	898	6.0	26	C-28
	76	973	6.0	35	C-35
ethene	38	903	6.5	10	E-10
	76	878	6.5	15	E-15
	76	908	6.5	20	E-20
	76	973	6.5	25	E-25
	76	983	6.5	27	E-27

* Obtained by measuring the weight loss of the CCA samples when heated in a continuous air flow up to 1023 K (15 K/min heating rate) in a Thermo Gravimetric Analysis apparatus.

** C or E stands for cyclohexene or ethene-prepared ; number represents weight percentage carbon.

to a heat treatment in order to improve the degree of alumina surface coverage. This involved heating the sample up to 1073 K (heating rate 10 K/min) under continuous N_2 flow for several hours. For experimental details see Table 2. Furthermore on a cyclohexene type as well as on an ethene type CCA sample already subjected to a heat treatment, an oxidative treatment was applied in order to increase the surface heterogeneity of the carbon deposit. In the oxidative treatment the CCA samples were subjected to a N_2 flow saturated with water vapour (p_{H_2O} = 17 torr). For experimental details see Table 2.

Table 2 : Treatments applied to CCA samples

sample	treatment*	temperature (K)	time (h)	notation* final sample**
C-20	H	1073	24	C-20-H
C-28	H	1073	9.5	C-27-H
C-28	H+O	1073(H)	9.5(H)	C-27-HO
		773(O)	48(O)	
E-25	H+O	1073(H)	3(H)	E-20-HO
		1073(O)	3(O)	

* H,O stands for Heat or Oxidative treatment respectively.

** Since during the treatments variations in carbon content might occur, the weight percentage carbon was measured after the treatment. Especially the ethene-prepared CCA sample had lost a considerable amount of carbon, probably due to the high temperature during the oxidative treatment.

Texture, XPS and ^{13}C-MAS-NMR experiments

Surface characteristics of the supports were studied by means of the adsorption-desorption isotherms of N_2 at 77 K measured on a Carlo-Erba sorptomatic 1800 apparatus. The surface areas of the various samples were calculated using the BET equation, pore size distributions in the meso pore range were determined using the Kelvin equation assuming a cylindrical pore model. Prior to the actual measurements

the samples were outgassed at 423 K in vacuum (1.3 x 10^{-5} torr). Total pore volumes were measured by water titration.

X-ray photoelectron spectroscopy was used to measure the surface characteristics of the CCA supports. The measurements were carried out on a Physical Electronics 550 XPS/AES spectrometer equipped with a magnesium X-ray source (E = 1253.6 eV) and a double pass cylindrical mirror analyzer. The powdered samples were pressed on a stainless steel mesh which was mounted on top of the specimen holder. C 1s and Al 2p photoelectron signals were collected in steps of 0.05 eV. Data acquisition time was varied according to the intensity of the signals. The intensity of a given photoelectron peak was calculated from the peak area after correction for inelastic backscattered electrons. The pressure during the measurements did not exceed 5 x 10^{-8} torr and the temperature was approximately 293 K. In some cases a specimen neutralizer (low energy electron gun) was used to study the insulating or conducting properties of the CCA samples.

^{13}C-MAS-NMR spectra were recorded on a Bruker CXP-300 spectrometer. Typically 0.12 g of solid sample was used. 90 pulses were applied at 75.476 MHz at 20 s intervals. 400 FID's were accumulated in 2K data points zero-filled to 8K, followed by Fourier transformation (line broadening 100 Hz). No crosspolarization was applied. The chemical shift is measured with respect to TMS.

Catalyst preparation and activity measurements.

The various CCA samples were impregnated (pore volume impregnation) with aqueous solutions of cobalt nitrate (Merck, "for analysis"). The support surface loading was kept in the range of 0.4-0.7 Co atoms per nm^2 support surface area. After impregnation the samples were dried in air starting at 293 K and slowly increasing to 383 K where they were kept overnight. The catalysts were not

subjected to a calcination procedure. Prior to the activity measurements the catalysts were sulfided in situ in a H_2S/H_2 flow (10 mol% H_2S, total flow rate 60 ml/min) using the following temperature program : linear increase from 293 K to 673 K in 1 h and holding at this temperature for two additional hours. After sulfiding, a flow (50 ml/min) of thiophene (6,2 mol%) in H_2 was led over the catalyst at 673 K. Thiophene conversion (typically between 4-6%) was measured at different time intervals by on-line gas chromatography. First order rate constants for thiophene HDS were calculated after 2 h run, and used to obtain the HDS activity per mol Co (indicated as QTOF value = Quasi Turn-Over Frequency).

THEORY

When depositing carbon on the alumina surface, the textural and surface properties of the product CCA material depend not only on the carbon content but also on the way in which carbon is deposited on the alumina. Consider for instance the B.E.T. surface area of CCA carriers. This will be given by the formula :

$$S_{CCA}(m^2/g) = W_{Al} \cdot S_{Al} \cdot (1-f) + W_C \cdot S_C$$

where S_{Al}, S_C, f, W_{Al} and W_C stand for the surface area of the alumina (m^2/g Al_2O_3), the surface area of the carbon deposit (m^2/g C), the fraction of the alumina surface covered by carbon, the weight fraction alumina in the CCA sample, and the weight fraction carbon in the CCA sample, respectively. It can be easily understood that if the deposited carbon structures have greater surface areas than the fraction of the alumina which they cover and the volume-to-surface ratio is small, then the surface area of CCA samples can easily surpass that of the original alumina

(for instance if the carbon is deposited as small hemispherical particles). However, if carbon is layed down as a monolayer or if flat epitaxial multilayer patches of carbon are formed, the surface area of the resulting CCA sample (normalized on a per gram basis) will decrease with increasing amount of carbon deposited. Thus given the weight fraction carbon deposited and the surface areas of the CCA samples it is possible to get some indication of the carbon morphology.

Another very important parameter related to the carbon morphology of CCA-type supports is the degree of carbon coverage (f) of the alumina surface. An indication of this characteristic can be obtained by comparing the experimentally derived CCA pore size distributions with the ones calculated under the assumptions that the carbon is uniformly deposited (f=1) over the entire alumina surface and that the pores are cylindrical. These pore size distributions can be obtained as follows : The pore volume $V_i(CCA)$ associated with a pore radius $r_i(CCA)$ of a uniformly (thickness d) carbon-covered alumina support is calculated from the experimentally derived pore volume $V_i(Al)$ associated with a pore radius $r_i(Al)$ [equal to $r_i(CCA) + d$)] of the alumina support by the formula :

$$V_i(CCA) = V_i(Al) [1 - d/r_i(Al)]^2.$$

This was done over the entire pore radius range (1.5-100 nm) taking sufficiently small pore radii intervals. In this way the complete pore size distribution was calculated for CCA samples with a 0.5 and 1.0 nm thick (d) uniform carbon layer deposited on the alumina surface. These are depicted in Fig. 1 together with that of the original alumina. Comparison of the experimentally obtained pore size distributions of the various CCA samples with the theoretical ones representing uniform carbon coverage, can give an indication of the carbon deposition in a certain

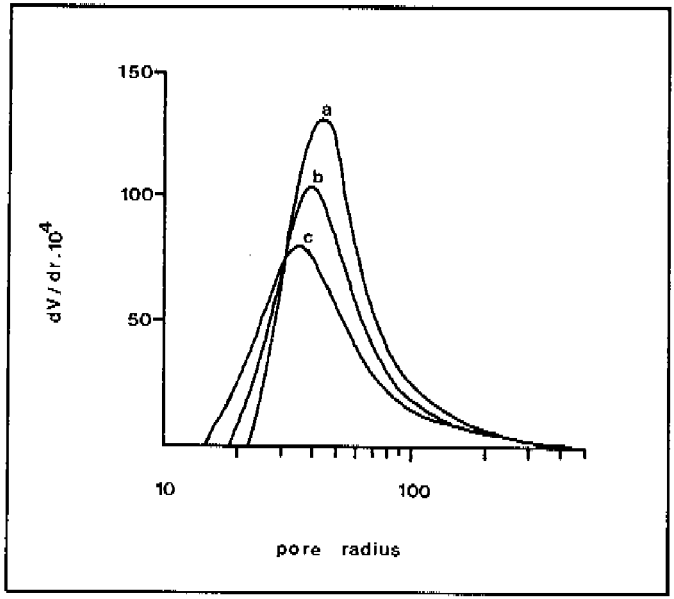

Fig. 1 Experimentally determined pore size distribution of Al_2O_3 (a) and theoretically determined pore size distribution of CCA samples assuming complete alumina surface coverage by a carbon layer of 0.5 nm thickness (b) corresponding to 19.5 wt% carbon and 1.0 nm thickness (c) corresponding to 32.7 wt% carbon.

pore radius range.

A more direct measurement of the average degree of carbon coverage of the alumina surface can be obtained by XPS measurements. The theoretical calculations predicting the XPS intensity ratio of a catalyst phase deposited on a porous carrier material outlined by Kerkhof and Moulijn (13), were used to calculate the degree of alumina surface coverage of our CCA samples. We used the model in its most general form (equation 10 of ref 13) which calculates the

fraction of the electrons (C 1s and Al 2p) passing through the support layers as well as through the deposited carbon layers. The experimental intensity ratios for a given weight% carbon of the CCA samples were computer fitted to the theoretical ones using the surface coverage (f) as variable. The XPS parameters used are collected in Table 3.

Table 3 : XPS parameters

D_{Al}*	0.848×10^{-3}	t***	2.07 nm
D_C*	1.032×10^{-3}	λ_{AlC}****	1.56 nm
σ_{Al}**	0.573	λ_{CC}****	1.35 nm
σ_C**	1	λ_{CAl}****	1.40 nm
ρ_C	1.8 g/ml	λ_{AlAl}****	1.63 nm

* Detector efficiencies = E_{kin}^{-1}.
** Cross sections according to ref. 14.
*** Support layer thickness t = 2/ $\rho_{Al} \cdot S_{Al}$.
**** Electron escape depths according to ref. 15.

RESULTS

General aspects of the CCA samples.

All CCA samples were dark black with the exception of the C-11 and E-10 samples which were greyish. Another aspect of the carbon deposit on the alumina is the electrical (and thermal) conductivity of CCA samples compared to the insulating properties of alumina. An indication for the presence of conducting and insulating domains on the surface of the CCA samples was obtained by XPS. During XPS data acquisition, the insulating part of the sample tends to acquire a steady-state positive charge of a few eV's, while the conducting domains remain neutral. As a result two peaks will appear in the spectrum. Low energy electrons from a flood gun were supplied to the sample to neutralize the charge of the insulator parts. By changing the energy of these electrons a distinction between insulation and

conducting phases of the sample can be made, since the peaks of the insulator parts will move relative to those of the conducting parts. In the low carbon content samples a major insulating character of both the Al and the C spectral peaks was observed. Increased carbon content lowered the charging effects until in the high carbon content samples (wt% C > 25) only conductive properties were observed. A larger

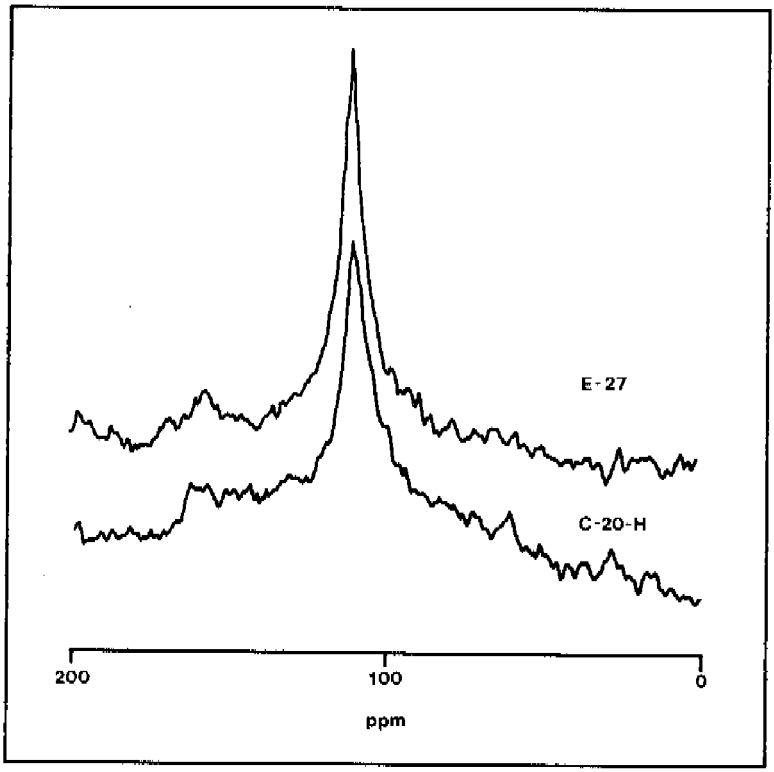

Fig. 2 ^{13}C-MAS-NMR spectra of a cyclohexene- (C-20-H) and an ethene-prepared (E-27) CCA sample.

contribution of insulating phase was observed for the cyclohexene type samples compared to ethene type samples of equal carbon content. The heat treated cyclohexene type CCA supports behaved comparable to ethene type samples. To get some structural information of the carbon deposit, ^{13}C-MAS-NMR spectra were recorded of an ethene- (E-27) and cyclohexene- (C-20-H) prepared sample (cf. Fig. 2). Both spectra are similar, viz., only one broad peak proportional to the carbon content, located at 110 ppm is observed. The chemical shift indicates olefinic or aromatic character (sp^2 hybridisation) of the carbon atoms, although the chemical shift is somewhat low for this class of compounds (120-150 ppm). The spectra measured of an activated carbon (Norit RX3 extra) and a carbon black (Monarch 1300) were, however, similar to those described for the CCA samples.

Texture and surface properties of CCA samples.

Cyclohexene-prepared samples.

In Fig. 3 the pore size distributions of some cyclohexene type samples and of the pure Al_2O_3 reference sample are plotted. As can be seen the pore size peak shifts towards lower radius and decreases in height with increasing amount of carbon deposited. Comparison of these experimentally found pore size distributions with the corresponding (same wt% C) theoretical distributions for the uniformly deposited carbon samples as outlined in the theoretical section, indicates that in the prepared CCA samples : (i) the pore size peaks are lower, (ii) the peaks have their maximum at lower pore radius and (iii) a considerable amount of pore volume is present in pores with radii smaller than 2.0 nm. These results already indicate that carbon coverage of the alumina surface is not uniform. It seems as if more carbon is deposited in the wider pores than in the narrow pores of the alumina. This is confirmed by the observation that the

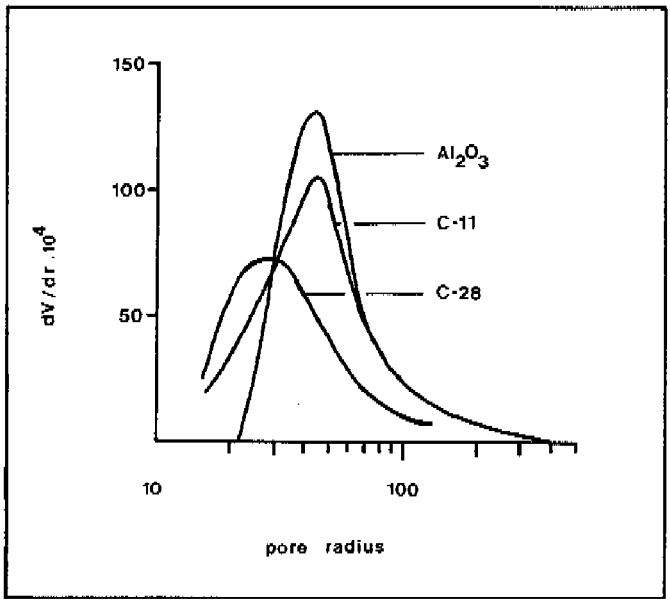

Fig. 3 Pore size distributions of Al_2O_3 and two cyclohexene-prepared (C-11, C-28) CCA samples.

N_2 adsorption - desorption hysteresis curve, which indicated mainly cylindrical pores for the alumina sample, changes with increasing carbon deposition towards the inkbottle type. In Table 4 surface area distributions, pore volumes and XPS results are listed. A decrease in pore volume with increasing carbon deposition can be noticed. On the other hand surface areas remain remarkably high. The micropore surface area of these CCA samples has increased relative to the alumina sample, which indicates that small pores (e.g. cracks) are present in the carbon layer. Compared to activated carbons, however, the CCA type carbon materials demonstrate high mesoporosity combined with relatively low

Table 4 : Textural and surface properties of CCA supports

support	S_{BET} (m^2/g)	S r>1.5 nm (m^2/g)	% micropores (r<1.5 nm)	pore volume ml/g	XPS I_C/I_{Al}	alumina surface coverage
Al_2O_3	270	257	5	1.9		
*C-11	304	252	17	1.6	-	-
C-20	-	-	-	1.4	0.9	0.14
C-28	304	210	31	1.0	2.4	0.37
C-35	-	-	-	1.1	-	-
E-10	-	-	-	2.1	-	-
E-15	334	274	18	2.0	1.0	0.19
E-20	304	235	23	2.0	1.8	0.37
E-25	-	-	-	1.6	3.0	0.65
E-27	276	214	22	1.5	3.6	0.77
C-20-H	264	202	23	1.6	1.7	0.34
C-27-H	269	192	29	1.1	2.9	0.51
C-27-HO	299	215	28	1.1	2.8	0.49
E-20-HO	-	-	-	2.0	2.3	0.68
NORIT RX3 extra	1190	250	79	1.0		

* support notation cf. Table 1 and 2.

microporosity.

As was expected the C 1s/Al 2p XPS intensity ratio increases with increasing amount of carbon deposited. Very striking are the relatively low alumina surface coverages especially for the low carbon content samples. However, with increasing carbon deposition the surface coverage seems to increase.

Ethene-prepared samples.

Fig. 4 shows the corresponding pore size distributions of the ethene type CCA samples including also the pure alumina

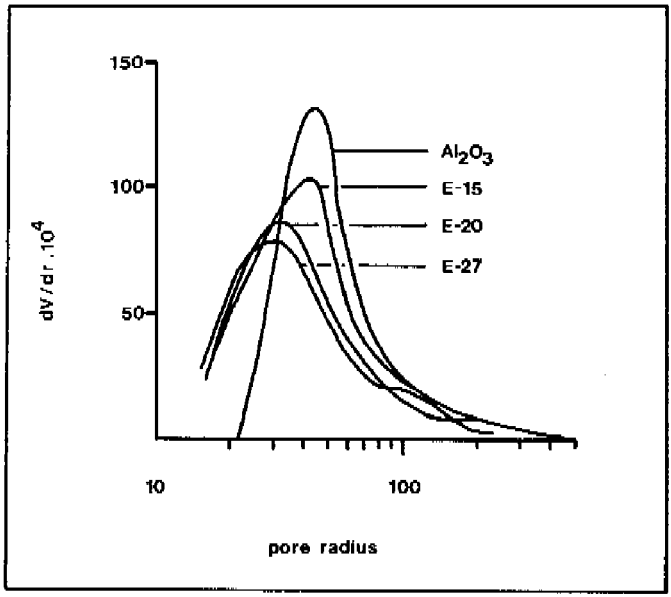

Fig. 4 Pore size distributions of Al_2O_3 and three ethene-prepared (E-15, E-20, E-27) CCA samples.

support. The same features found for the cyclohexene-prepared CCA samples apply for this series of CCA samples : shift in pore radius peak and decrease in height of this peak with increasing amount of carbon deposited, as well as a considerable amount of porosity in pores with radii smaller than 2.0 nm. It is noticed however, that the pore size peaks of the ethene type samples remain somewhat higher compared to those of the corresponding cyclohexene type samples, which already indicates that the carbon is more uniformly spread over the alumina surface . In Table 4 the textural data of the ethene type CCA's are collected. Very striking is the high pore volume of these

samples. Although this can be attributed to the formation of macropores, since no increase in meso- or micropore volume was observed for these samples compared to corresponding cyclohexene type samples, this result remains intriguing. Perhaps the preparation of the carbon-covered alumina with ethene as hydrocarbon causes a conglomeration of the precursor alumina particles with the pyrolyzed carbon substance as binder, inducing an extra macropore volume. The B.E.T. surface area of the samples gradually decreases with increasing amount of carbon deposited. This again points to a more uniform type of coverage, although sufficient roughness of the carbon deposit (e.g. cracks) must be present in order to explain the high surface areas. The micropore surface area remains about 20% of total surface area, which is low compared to activated carbons.

The XPS results are also collected in Table 4. With increasing carbon content the C 1s/Al 2p intensity ratio increases. The surface coverage increased drastically with increasing carbon content. Interestingly, the ethene type samples have surface coverages twice as high as cyclohexene-prepared samples of the same carbon content, reaching a value of 77% in the highest carbon content sample.

Treatments on cyclohexene- and ethene-prepared samples.

In the previous paragraphs it was demonstrated that the alumina surface coverage was not uniform, especially not for cyclohexene-prepared samples. In order to improve this, two cyclohexene type CCA (C-20,C-28) samples were subjected to a heat treatment which was expected to cause spreading of the carbon over the alumina and simultaneously elimination of the micropores (cracks) in the carbon layer. This technique has been reported to be useful for modifying the nature of the pore system in glassy carbon samples (16). As a result of the heat treatment only some minor changes in the carbon content of the samples were observed, indicating that essentially no carbon was lost during the heat

treatment. Thus a straightforward comparison can be made between C-20, C-20-H and C-28, C-27-H (H stands for heat treatment). As shown in Table 4 surface coverages increase markedly upon heat treatment but still remain below uniform coverage. The textural properties of these heat treated samples undergo only minor changes compared to untreated samples, viz., a slight decrease in surface area and some increase in pore volume and height of the pore size peak is noticed (more uniform type coverage). It is to be expected that the carbon surface of the CCA prepared samples and especially those which were subjected to the heat treatment are very inert. As a consequence the dispersion of the carbon-supported Co phase will be poor. In order to improve on the affinity of the carbon surface of the CCA samples towards the Co phase, a steam oxidation procedure was applied. Two samples were oxidized (C-27-H and E-25-H), which had been subjected to a heat treatment first. Since it is to be expected that the stream oxidation procedure applied will cause some loss in carbon due to gasification, the carbon content of the oxidized samples was measured. It was found that no carbon loss had occurred for the C-27-H sample (thus denoted C-27-HO), but considerable gasification had occurred on the E-25-H sample since only 20 wt% was found (E-20-HO). The latter should therefore be compared with the E-20 sample. Both oxidized samples show a high degree of alumina surface coverage, indicating that the oxidation treatment leaves the coverage intact.

Catalytic properties of CCA-supported Co-sulfide catalysts.

In Table 5 the amount of Co in CCA-supported sulfided cobalt catalysts (Co/CCA) and the corresponding catalytic activities per mol Co (QTOF in mol thiophene converted per mol Co per s) are collected. Table 5 also includes the HDS activities measured for Co sulfide catalysts supported on Al_2O_3 and activated carbon. As can be noticed, a very

Table 5 : Catalytic properties of Co/CCA catalysts

support	weight % Co	QTOF x 10^2 (mol thiophene/mol Co.s)
Al_2O_3	2.3	0.7
*C-11	2.2	0.8
C-20	1.6	0.9
C-28	1.8	1.2
C-35	1.4	1.6
E-10	1.5	1.1
E-15	1.5	1.2
E-30	1.2	1.5
E-25	1.3	1.8
E-27	1.6	2.0
C-20-H	1.3	1.3
C-27-H	1.8	1.6
C-27-HO	2.1	1.8
E-20-HO	1.0	2.4
Norit RX3 extra	10.05	5.1

* support notation cf. Table 1 and 2.

striking large discrepancy in HDS activity exists between the alumina- and activated-carbon supported catalysts as was reported earlier (9,10). The HDS activity of the sulfided Co on cyclohexene type CCA catalysts increases steadily with increasing amount of carbon present in the CCA carrier. This leads to an activity in the C-35 sample which is twice as high as that of the corresponding pure alumina-based catalyst. Co catalysts deposited on ethene type CCA supports behave analogous to the cyclohexene type serie, namely a steady increase in activity is observed with increasing amount of carbon in the support. However, the ethene type catalysts are more active than the corresponding

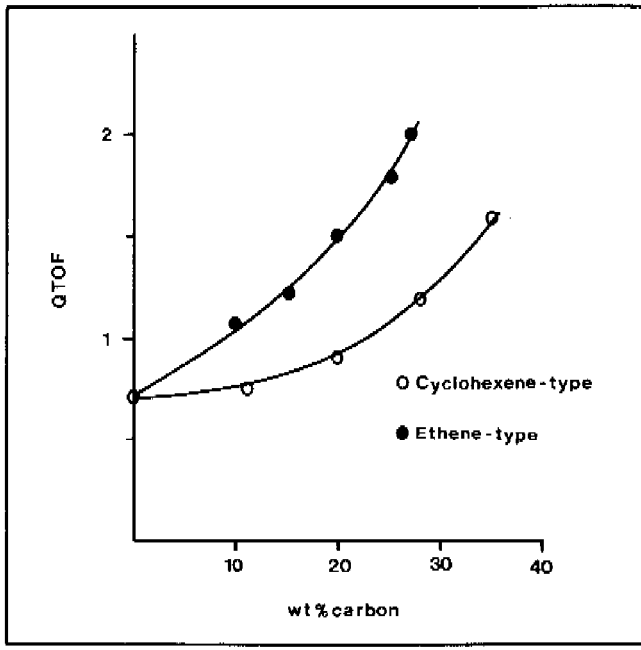

Fig. 5 HDS activity per mol Co (QTOF value) of sulfided Co/CCA catalysts plotted relative to the weight% carbon of the support.

(same wt% carbon) catalysts based on cyclohexene type supports. In Fig. 5 the HDS activity behaviour of the Co/CCA catalysts is shown as a function of the wt% carbon present in the CCA carriers. Fig. 5 suggests that the HDS activity behaviour of the sulfided Co/CCA catalysts is closely related to the degree of alumina surface coverage by carbon. This is emphasized by the observation (Table 5) that the HDS activity of Co sulfide on the C-20-H and C-27-H heat treated supports is considerably higher than that of Co sulfide on the C-20 and C-28 supports (Recall that as a

result of the heat treatment spreading of the carbon on the alumina surface occurred, increasing the degree of surface coverage). Finally, it can be seen that the catalysts prepared on the heat treated and subsequently oxidized supports, have a high activity. In order to see more clearly the effect that a heat and oxidative treatment of the CCA supports has on the HDS activity of a supported cobalt catalyst, one should compare the HDS activity of the following series of catalysts : (i) Co/C-28, Co/C-27-H, Co/C-27-HO (ii) Co/C-20, Co/C-20-H (iii) Co/E-20, Co/E-20-HO. As can be seen in Table 5 both the heat treatment and the oxidative treatment have a positive effect on the HDS activity of supported cobalt catalysts.

DISCUSSION

Pyrolytic carbons have been applied in different research areas. Most of the related literature deals with the deposition of pyrolytic carbon into porous carbon substrates (commonly called infiltration) in order to obtain an appreciable densification of the carbon material. Numerous theories have been proposed in this respect to describe the mechanism, kinetics and the structure of pyrolytic carbon formation generally at high temperatures (> 1273 K) (17). The salient conclusions of these studies with regard to the present study are : (i) below 1473 K and at low hydrocarbon partical pressure a high-density layered pyrolytic carbon is produced (density = 2g/ml) with an aromatic character : (ii) the growth of pyrolytic carbon in the pores of an aggregate can be treated in a manner analogous to the oxidation of porous carbons with gases. In order to obtain a uniform carbon deposition the temperature and the reaction rate should be kept low. In the field of chromatography pyrolytic carbon-coated silica particles were prepared and evaluated for their use as adsorbents in gas-liquid chromatography

(18,19). It was found (18) that deposition of up to 15 wt% carbon did not reduce the surface area significantly, suggesting that the effect of surface area decrease due to pore plugging is compensated by the effect of the surface area increase due to the porosity of the carbon coating. In the production of aluminium chloride from alumina or bauxite, the deposition of pyrolytic carbon on the oxide surface was studied in view of its reductive properties on the chlorination of the alumina or bauxite (20). General conclusions of this work regarding the CCA properties were that deposition of carbon on alumina (using acetylene, ethene or ethane diluted in N_2) at a temperature of 1073 K proceeds slowly and that up to about 10 wt% carbon deposited the surface area of the CCA sample increased or remained the same relative to the pure alumina sample. In the patent by Youtsey (12), applied in the present study as a guide for CCA preparation, the conductive properties of the final material were of interest and no information was included on the textural or coating characteristics of the CCA samples. Depending on the amount of carbon deposited it was found possible to prepare semi-conducting or conducting CCA samples. The reason for this was the high density of conjugated double bonds in the carbon deposit. Finally, in the literature only one example was found in which CCA-type materials were used as supports for HDS catalysts (21). The impetus behind the application of this support was to neutralize the acidity of the alumina support. No data on the support nor catalyst properties were given in the paper. Despite the above cited research efforts, no clear picture of the textural and surface properties of CCA-type materials and their relation with process parameters such as amount of carbon deposited, pyrolysis temperature, pressure and hydrocarbon used, has emerged. Thus, we have found it important to characterize these CCA properties since they are of vital interest when using CCA materials as supports for catalyst systems.

It was observed that the textural properties of the CCA samples were largely dependent on the amount of carbon deposited as well as on the type of hydrocarbon used for the pyrolysis. As a general observation we can conclude that presently prepared CCA samples had narrow pore size distributions situated in the 2.5-10 nm pore radius range, combined with meso- and macropore surface areas reaching values of 190-270 m^2/g. The micropore surface area never exceeded 30%of the total B.E.T. surface area. It was suggested from inspection of the pore size distributions that more carbon was deposited in the larger pores of the alumina than in the narrow pores, indicating that no uniform coverage of the alumina surface by carbon was obtained. This was confirmed by the XPS measurements. In addition they indicated that the alumina surface coverage increased with increasing carbon deposition and was much higher for the ethene type CCA samples than for the cyclohexene type samples. From these results two general conclusions can be drawn. Firstly, the rate of diffusion of the carbon-yielding hydrocarbon influences carbon deposition. Secondly, carbon deposition occurs on exposed alumina surface, rather than on carbon. The latter conclusion is based on the observation that the alumina surface coverage increased with increasing carbon deposition. In order to suppress the diffusion problems we prepared cyclohexene type CCA samples at lower temperatures (788 K). The surface coverages measured were, however, equal to those of the corresponding samples prepared as described in Table 1. It might be argued that application of methane as carbon-yielding hydrocarbon could result in a better alumina surface coverage. However, these methane type CCA samples would require high preparation temperatures in order to obtain sufficient carbon deposition within a reasonable time period. At these temperatures one would be confronted with the problem of the stability of the alumina support.

The heat treatment experiments point to a remarkable

increase in alumina surface coverage at a given carbon content. During the prolonged pyrolysis hydrogenation of the carbon coating will take place. The resulting product will adhere much better to the surface and as a consequence, the alumina surface coverage will be improved. These experiments confirm the conclusion that the carbon preferentially deposites on the alumina support rather than agglomerates.

HDS activity of Co/CCA catalysts increased with increasing carbon deposition on the support, in both the cyclohexene and ethene-prepared CCA supports. It became clear that the degree of alumina surface coverage is the main factor determining catalyst activity. As shown in Fig. 6 a correlation can be found between the alumina surface coverage and the activity of a supported Co catalyst for the unoxidized CCA samples. This catalytic behavior can be explained as follows. During impregnation the Co ions can get attached either to the uncovered alumina surface or to the carbon surface of the CCA support. Two conditions have to be fulfilled in order that a linear correlation holds between activity and alumina surface coverage : (i) the distribution of the Co phase between the alumina and carbon surfaces must be proportional to the mutual ratio of the two surface areas, and (ii) the Co phases deposited on the alumina and carbon surface have to be considered as individual non interacting entities with QTOF values of 0.7 x 10^{-3} s^{-1} and 2.5 x 10^{-3} s^{-1} (extrapolation in Fig. 6 to f=0 and f=1 respectively). These conditions seem reasonable in view of the fact that the amount of Co deposited is low compared to the available support surface areas. Thus the resulting QTOF value of Co deposited on an unoxidized CCA material having an alumina surface coverage f is given by the formula :

$$QTOF\ (x\ 10^{3}) = 2.5\ f + 0.7\ (1 - f)$$

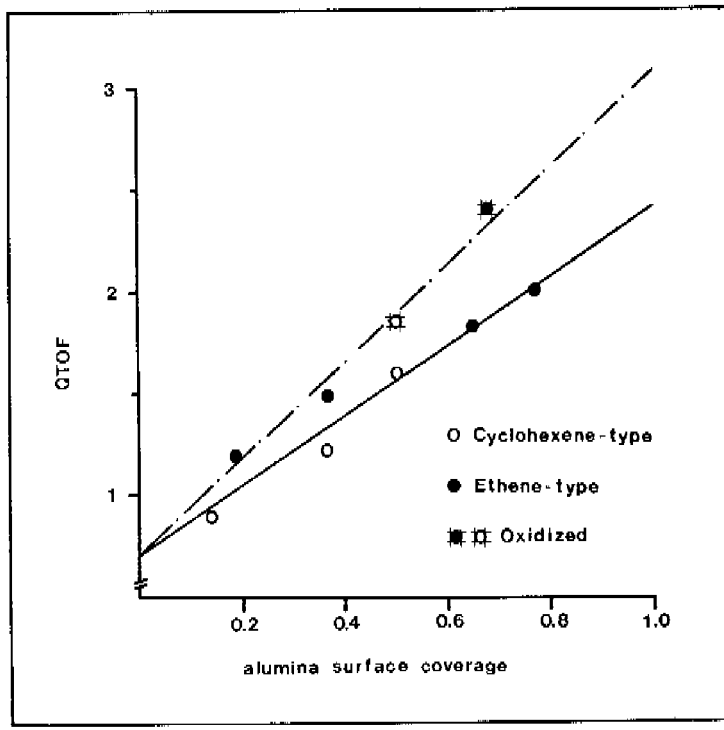

Fig. 6 HDS activity per mol Co (QTOF value) of sulfided Co/CCA catalysts versus the degree of carbon coverage of the alumina surface as measured by means of XPS.

The intrinsic activity of Co deposited on the unoxidized carbon layer (2.5×10^{-3} s^{-1}) is lower than the value reported for activated carbon supported Co phase (5.1×10^{-3} s^{-1}), probably due to a difference in Co dispersion. More sintering of the Co phase will take place on the highly inert pyrolytic carbon surface which has very few anchorage

sites for the Co phase. This is emphasized by the experiments in which the carbon surface of CCA samples was oxidized, showing a considerable increase in activity of deposited Co catalysts (cf. Table 5 and Fig. 6). Extrapolation of the HDS activity of Co catalysts deposited on these oxidized CCA supports to f=1 results in a QTOF value of around 3.0×10^{-3} s^{-1}.

Summarizing our results we conclude that the CCA materials combine several favourable properties for use as supports for sulfide catalysts. The textural properties are such that the major part of the pore radii are located in the 2.0-20 nm range, while microporosity never exceeds 30% of the total BET surface area. The carbon coating effectively shields the reactive alumina surface from the catalytic phase. Hence, due to the absence of strong metal-support interactions, catalysts can be prepared with remarkably higher HDS activities compared to the conventional alumina-supported catalysts.

REFERENCES

1. Mc Culloch, D.C., in "Applied Industrial Catalysis", (Leach, B.E., ed.), vol 1, p. 69, Academic press, New York (1983).
2. Grange, P., Catal. Rev.-Sci. Eng. 21 (1), 135 (1980).
3. Burggraf, L.W., Leyden, D.E., Chin, R.L. , and Hercules, D.M., J. Catal. 78, 360 (1982).
4. Vissers, J.P.R., Bachelier, J., ten Doeschate, H.J.M., Duchet, J.C., de Beer, V.H.J., and Prins, R., in "Proceedings of 8th International Congress on Catalysis, Berlin,1984 " p. II-387, Verlag Chemie, Weinheim, 1984.
5. Bachelier, J., Duchet, J.C., and Cornet, D., Bull. Soc. Chim. Fr. 1, 221 (1979).
6. Lycourghiotis, A., Vattis, D., and Aroni, P., Z. Phys. Chem. Neue Folge 121, 257 (1980).

7. Lycourghiotis, A., Tsiatsios, A., and Katsanos, N.A., Z. Phys. Chem. Neue Folge 126, 95 (1981).
8. de Beer, V.H.J., van Sint Fiet, T.H.M., Van der Steen, G.H.A.M., Zwaga, A.C., and Schuit, G.C.A., J. Catal. 35, 297 (1974).
9. de Beer, V.H.J., Duchet, J.C., and Prins, R., J. Catal. 72, 369 (1981).
10. Vissers, J.P.R., Mercx, F.P.M., de Beer, V.H.J., and Prins, R., J. Catal. to be published, chapter 4 of this thesis.
11. Vissers, J.P.R., de Beer, V.H.J., and Prins, R., Applied Catal. to be published, chapter 8 of this thesis.
12. Youtsey, K.J., Holt, W.C., Carnahan, R.D., and Spielberg, D.H., US Patent 4,018,943 (1977).
13. Kerkhof, F.P.J.M., and Moulijn, J.A., J. Phys. Chem. 83, 1612 (1979).
14. Scofield, J.H., J. Electron Spectrosc. 8, 129 (1976).
15. Penn, D.R., J. Electron Spectrosc. 9, 29 (1976).
16. Walker Jr, P.L., in "Proceedings Fifth Industrial Conference on Carbon and Grafhite", London, Soc. Chem. Ind., 427, 1978.
17. Kotlensky, W.V., in "Chemistry and Physics of Carbon", (P.L. Walker, Ed.), Vol. 9, p. 173, Dekker, New York, 1973.
18. Colin, H., and Guishon, G., J. of Chromatography 126, 43 (1976).
19. Leboda, R., Waksmundzki, A., Chromatographia 12, 207 (1979).
20. Alder, H.P., Geisser, H., Baiker, A., Richarz, W., "Proceedings of 108th AIME, New Orleans, 1979", p. 337, 1979.
21. Kiezel, L., and Rutkowsky, M., Pol. PL 108,972 (1978).

SUMMARY AND CONCLUSIONS

Hydrotreatment of petroleum feedstocks comprising reactions such as hydrodesulfurization (HDS) and hydrodenitrogenation (HDN) has become of increasing importance in the last decades. The stringent prescriptions concerning the amount of sulfur and nitrogen contaminants in ecologically acceptable gas, liquid and solid fuels as well as the increasing need for processing of still heavier and dirtier feedstock supply a continuous drive to the research and development of hydrotreating catalysts and the process technology involved. The nowadays commercially applied catalysts consist of molybdenum (or tungsten) sulfide promoted with cobalt (or nickel) sulfide supported on a porous alumina carrier. Only in comparatively recent times, detailed fundamental information on the structure and related catalytic properties of these complicated catalytic ensembles has been derived. Thus, it became clear that there was no need for the exclusive use of alumina as a support material for these sulfide catalysts. On the contrary, it was found that substantially more active catalysts could be prepared on relatively inert carbon support materials. In addition, it was suggested that the use of carbon supports enables one to study the true catalytic properties of well-dispersed metal sulfides.

These findings were the outset of the research presented in this study which contains the results, both from a fundamental and practical point of view, concerning the use of carbon substrates as support materials for hydrotreating or more specifically, HDS catalysts. Due to the fact that in the literature not very much attention has been paid to this subject, it was decided to explore the properties of these carbon-supported catalysts in a wide context. The present investigation can be subdivided in two parts : the first part, comprising chapters 2 to 5, is focussed on the

structure and catalytic properties of the metal sulfide phase (especially Mo and Co) supported on a Norit activated carbon ; the second part comprising chapters 6 to 9 is focussed on the influence of the textural and surface characteristics of various carbon supports on the dispersion and catalytic properties of deposited Mo and Co catalysts. The main techniques applied were : atmospheric thiophene HDS experiments, X-ray photoelectron spectroscopy, dynamic oxygen chemisorption, Fourier transform infrared spectroscopy, pore size distribution measurements and temperature programmed sulfidation.

Preparation of the carbon-supported catalysts involved a standard pore volume impregnation with aqueous solutions of the appropriate metal salts, followed by drying. In this precursor state the Mo phase supported on activated carbon was found to be highly dispersed as isolated or polymerized monolayer species at Mo loadings below 3 wt% and as very tiny three dimensional particles at higher loadings. In contrast herewith, the precursor Co phase in activated carbon-supported Co catalysts appeared to be inhomogeneously dispersed on the carbon surface, yielding a considerable enrichment at the outer surface of the support particles. An explanation for this dispersion was that during impregnation the carbon surface becomes positively charged due to adsorption of protons from the solution. As a result the molybdate anions present in the solution adsorb on the carbon surface due to electrostatic attraction. Cobalt cations on the contrary are not adsorbed because of electrostatic repulsion. Hence, the inhomogeneous dispersion of Co is understood to result from transport of the Co solution to the outer part of the support grains during the drying procedure.

Upon sulfidation in a 10% H_2S in H_2 mixture, the precursor Mo and Co phases were quantitatively converted into their sulfide phases, viz. MoS_2 and Co_9S_8. Sulfidation, which was complete at temperatures below 573 K, proceeded via a

mechanism of O-S substitution reactions and by reduction via cleavage of part of the metal-S bonds. Furthermore, the dispersion of the catalysts significantly decreased during sulfidation. These findings demonstrate the weak interaction of the carbon surface with the deposited catalytic phase, a situation which is clearly completely different from that observed for alumina-supported Mo and especially Co catalysts where strong metal-support interactions are present necessitating high sulfiding temperatures (>700 K) in order to obtain complete sulfidation of the precursor catalysts.

The thiophene HDS activity of activated carbon-supported sulfided Mo catalysts was found to be much higher than the corresponding activity for alumina-supported Mo catalysts. Dynamic oxygen chemisorption measurements indicated a higher fraction of active sulfide surface area and a higher turn-over frequency of the sites for the carbon-supported Mo catalysts compared to the alumina-supported ones. It was concluded that the interaction of the alumina oxygen anions with the Mo atoms in the sulfide caused an extra charging of the Mo atoms which lowered their capability for S-hydrogenolysis. Experimental evidence supporting this finding was found in a correlation between the catalytic activity of second and third row metal sulfides supported on activated carbon, and the shift in XPS binding energy between metal and metal sulfide phases, which demonstrated that superior catalysts have a small charge on the metal atom in the sulfide phase (preserve a high degree of metal character).

The activated carbon-supported sulfided Co catalysts demonstrated very high HDS activities which were by far superior to those of corresponding carbon- or alumina-supported molybdenum catalysts. Extrapolation to optimal atomic dispersion indicated that Co atoms had a seven-fold higher HDS activity than optimally dispersed Mo. Comparison of these activity data with those obtained for

carbon-supported Co-Mo shows that the so-called promotor effect in sulfided Co-Mo catalysts is primarily caused by the exceptionally high catalytic activity of Co sites and that the role of MoS_2 in these catalysts is mainly to function as a support for the atomic dispersion of the Co atoms on its surface. The latter finding is in complete agreement with the Co-Mo-S model described by Topsøe and coworkers. In this respect, it would be of interest to see if the above conclusion regarding the role of Co as promotor atom also applies when Ni instead of Co is added or when W sulfide instead of Mo sulfide is used, and furthermore whether it also holds for other reactions and reactants.

The atmospheric thiophene HDS activities measured for carbon-supported transition metal sulfide catalysts ranging from group VI to group VIII c resembled very much the HDS activities reported for the corresponding unsupported sulfides. Typical volcano curves were obtained for second and third row metal sulfides when activity was plotted as a function of the periodic position of the transition metal. Maximum activity was measured for Rh in the second and Ir in the third row. First row elements showed a twin-shaped pattern with maximum activity located at Cr and Co. In this regard it would be interesting to see whether the same relation between activity and periodic position holds for other catalytic reactions such as hydrodenitrogenation, hydrodeoxygenation, and aromatic hydrogenation.

The above described findings of the carbon-supported catalysts, show that due to the weak interaction of the carbon surface with the deposited catalytic phases, these catalysts show some remarkable properties which are very different from those observed for alumina-supported systems. Upon sulfidation, unhampered formation of the actually active metal sulfide phase is achieved at low temperatures. This metal sulfide phase is free of strong interactions with the support and as a consequence shows a remarkable high HDS activity. Hence, the advantages of carbon as a support

material are that the true catalytic properties of well-dispersed metal sulfides present in their most active form can be studied, and that by comparison with alumina-supported catalysts the effect of strong metal-support interactions on the structural and catalytic properties of the metal sulfide phase can be identified.

The role of the carbon surface oxygen functionality on the dispersion of the Mo phase was studied by means of Fourier transform infrared spectroscopy (FTIR) and XPS on carbon black-supported Mo catalysts which differ in Mo dispersion. This study was based on the supposition that, if a chemical reaction takes place between the molybdate ions and a specific carbon surface oxygen group, a change in the spectral characteristics of the impregnated compared to the unloaded carbon blacks will become apparant. Some evidence was found in the FTIR spectra of the samples with the highest Mo dispersion that the molybdate ions interact with carbon surface aryl-ether functional groups. However, since no major changes were observed in the XPS and FTIR spectra of the impregnated compared to the unloaded carbon black samples, it was suggested that the role of the oxygen functional groups on the dispersion of the catalysts might be of secondary importance. Then, the presence and amount of reactive carbon surface atoms could be the major factor influencing the active phase dispersion.

The thiophene HDS activity of activated carbon-supported Mo catalysts was found to decrease drastically with increasing amount of phosphate present on the carbon surface. Thus, in order to obtain highly active Mo catalysts supported on carbon, the phosphate impurity level of the carbon should be kept low. It was shown that phosphate combines with molybdate to form a 12-molybdophosphate complex in the precursor catalysts. Upon sulfidation this complex readily converts into a MoS_2-P species which has poor HDS properties. The exact nature by which phosphorus influences the MoS_2 phase remains

unknown for the moment, but additional XPS and ^{31}P solid state MAS NMR measurements on sulfided phosphorus containing Mo catalysts might clarify this. Nevertheless in view of the above results it can be concluded that in phosphate containing alumina-supported catalysts, where a distinct promotion effect of P on the HDS activity is observed, no MoS_2-P species are formed.

Since activated carbons are essentially microporous, and therefore of little use as support for HDS catalysts under industrial conditions, two types of mesoporous carbons, carbon black composites and carbon covered alumina were prepared and evaluated with respect to their textural and surface properties for use as carrier materials for sulfide catalysts. Pore size distributions of the composites could be varied by selecting carbon black substrates differing in primary particle size. Promising textural properties were obtained for the composites prepared (BET surface area ranging from 120-730 m^2/g with predominant porosity in the mesoporous range). However, it was found that reasonable dispersions of the Mo phase were obtained only after the composites had been subjected to an oxidative treatment to increase their surface heterogeneity and thus their affinity towards the deposited Mo phase. Carbon covered alumina carrier materials were prepared via pyrolysis of cyclohexene or ethene on the surface of a gamma-alumina. Narrow pore size distributions were obtained in the 2.5-10 nm pore radius range and meso- plus macropore surface areas reached values of 190-270 m^2/g. The alumina surface coverage was not uniform but a value of 77% could be reached for a 27 wt% C on alumina sample. The thiophene HDS activity of Co sulfide supported on the prepared carbon covered aluminas was found to increase linearly with increasing alumina surface coverage by carbon, demonstrating the shielding of the carbon layer to reduce or eliminate strong cobalt-alumina support interactions. Oxidation of the carbon surface prior to introduction of cobalt led to an

improvement of the HDS activity. It was found, however, that the catalytic activity of the Mo and Co catalysts supported on the carbon black composite and carbon covered alumina supports, respectively, were lower than those measured for the corresponding catalysts based on the activated carbon support. Thus it becomes clear that the possible advantage of carbon black composites and carbon covered alumina with regard to a more optimal pore size distribution is not prominent, at least when thiophene is employed as a probe molecule for HDS and that further development work is necessary before carbon black composites or carbon covered alumina's can be used in the industry.

Overlooking the results described in the present investigation it is obvious that the carbon-supported sulfide catalysts contain interesting as well as promising properties both from a fundamental and practical point of view. It is evident, that by carefully balancing the textural and surface properties of carbon supports, the research efforts on this type of catalysts will pay-off in the near future.

SAMENVATTING EN CONCLUSIES

Ontzwaveling en ontstikstoffing van aardoliefracties (hydrotreating) is de laatste decennia in belangrijke mate toegenomen. De strenge eisen wat betreft het zwavel- en stikstofgehalte in ecologisch aanvaardbare gasvormige, vloeibare en vaste brandstoffen als mede de toenemende noodzaak voor het verwerken van zwaardere oliefracties hebben het onderzoeks- en ontwikkelingswerk van hydrotreating katalysatoren en de daarbij behorende procestechnologie in sterke mate gestimuleerd. De heden ten dage commercieel gebruikte katalysatoren bestaan uit molybdeen- (of wolfraam-) sulfide gepromoteerd met kobalt- (of nikkel) sulfide aangebracht op een poreuze aluminiumoxide drager. Gedetailleerd fundamenteel inzicht in de structuur en de hieraan verbonden katalytische eigenschappen van deze ingewikkelde katalysatorsystemen heeft men pas recentelijk verkregen. Hieruit bleek dat het exclusieve gebruik van alumina als dragermateriaal voor sulfidische katalysatoren niet noodzakelijk was. Integendeel, het bleek dat katalysatoren met een aanmerkelijk hogere activiteit konden worden bereid indien kool als dragermateriaal werd aangewend. Tevens werd gesuggereerd dat het gebruik van kool als dragermateriaal het mogelijk maakte om de ware katalytische eigenschappen te bestuderen van goed gedispergeerde metaalsulfide deeltjes.

Deze bevindingen waren de start van het in dit proefschrift beschreven onderzoek welk fundamentele zowel als praktische resultaten bevat aangaande het gebruik van kool als dragermateriaal voor hydrotreating, of meer specifiek, ontzwavelings-(HDS) katalysatoren. Gezien het feit dat er in de literatuur niet veel aandacht besteed werd aan dit onderwerp, werd besloten de eigenschappen van sulfidische katalysatoren op kool te bestuderen in een brede context. De resultaten kunnen dan ook in twee delen worden

ingedeeld : het eerste deel (hoofdstuk 2 tot en met 5) bevat de resultaten met betrekking tot de structuur en katalytische eigenschappen van metaalsulfide deeltjes (in het bijzonder Mo en Co) gedragen op een Norit aktieve kool ; het tweede deel (hoofdstuk 6 tot en met 9) beschrijft de invloed van textuur en oppervlakte-eigenschappen van verschillende kooldragers op de dispersie en katalytische eigenschappen van Mo en Co katalysatoren aangebracht op de diverse dragers. De volgende technieken werden toegepast ; atmosferische thiofeen ontzwavelingsexperimenten, rontgen-fotoelectronspectroscopie, dynamische zuurstof chemisorptie, Fourier transform infrarood spectroscopie, poriedistributie bepalingen en temperatuur geprogrammeerde inzwaveling.

De kool-gedragen katalysatoren werden bereid door middel van een standaard porie-volume impregnatie van de drager met een waterige metaalzout oplossing, gevolgd door drogen. Voor de gedroogde actieve kool-gedragen Mo katalysatoren bleek de Mo fase zich goed gedispergeerd te bevinden aan het kooloppervlak hetzij als geïsoleerde of gepolymeriseerde monolaag plakjes bij Mo beladingen beneden de 3 gewichtsprocent en als zeer kleine drie dimensionale deeltjes bij hogere beladingen. In tegenstelling hiermee bleek dat in gedroogde katalysatoren van Co op actieve kool de Co fase inhomogeen verdeeld was over het drageroppervlak en zich voornamelijk aan het buitenoppervlak van de dragerdeeltjes bevond. Een verklaring hiervoor werd gevonden in het feit dat het kooloppervlak tijdens de impregnatiestap protonen adsorbeert en hierdoor positief geladen wordt. Dit resulteert in een adsorptie van de molybdaatanionen uit de impregnatieoplossing. Cobalt cationen worden echter niet geadsorbeerd ten gevolge van de electrostatische repulsiekrachten. De inhomogene dispersie van Co volgt dan ook uit het feit dat transport van de Co oplossing plaats vindt naar het buitenoppervlak van de dragerdeeltjes tijdens de droogprocedure.

Inzwaveling van de gedroogde katalysatoren in een 10%

H_2S/H_2 mengsel resulteert in een kwantitatieve omzetting van de metaalzouten in hun sulfide vorm : MoS_2 en Co_9S_8. Deze inzwaveling was beëindigd bij temperaturen beneden de 573 K en verliep door middel van O-S substitutie reacties en reductie via het breken van een deel van de gevormde metaal-S bindingen. Daarenboven trad sintering op van de actieve fase gedurende de inzwaveling. Deze bevindingen wijzen op een geringe interactie tussen het kooloppervlak en de katalytisch actieve fase, een situatie die duidelijk verschilt van die in alumina- gedragen systemen, waar sterke metaal-drager interacties een hoge inzwavelingstemperatuur (>700 K) vereisen wil men de gedroogde katalysatoren volledig inzwavelen.

De thiofeen-ontzwavelingsactiviteit van Mo-sulfide katalysatoren gedragen op actieve kool bleek vele malen hoger dan de overeenkomstige activiteit van Mo systemen op alumina. Dynamische zuurstofchemisorptie experimenten duiden op een lagere fractie van het actief sulfide oppervlak en een lagere turn-over frequency van de sites voor alumina katalysatoren vergeleken met de kool gedragen systemen. De conclusie was dat de interactie tussen de zuurstofanionen van het alumina en de Mo atomen in het sulfide een extra lading op de Mo atomen met zich meebracht, waardoor de ontzwavelingscapaciteit van deze Mo atomen verkleind wordt. Een experimenteel bewijs hiervoor werd gevonden in de correlatie tussen katalystische activiteit van tweede en derde rij overgangsmetaalsulfiden en de verschuiving in XPS-bindingsenergie tussen het metaal en metaalsulfide, welke aantoonde dat katalysatoren met een hoge ontzwavelingsactiviteit slechts een geringe lading op het metaalatoom in het sulfide hadden (hoge mate van metallisch karakter).

Cobalt sulfide katalysatoren op actieve kool bleken een uitermate hoge ontzwavelingsactiviteit te bezitten, welke beduidend hoger was dan die van de overeenkomstige Mo katalysatoren op kool of alumina. Bij extrapolatie naar

optimale atomaire dispersie bleek de ontzwavelingsactiviteit van Co atomen zeven maal groter te zijn dan die van Mo atomen. Een vergelijking met de activiteit van Co-Mo katalysatorsystemen toonde aan dat het zogenoemde promotoreffect in deze katalysatoren het gevolg is van de hoge ontzwavelingsactiviteit van sites gelokaliseerd op Co atomen en dat de rol van MoS_2 in deze katalysatoren beperkt blijft tot het optimaal dispergeren van de Co atomen aan zijn oppervlak. Dit laatste is in overeenstemming met de resultaten van het Co-Mo-S model van Topsøe en medewerkers. In deze context lijkt het interessant om na te gaan of de bovenstaande conclusies aangaande de rol van Co in gepromoteerde katalysatoren ook van toepassing is wanneer Ni i.p.v. Co als promotor wordt toegevoegd, of wanneer W sulfide i.p.v. Mo sulfide wordt aangewend, alsook bij andere reacties dan HDS.

De thiofeen-HDS-activiteiten gemeten bij atmosferische druk voor overgangsmetaalsulfide katalysatoren op kool, gaande van groep VI tot en met groep VIII c, geleken sterk op de HDS-activiteiten beschreven in de literatuur voor overeenkomstige ongedragen sulfides. Typische klokkurven werden verkregen wanneer de activiteit werd uitgezet t.o.v. de positie van het overgangsmetaal in het periodiek systeem. De hoogste activiteit werd gemeten voor Rh in de tweede rij en Ir in de derde rij. De overgangsmetaalelementen van de eerste rij vertoonden een verloop met een dubbel maximum, met Cr en Co als meest actieve elementen. In dit opzicht zou het interessant zijn om na te gaan of dezelfde relatie tussen activiteit en plaats in het periodiek systeem ook voor andere katalytische reacties zoals ontstikstoffing, ontzuurstoffing en aromaat-hydrogenering geldt.

Uit de resultaten beschreven in het voorgaande blijkt dat kool-gedragen sulfidische katalysatoren, mede dank zij de zwakke interactie tussen het kooloppervlak en de actieve fase, uitzonderlijke katalytische eigenschappen bezitten welke duidelijk verschillend zijn van die van alumina-

gedragen systemen. Tijdens het inzwavelen kan de sulfide- fase zich onbelemmerd vormen bij relatief lage temperaturen. De gevormde metaalsulfide fase vertoont geen sterke interactie met de drager en heeft daardoor een hoge ontzwavelingsactiviteit. De voordelen die verbonden zijn aan het gebruik van kool als dragermateriaal zijn dus, dat de ware katalytische activiteit van goed gedispergeerde metaalsulfide deeltjes in hun meest actieve vorm bestudeerd kan worden en dat door een vergelijk te maken met alumina gedragen systemen, de invloed van de sterke metaal-drager interactie op de structuur en katalytische eigenschappen van een metaalsulfide fase geïdentificeerd kan worden.

De invloed van de zuurstofhoudende functionele groepen op de dispersie van Mo op roet katalysatoren (met verschillende Mo dispersies) werd bestudeerd met behulp van Fourier-transform infraroodspectroscopie (FTIR) en rontgen-fotoelectronspectroscopie. Het uitgangspunt was dat indien er een chemische reactie zou plaatsvinden tussen de molybdaationen en een specifieke zuurstofgroep aan het kooloppervlak, dit een verandering in de spectra van de zuurstofhoudende groepen van de gedroogde katalysatoren ten opzichte van de onbeladen roeten zou teweegbrengen. In de FTIR spectra van de katalysatoren met de hoogste Mo dispersie werden aanwijzingen gevonden die duiden op een reactie tussen molybdaationen en aryl-ethergroepen van het kooloppervlak. Echter omdat de spectrale wijzigingen eerder minimaal waren, bestaat de mogelijkheid dat de zuurstofhoudende groepen van het kooloppervlak geen directe invloed op de dispersie van de Mo-fase uitoefenen. In dat geval zouden de reactieve oppervlakte-koolstofatomen een bepalende rol voor de Mo-dispersie kunnen spelen.

Een sterke daling in de katalytische activiteit van kool-gedragen Mo-katalysatoren werd waargenomen bij toenemende hoeveelheid fosfaat aanwezig op het kooloppervlak. De hoeveelheid fosfaat-onzuiverheden in kooldragers dient dan ook laag te zijn wil men hoge

ontzwavelingsactiviteiten bereiken. Het aanwezige fosfaat reageerde met de geïmpregneerde molybdaationen onder de vorming van een 12-molybdofosfaat complex welk bij inzwaveling werd omgezet in een MoS_2-P deeltje met een lage ontzwavelingsactiviteit. De manier waarop fosfor de activiteit van een MoS_2 deeltje verlaagt werd niet helemaal duidelijk ; hierin zouden aanvullende XPS en ^{31}P vaste stof MAS-NMR metingen aan de sulfidische Mo-P katalysatoren opheldering kunnen brengen. Er kan echter wel geconcludeerd worden dat in fosfaat bevattende Mo katalysatoren op alumina, waarin in tegenstelling tot de kool gedragen systemen een stijging in activiteit met fosfaatgehalte wordt waargenomen, geen MoS_2-P deeltjes gevormd worden.

Gezien het feit dat actieve kool voor het merendeel microporeus is en daardoor niet echt geschikt is als drager voor sulfidische katalysatoren onder industriële condities, werden twee soorten mesoporeuze kool, composieten en met kool bedekt alumina, bereid en geëvalueerd op hun hoedanigheid als drager voor sulfidische katalysatoren. Het bleek mogelijk de poriestraalverdeling van composieten te variëren door roetdeeltjes te gebruiken met verschillende primaire deeltjesgrootte. De textuureigenschappen van de composieten waren veelbelovend (BET oppervlak van 120-730 m^2/g hoofdzakelijk gelegen in het mesoporiëngebied). Het bleek echter noodzakelijk de composieten vooraf aan een oxidatiebehandeling te onderwerpen om zodoende de oppervlakte-heterogeniteit te verhogen en dus de affiniteit voor de Mo fase, om redelijke Mo dispersies te verkrijgen in de katalysatoren. De met kool bedekte alumina dragermaterialen werden bereid via de pyrolyse van cyclohexeen of etheen aan het alumina-oppervlak. De bereide preparaten vertoonden nauwe poriestraalverdelingen in een gebied met een poriestraal gelegen tussen 2.5 en 10 nm en met een meso -en macroporie-oppervlak van 190-270 m^2/g. De bedekking van het alumina-oppervlak door kool bleek niet uniform. Een bedekkingsgraad van 77% werd bereikt voor een

preparaat dat 27 gewichtsprocent kool bevatte. De thiofeen-ontzwavelingsactiviteit van Co-sulfide aangebracht op de met kool bedekte alumina dragers bleek lineair toe te nemen met de bedekkingsgraad van het alumina-oppervlak. Hieruit blijkt dat het koollaagje voldoende afscherming biedt en zodoende de sterke interactie tussen het kobalt- en het alumina-oppervlak gedeeltelijk of volledig elimineert. De katalytische activiteit van de Mo- en Co-katalysatoren aangebracht op de composiet en met kool bedekte alumina-dragermaterialen bleef echter beduidend onder het niveau van de overeenkomstige actieve kool gedragen katalysatoren. Dit wijst erop dat de mogelijke voordelen van de composieten en de met kool bedekte alumina dragermaterialen met betrekking tot de betere textuureigenschappen, niet echt vooraanstaand zijn gezien de ontzwavelingsactiviteit van de hierop bereide katalysatoren, en dat verdere ontwikkeling noodzakelijk is alvorens de composieten of met kool bedekt alumina industrieel toepasbaar zijn.

Terugblikkend op de resultaten beschreven in dit proefschrift, kan gesteld worden dat de sulfidische katalysatoren gedragen op kool zowel fundamenteel interessante als praktisch veelbelovende katalytische eigenschappen bezitten. Het is duidelijk dat door een juiste keuze van textuur- en oppervlakte-eigenschappen van de kooldragermaterialen, de onderzoeksinspanningen aangaande dit katalysatorsysteem praktisch bruikbare resultaten zal opleveren.

ACKNOWLEDGEMENTS

We gratefully acknowledge :

Norit B.V., especially Dr. A.R.P. van Heiningen (presently at Mc Gill University, Canada) and Dr. T. Wigmans for providing activated carbon support samples and for stimulating discussions.

Akzo Chemie Nederland B.V. (Ketjen Catalysts) and Eskens' Handelsmij B.V. for the provision of commercial catalysts, alumina carriers and carbon blacks.

Dr. J.J.G.M. van Bokhoven (Prins Mauritz Laboratory,TNO) and Mr. J. Teunisse (Delft University of Technology) for textural measurements.

Drs. B. Scheffer for recording of the TPS spectra and useful discussions on the interpretation of the results.

Dr. D. Schrijvers from the RUCA Centra for High Voltage Electron Microscopy in Antwerp for recording the Transmission Electron Micrographs.

Dr. J. de Haan and Mr. L. van de Ven for measuring the MAS-NMR spectra.

Prof. Dr. J.C. Duchet for enlightening discussions on HDS catalysis and for his remarks at the manuscripts.

The information included in chapters 2, 8 and 9 of this thesis is partly derived from a contract (EH-C-50-017-NL) concluded with the European Community.

DANKWOORD

Aan het slot van dit proefschrift wens ik al degenen die tot de voltooiing van dit werk hebben bijgedragen, te bedanken :

Mijn ouders, omdat ze me steeds in de gelegenheid hebben gesteld te studeren; San de Beer (sous-chef en zwavelees in hart en nieren) voor z'n stimulerend enthousiasme en kollegialiteit, z'n klimpartijen in de telefoon en opbouwende kritiek op mijn manuscripten (zonder hem had dit proefschrift er aanmerkelijk anders uitgezien); Niels Groot (gnoor, schroot, gnook, etc.) voor de prettige samenwerking zowel op wetenschappelijk als sportief (rondjes Karpendonk) vlak; Eugene van Oers (EVO), voor de vele experimenten die hij ten behoeve van het onderzoek heeft verricht; Theo Lensing, Henk ten Doeschate, Frans Mercx, Stefan Bouwens, Jan-Willem van Dijk, Arie Volmer en Paul Wijnands voor het werk dat zij in het kader van hun S8-praktikum of afstudeerwerk ten behoeve van dit onderzoek hebben verricht; Roel Prins omdat hij het aandurfde met een Belg van wal te steken; Wout van Herpen, voor het ontwerpen, maken, onderhouden en repareren van apparatuur; Adelheid Elemans-Mehring, voor de vele elementanalyses; Jos van Wolput, voor zijn deskundige assistentie bij de FTIR metingen; en alle leden van de vakgroep voor de prettige sfeer tijdens het werk.

Tot slot maar eigenlijk op de eerste plaats wil ik Ingrid bedanken voor de steun die ik aan haar heb gehad tijdens de afgelopen vier jaar.

LEVENSBERICHT

Jan Paul Rene Vissers werd geboren op 16 oktober 1957 te Merksem.

In juni 1975 behaalde hij, aan het Onze-Lieve-Vrouw van Lourdes College, het diploma van het secundair onderwijs, richting wetenschappelijke B.

Hierna vervolgde hij zijn studies aan de universiteit van Antwerpen (Rijksuniversitair Centrum Antwerpen en Universitaire Instelling Antwerpen). In juli 1980 behaalde hij, na zijn afstudeerwerk te hebben verricht in de vakgroep structuurchemie o.l.v. Prof. dr. H. Geise aan "Molecuulstructuurbepaling van Dimethylether met behulp van Electronendiffractie en Microgolfdata", met grote onderscheiding, het licentiaatsdiploma in de wetenschappen, groep scheikunde.

Op 1 oktober 1980 startte hij aan de Technische Hogeschool Eindhoven met een promotie-onderzoek naar de structuur en katalytische eigenschappen van sulfidische katalysatoren op kool, resulterend in dit proefschrift.

Op 14 april 1984 trad hij in het huwelijk met Ingrid Declercq.

Sinds 1 oktober 1984 vervult hij zijn militaire dienstplicht.

Stellingen behorende bij het proefschrift van J.P.R. Vissers

1. Het verdient aanbeveling om de combinatie van dynamische zuurstofchemisorptie en rontgen-fotoelectronspectroscopie, waarmee men inzicht kan verkrijgen over het al of niet homogeen gedispergeerd zijn van metaalsulfide deeltjes op een koolstofdrager, ook te toetsen aan katalysatoren zoals cobalt- en ijzersulfide op koolstof.

2. Bij hun "herinterpretatie" van het infraroodspectrum van $CuCl.C_2H_4$ op basis van berekeningen aan $Cu^+.C_2H_4$, waarin Cu d_{yz} C_2H_4 * backdonatie onbelangrijk blijkt te zijn, houden Merchan et al. er onvoldoende rekening mee dat Cu^+ geen goed model voor CuCl is.

   M. Merchan, R. Gonzalez-Luque, I. Nebot-Gil and F. Tomas, Chem. Phys. Lett. 112, 412 (1984).

3. De bewering van Raesky, dat de door hem gemeten gauche-trans konformerenverhouding in de vloeistoffase van methoxy dichlorofosfinoxide, $CH_3OP(O)Cl_2$, kan worden verklaard gebaseerd op verschillende statistische gewichtsfactoren voor de onderscheiden konformeren, is onjuist.

   O.A. Raesky, J. Mol. Struct. 19, 275 (1973).

4. Gezien de slechte reproduceerbaarheid en het moeilijk te bepalen eindpunt, verdient het aanbeveling de "Tellertest" methode welke het ontvettend vermogen van een detergent bepaalt, niet als aanvaardingscriterium voor detergenten te gebruiken.

   Belg. Mil. Spec. betreffende de proefmethoden voor zepen en detergenten (1972).

5. De bewering van Murrel en Garten als zou Fe^{2+} monoatomair verankerd zijn aan de coordinatief onverzadigde sites van de TiO_2 drager, is onvoldoende onderbouwd.

L.L. Murrel and R.L. Garten, Appl. Surf. Sci. 19, 218 (1984).

6. De conclusie als zouden kleine (1 nm) MoS_2 deeltjes in gesulfideerde Mo/Al_2O_3 katalysatoren aanwezig zijn, is niet in overeenstemming met de EXAFS resultaten welke duiden op een zesvoudige zwavelomringing van het Mo atoom.

B.S. Clausen, H. Topsoe, R. Candia, J. Villadsen, B. Lengeler, J. Als-Nielsen and F. Christensen, J. Phys. Chem. 85, 3868 (1981).

7. Bij de interpretatie van de textuureigenschappen van met koolstof bedekte poreuze materialen, dient rekening te worden gehouden met de structuureigenschappen van het koolstof en de wijze waarop het koolstof zich aan het oppervlak bevindt.

R. Leboda, Chromatographia 13, 549 (1980).
H.P. Alder, H. Geisser, A. Baiker and W. Richarz, " 108th AI ME Annual meeting, New Orleans, 1979", p. 337 (1979).

8. Door te stellen dat badminton een tweederangs tennis is, laat men duidelijk zijn gebrek aan kennis (en kunde) omtrent beide sporten blijken.

9. Aangezien de creativiteit van een groep groter is dan de som der individuele creativiteiten van de groepselementen, is samenwerking in wetenschappelijk onderzoek een absolute noodzaak.

10. Wanneer politici beweren dat nucleaire bewapening de enige manier is om de vrede te bewaren, bedoelen ze eigenlijk de "eeuwige vrede".

26 maart 1985